Molecular Control of Organogenesis, Cell Fate Specification and Cell Differentiation

Genetic and Experimental Studies in the Mouse

Maha Abdelghaffar Abdelgawwad El Shahawy

Department of Oral Biochemistry,
Institute of Odontology
Sahlgrenska Academy, University of Gothenburg

UNIVERSITY OF GOTHENBURG

Gothenburg 2019

Molecular Control of Organogenesis, Cell Fate Specification and Cell Differentiation: Genetic and Experimental Studies in the Mouse

maha.el.shahawy@odontologi.gu.se

ISBN 978-91-7833-203-8 (print)
ISBN 978-91-7833-204-5 (PDF)

Printed in Gothenburg, Sweden 2019
Printed by BrandFactory

To my family

With love

Molecular control during embryonic development

Molecular Control of Organogenesis, Cell Fate Specification and Cell Differentiation: Genetic and Experimental Studies in the Mouse

av Maha Abdelghaffar Abdelgawwad El Shahawy

Department of Oral Biochemistry, Institute of Odontology
Sahlgrenska Academy, University of Gothenburg
Gothenburg, Sweden

ABSTRACT

Deciphering the mechanisms controlling normal development sheds light onto the etiopathogenesis of congenital malformations and diseases, and knowledge of the expression patterns of proteins and/or their encoding genes is necessary to understand developmental pocesses. Good models to study developmental processes, such as morphogenesis, tissue patterning, cell fate specification and cell differentiation include developing teeth and tongue.

Carbonic anhydrases (CAs) are involved in several physiological processes and diseases, yet which of these enzymes are produced, and which cells express them during odontogenesis is unknown. To fill in this knowledge gap, we used biochemical and molecular analyses in developing mouse teeth. We revealed dynamic expression patterns of eight CAs during tooth formation, and showed that CAs are not produced solely by cells involved in enamel and dentine secretion and biomineralization. Furthermore, we showed that CAXIII protein was enriched in LAMP1/2-expressing vesicles, suggesting lysosomal localization, and that CAIII expression was confined to root odontoblasts. Our data suggest developmental regulation of CA expression, and that CAs participate in several biological events inherent to tooth-forming cells (study I).

The Hedgehog (Hh) and retinoic acid (RA) pathways play key roles during embryogenesis and tissue homeostasis. Both pathways are active in same or adjacent tissues. However, whether these pathways interact is largely unexplored. Furthermore, whether Sonic Hedgehog (SHH) signaling triggered by SHH, a Hh ligand, controls tongue development *in vivo* is unknown. To address these issues, we generated and studied mice genetically lacking SHH signaling (studies II and III). We revealed that in the developing tongue SHH abates RA activity through the RA-degrading enzymes CYP26s, and that epithelial cell fate specification is regulated by antagonistic SHH and RA activities, wherein SHH inhibits, whereas RA promotes taste placode and minor salivary gland formation. Furthermore, we showed that SHH signaling is required to prevent ectopic Merkel cell specification in the lingual epithelium (study II). We also revealed interactions between the Hedgehog and RA pathways in other embryonic structures (study III). Our findings (studies II and III) show that properly calibrated SHH and RA activities are crucial for adequate development, and are expected to be of interest, as deregulation of Hh/SHH signaling leads to congenital malformations and neoplasia.

Keywords: Carbonic anhydrase, *CRE/LoxP*, Glands, Merkel cells, Metaplasia, Patterning, Retinoic acid, Sonic Hedgehog, Tongue, Tooth

ISBN: 978-91-7833-203-8 (PRINT)
ISBN: 978-91-7833-204-5 (PDF)

Sammanfattning på svenska

En detaljerad kartläggning av de mekanismer som styr normal utveckling av kroppens vävnader och organ ger viktig information om orsaker och sjukdomsmekanismer för medfödda missbildningar och sjukdomstillstånd, och kunskap om expressionsmönster för de proteiner som är involverade och deras gener är av utomordentlig vikt för att förstå olika utvecklingsbiologiska skeenden. Såväl tandutveckling som bildandet av tungan utgör goda modeller för att studera utvecklingsbiologiska processer såsom morfogenes samt specificering och differentiering av olika celltyper.

Karboanhydraser (CA), en familj av enzymer, är viktiga i många fysiologiska processer, men trots detta är det inte känt vilka av dessa enzymer som bildas under odontogenesen och i vilka celler detta sker. För att råda bot på denna kunskapslucka analyserade vi musständer under utveckling. Vi kunde visa på dynamiska expressionsmönster för åtta CA i samband med tandutvecklingen, och fann också att produktion av CA inte begränsas till de celler som är involverade i sekretion och mineralisering av emalj och dentin. Vi kunde vidare visa att CAXIII var anrikat i vesiklar som uttrycker LAMP1/2, sannolikt således en lysosomal lokalisering, samt att CAIII-expression begränsades till odontoblaster i tandens rot. Våra resultat visar en utvecklingsberoende reglering av CA, samt att CA deltar i ett flertal biologiska skeenden i de tandbildande cellerna (Studie I).

Hedgehog (Hh) och retinoic acid (RA) och deras signalering är av central betydelse under embryogenesen och för vävnaders homeostas. Dessa signalvägar är ofta samtidigt aktiva i samma eller angränsande vävnader, men det är i stort sett okänt om dessa viktiga signalvägar på något sätt interagerar med varandra. Det är heller inte känt om och hur tungans utveckling *in vivo* kontrolleras av Sonic Hedgehog (SHH), en Hh-ligand. För att belysa dessa frågeställningar genererade vi genetiskt modifierade möss som saknade SHH-signalering och analyserade dessa (Studierna II & III). Vi kunde visa att SHH motverkar RA-signalering under tungans utveckling via RA-nedbrytande CYP26-enzymer. Vidare fann vi att specificering av tungepitelcellerna styrs av sinsemellan motverkande SHH- och RA-aktiviteter, där SHH inhiberar medan RA gynnar bildningen av smakplakoder och små salivkörtlar. Vi visade också att en intakt SHH-signalering erfordras för att förhindra ektopisk Merkel cell-specificering i tungans epitel (Studie II). Som en fortsättning har vi kunnat visa på interaktioner mellan Hedgehog- and RA-signalering också i andra embryonala strukturer (Studie III). Våra resultat (Studierna II & III) visar att noggrant kalibrerade SHH- och RA-aktiviteter är av avgörande betydelse för en problemfri embryonalutveckling. Resultaten är av intresse, då störningar i Hh/SHH-signalering orsakar såväl medfödda missbildningar som tumörutveckling.

List of papers

This thesis is based on the following studies, referred to in the text by their Roman numerals.

I. Reibring CG, El Shahawy M, Hallberg K, Kannius-Janson M, Nilsson J, Parkkila S, Sly WS, Waheed A, Linde A, Gritli-Linde A. Expression patterns and subcellular localization of carbonic anhydrases are developmentally regulated during tooth formation. *PloS One.* 2014 May 1;9(5):e96007.

II. El Shahawy M, Reibring CG, Neben CL, Hallberg K, Marangoni P, Harfe BD, Klein OD, Linde A, Gritli-Linde A. Cell fate specification in the lingual epithelium is controlled by antagonistic activities of Sonic hedgehog and retinoic acid. *PLoS Genet*. 2017 July 17; 13(7):e1006914.

III. El Shahawy M, Reibring CG, Hallberg K, Neben CL, Marangoni P, Harfe BD, Klein OD, Linde A, Gritli-Linde A. Sonic hedgehog signaling is required for *Cyp26* expression during embryonic development. *Manuscript.*

Content

Abbreviations

"+"	Wild type allele
4-OH-TAM	4-hydroxy-tamoxifen
acac	Acetic acid
ADH	Alcohol dehydrogenases
BMS493	Pan RAR antagonist
BOC	Brother of CDO (BOC)
CAs	Carbonic anhydrases
Car	Carbonic anhydrase gene
CARP	Carbonic anhydrase-related proteins
CD1530	Retinoic acid receptor γ selective agonist
CD2314	Retinoic acid receptor β selective agonist
CDO	Immunoglobulin/fibronectin-repeat-containing cell surface protein
Cre	(Cyclization recombination) recombinase
CV	Circumvallate papilla
CYP	Cytochrome P450 enzymes
DEAB	4-diethylaminobenzaldehyde
Dig	Digoxigenin
dpp	Day post-partum
E12	Embryonic day 12
EDTA	Ethylene diamine tetra-acetic acid
ER	Estrogen receptor
ERM	Epithelial rests of Malassez
ETOH	Ethanol
EVC	Ellis van Creveld syndrome protein
Fgfr/FGFR	Fibroblast growth factor receptor
"f"	Floxed allele
Foxa1/FOXA1	Forkhead box A1 (gene/protein)
FP	Fungiform placode
FuP	Fungiform papilla
GAS1	Growth-arrest specific gene 1
GFP	Green fluorescent protein
GIT	Gastrointestinal tract
Gli/GLI	Glioma-associated oncogene (gene/protein)
Hh	Hedgehog
Hsp/HSP	Heat shock protein (gene/protein)
IHC	Immunohistochemistry
IHH	Indian Hedgehog
ISH	*In situ* hybridization
K	Keratin

LacZ	*E. coli* gene encoding β-galactosidase enzyme
LAMP	Lysosome associated membrane protein
LE	Lingual epithelium
LM	Lingual mesenchyme
LoxP	Locus of crossing-over of P1
LRPs	Low-density lipoprotein co-receptors
MA	Maturation-stage ameloblast
"n"	Null allele
NCC	Neural crest cell
P0	At birth
PBS	Phosphate-buffered saline
PFA	Paraformaldehyde
PL	Papillary layer
Ptch/PTCH	Patched (gene/protein)
RA	Retinoic acid
RMA	Ruffle-ended maturation-stage ameloblast
RT-qPCR	Reverse transcription quantitative polymerase chain reaction
Aldh1a/RALDH	Retinaldehyde dehydrogenase (gene/protein)
RAR/RAR	Nuclear retinoic acid receptor (gene/protein)
RARE	Retinoic acid response element
RDH	Retinol dehydrogenase
RXR/RXR	Nuclear retinoid X receptors (gene/protein)
SAG	Smoothened agonist
Shh/SHH	Sonic hedgehog (gene/protein)
Smo/SMO	Smoothened (gene/protein)
SMA	Smooth-ended maturation-stage ameloblast
Spry2	Sprouty2
SOX2	SRY (sex determning region Y)-box2, transcription factor
SUFU	Suppressor of fused
TAM	Tamoxifen
VitA	Vitamin A
Wnt/Wnt	Homologue of wingless (gene/protein)
WMISH	Whole mount *in situ* hybridization

1. Review of literature

1.1 Introduction

During early stages of development, many organs, notably those that develop through reciprocal epithelial-mesenchymal interactions, share similar molecular and morphogenetic processes, even though the final outcome is different. Therefore studying and deciphering the cellular and molecular events controlling development of one organ provides insights into the mechanisms underlying the formation of other organs. Examples include ectodermal derivatives such as glands, feather and hair follicles, palate, and teeth, as well as endodermal derivatives, including, lungs, trachea and eosophagus (**Chuong et al., 2000; Gritli-Linde 2007; 2008; Jussila and Thesleff 2012; Rishikaysh et al. 2014; Lan et al. 2015**).

Structures such as developing glands, feather and hair follicles, *rugae palatinae*, teeth, and taste papillae/taste buds arise from seemingly homogeneous epithelial sheets, making them attractive models to dissect the mechanisms controlling tissue patterning and cell fate specification.

Organogenesis, tissue patterning, cell fate specification and cell differentiation are regulated by numerous proteins and small molecules, including signaling molecules, transcription factors, enzymes and extracellular matrix components. Signaling pathways such as the retinoic acid (RA), Hedgehog (Hh), Fibroblast growth factor (FGF) and Wnt signaling cascades play key roles during embryogenesis, organogenesis and tissue homeostasis (**Briscoe and Thérond, 2013; Duester, 2013; Brewer et al., 2016; Itoh 2016; Wiese et al., 2018**), and deregulation of these pathways during development affects numerous tissues and organs (**Gritli-Linde, 2010; Briscoe and Thérond, 2013; Duester, 2013; Brewer et al., 2016; Itoh 2016; Wiese et al., 2018**).

Accumulating evidence shows that signaling pathways interact whithin networks to drive development, as shown for example in developing hair follicles (**Rishikaysh et al. 2014**), teeth (**Jussila and Thesleff, 2012**), palate (**Gritli-Linde, 2007, 2008; Lan et al., 2015**) and limbs (**Tickle, 2006**). It is therefore important to delineate at which level and how signaling pathways interact to drive normal development, as this provides insights into the etiopathogenesis of congenital malformations.

Equally important is knowledge of the expression patterns of genes and/or their protein products (when and where they are expressed) in developing tissues and organs. Protein/gene marker expression within a cell or a tissue enables

identification of cell types and/or their functional status and helps in deciphering the etiology and mechanisms underlying abnormal development and disease. Furthermore, proteins expressed specifically in a given cell type can be used as tools to isolate and/or identify cells in future cell- and tissue-based therapies.

This work revealed the expression patterns of carbonic anhydrases (CAs) during tooth formation (sudy I). In addition, this work deciphered the *in vivo* role of Hedgehog signaling elicited by Sonic hedgehog (SHH) and revealed interactions between the SHH and the RA pathways during tongue development (study II), as well as interactions between the SHH and RA cascades in other embryonic structures (study III). SHH interacts with other signaling cascades such as the FGF and/or Wnt pathways in several developing organs, including the tongue and palate. I will therefore provide an overview of the Hedgehog/SHH, RA, Wnt and FGF signaling pathways. This is followed by a description of embryonic development of the organs studied and the current knowledge about the expression patterns and/or role of members of signaling pathways (with emphasis on the pathways that are relevant to this work in a given organ) in these organs. I will also provide an overview of the biology of CAs in dental and non-dental tissues. Finally, since this work is, to a large extent, based on the use of the *Cre/LoxP* system in mice, I will describe the *Cre/LoxP* approaches enabling the generation of genetically modified mice that have been used in the present work.

1.2 Signaling pathways

1.2.1 The Hedgehog signaling pathway

Hedgehog (Hh) signaling regulates many developmental processes in both vertebrates and invertebrates. The Hh signaling pathway is, to some extent, conserved among organisms and is important for cell proliferation, cell differentiation, migration, survival and cell fate determination (**McMahon et al., 2003; Hui and Angers, 2011; Lee et al., 2016**).

Sonic hedgehog (SHH) is a member of the Hh family of secreted proteins, which in mammals also includes Indian Hedgehog (IHH) and Desert Hedgehog. SHH ligand is synthesized as a pre-protein that is subsequently processed to its active form (**Lee et al., 2016**). SHH can act both as long-range and short-range morphogen (**Strigini and Cohen, 1997, Gritli-Linde et al., 2001; McMahon et al., 2003; Nagase et al., 2007; Lee al al., 2016**).

Patched1 (*Ptch1*) encodes a transmembrane Hh receptor, and *Smoothened* (*Smo*) encodes an obligatory factor for transduction of all Hh signaling (**McMahon et al., 2003**). In the absence of Hh ligands, PTCH1 protein localizes in the primary cilium, and inhibits signaling through inhibition of SMO activity. At the base of the primary cilium, Kinesin family member 7 and Protein kinase A mediate the

proteolytic processing of glioma-associated oncogene 3 (GLI3) to its repressor form, and to a lesser extent GLI2, thus keeping the Hh/SHH signaling cascade blocked and Hh target genes inactive.

In the presence of the Hh ligands, PTCH1 binds to the ligand and moves out of the primary cilium. This enables SMO to accumulate in the primary cilium and to associate with EVC (Ellis van Creveld syndrome protein) and EVC2. SMO activation leads to increased recruitment of SUFU (Suppressor of Fused), GLI2 and GLI3 to the cilium, dissociation of the SUFU-GLI complex within the cilium, and to translocation of full-lengh activator forms of GLI2 and GLI3 transcription factors to the nucleus, where they activate Hh target gene transcription (**Briscoe and Thérond, 2013**). *Ptch1* and *Gli1* are direct targets of Hh signaling, thus, their expressions identify cells and tissues responding to Hh activity (**McMahon et al., 2003**). Vertebrates, including mammals have a second *Patched* gene (*Ptch2*), and PTCH2 protein exhibits partial functional redundancy with PTCH1 (**McMahon et al., 2003; Lee et al., 2016**).

Hh protein activity and movement is regulated through various molecules. Dispatched, a membrane protein, regulates the release of Hh protein (**Farzan et al., 2008**). Heparan sulfate proteoglycans, notably a glypican family member, GPC3, has been shown to inhibit Hh signaling in vertebrates by competing with PTCH1 for Hh binding (**Jiang and Hui, 2008; Simpson et al., 2009**). Cholesterol derivatives (oxysterols) have been shown to activate Hh signaling **(Rohatgi et al., 2007; Simpson et al., 2009**). Similar to PTCH protein in *Drosophila* and vertebrates, in vertebrates Hedgehog-interacting protein 1 attenuates Hh movement by sequestering and endocytosing Hh ligand, and competes with PTCH for the ligand (**Jeong and McMahon, 2005; Torroja et al., 2005; Lee et al., 2016**). Studies in mice showed that Hh signal reception is positively regulated by other Hh-binding proteins, including the immunoglobulin/fibronectin-repeat-containing cell surface proteins (CDO), brother of CDO (BOC) and Growth-arrest specific gene 1 (GAS1), which enhance Hh ligand binding to PTCH1. In this event GAS1 cooperates with CDO (**Jiang and Hui, 2008**). In developing craniofacial structures, GAS1 and BOC can exhibit both redundant and well-defined functions (**Seppala et al., 2014**).

1.2.2 The Retinoic acid signaling pathway

Vitamins are essential organic molecules that cannot be synthesized by organisms and must be supplemented in the diet. The multifunctional vitamin A (VitA; retinol) is available in the liver, and as a provitamin in spinach, carrots and sweet potatoes (**Al Tanoury et al., 2013**).

Most of VitA functions are carried out by its active metabolite, retinoic acid (RA) (**Al Tanoury et al., 2013; Cunningham and Duester, 2015**). RA is produced from retinol via a two-step process. First, the oxidation of retinol to retinaldehyde, a reversible process, is catalyzed by either alcohol

dehydrogenases (ADH1, ADH3 and ADH4) or retinol dehydrogenases (RDH1 and RDH10). These retinol-oxidizing enzymes have overlapping and widespread expression patterns. The second step is the oxidation of retinaldehyde into RA in an irreversible reaction catalyzed by three retinaldehyde dehydrogenases (RALDH1, RALDH2, RALDH3) (**Duester, 2008; 2013**). The RALDHs have, to a large extent, non-overlapping expression patterns during embryogenesis. Although retinol is readily available to all tissues and cells via the circulatory system, only cells that express at least one of the RALDHs can oxidize retinaldehyde to RA (**Duester, 2008**).

RA signaling is transduced through two families of nuclear receptors. The nuclear RAR family of RA receptors consists of three isotypes (RARα, RARβ, RARγ). Genes encoding the three RAR subtypes exhibit differences in their sequence, implying specific function for each isotype. Each subtype is evolutionary conserved between human and mice. The RARs form heterodimers with another nuclear receptor family also consisting of three isoforms, the retinoid X receptors (RXRα, RXRβ, RXRγ) (**Henning et al., 2015**). In the cell nucleus the ligand binds to the RAR portion of the RAR/RXR heterodimer. The heterodimers act as a transcription factor that activates target genes through binding to retinoic acid response elements (RAREs) in the target's promoter region (**Henning et al., 2015**). In the absence of RA, RAR/RXR recruits members of the nuclear receptor co-repressor family of proteins and repress target genes. By contrast, upon ligand binding, RAR/RXR associate with co-activators, leading to activation of the same target genes (**Duester, 2008; Cunningham and Duester, 2015**).

The degradation of RA occurs through oxidation by the cytochrome P450 (CYP26) family of enzymes. There are three CYP26 subtypes (CYP26A1, CYP26B1, and CYP26C1). In mice *Cyp26* genes exhibit tissue specific expression patterns (**Duester, 2008**). Cells that express one of the *Cyp26* genes are protected from high levels of RA, whereas in cells that lack *Cyp26* expression, RA is intact and is able to elicit signaling (**Duester, 2008**).

VitA and RA are crucial for several biological processes such as differentiation and maintenance of epithelial cells, vision, immune function, reproduction and tissue homeostasis. VitA deficiency results in a wide variety of defects, including loss of vision, immunodeficiency, growth retardation, foetal resorption, shortening and thickening of bones, and testis atrophy. By contrast, VitA or RA excess are highly teratogenic, causing multiple developmental alterations, including craniofacial anomalies. The severity of defects caused by overexposure to VitA or RA depends on the dose of retinoids and gestational stage of the exposed embryos (**Shenefelt, 1972; Geelen and Peters, 1979; Yasuda et al., 1986; Elmazar et al., 1996; Padmanabhan, 1998; Young et al., 2000; Doldo et al., 2015**). In addition to the role of retinoids during development, accumulating evidence indicates that VitA deficiency or attenuated RA signaling are involved in tumorigenesis, and retinoids are used as

chemotherapeutic drugs (**Doldo et al., 2015; Alonso et al., 2016**). Notably, overexpression of *Cyp26a1* in mice has been shown to promote mutagen-induced skin carcinogenesis in mice (**Osanai et al., 2018**) and SHH-mediated upregulation of *CYP26A1* in the bone marrow stroma protects tumor cells against differentiation and chemotherapy (**Alonso et al., 2016**).

1.2.3 The Wnt signaling pathway

The Wingless/int1 family (Wnt) comprises secreted glycoproteins found in all animals. The *Wnt* gene family includes 19 members. Wnt proteins are palmitoylated by the palmitoyl transferase Porcupine. In multicellular organisms Wnt signaling is crucial for development and tissue homeostasis (**Nusse and Clevers, 2017**). Deregulation of Wnt signaling leads to cancer and is involved in inflammatory, metabolic, and neurological disorders (**Acebron and Niehrs 2016**). Wnt signaling is classically divided into canonical and non canonical pathways. The canonical pathway, the most widely studied, is also known as the Wnt/β-catenin pathway. β-catenin-independent Wnt signaling pathways, include the Wnt/planar cell polarity and Wnt/Ca2+ pathways (**Zhan et al., 2017**).

In canonical Wnt signaling, the absence of Wnt ligand, causes the scaffolding protein AXIN to form a destruction complex with Adenomatous Polyposis Coli, glycogen synthase kinase 3 and casein kinase 1, resulting in phosphorylation of AXIN-bound β-catenin by the serine/threonine kinases casein kinase 1 and glycogen synthase kinase 3. Phosphorylated β-catenin is thereafter ubiquitinated by β-TrCP, and directed to proteosomal degradation. In this case, the absence of nuclear β-catenin localization leads to formation of a repressor complex that represses target genes. Wnt signaling is initiated upon binding of Wnt ligand to Frizzled receptors and low-density lipoprotein co-receptors (LRP) 5/6. Subsequently glycogen synthase kinase 3 and casein kinase 1 phosphorylate LRPs and recruit Dishevelled proteins to the cell membrane, where they form activated polymers. The destruction complex is inhibited by Dishevelled polymers, resulting in stabilization of β-catenin and its subsequent translocation into the nucleus. Nuclear β-catenin forms an active complex with other factors, including Lymphoid enhancer factor and T-cell factor, leading to activation of target gene transcription, including genes encoding C-Myc and Cyclin D1 (**Acebron and Niehrs 2016; Zhan et al., 2017**).

Wnt-β-catenin signaling is modulated by different factors. Secreted Wnt antagonists such as members of the Secreted Frizzled-related protein family and Wnt inhibitory factor bind to Wnt ligands, preventing their binding to Wnt receptors. The Dickkopf and the Sclerostin/SOST families of Wnt inhibitors bind to LRP5/6, and this likely prevents Wnt-induced formation of the Frizzled-LRP5/6 dimers. Wnt/β-catenin signaling is activated through secreted agonists such as Norrin and R-spondin proteins (**Dijksterhuis et al., 2014; Nusse and Clevers, 2017; Zhan et al., 2017**).

1.2.4 The Fibroblast growth factor signaling pathway

Secreted Fibroblast growth factors (FGFs) are widely expressed. These factors are crucial for early embryonic development, and play key roles during repair, regeneration, and maintenance of adult tissues. At the cellular level, secreted FGFs regulate multiple processes such as cell proliferation (as positive or negative regulators), migration, differentiation and survival. The FGF family consists of 22 members that are classified into 7 subfamilies known as FGF/1/2/5, FGF/3/4/6, FGF/7/10/22, FGF/8/17/18, FGF/9/16/20, FGF/11/13/14 and FGF/15/19/21/23 families. FGF signaling is activated through binding of the FGF ligand to FGF receptors (FGFR) (**Ornitz and Itoh 2015; Itoh, 2016**).

Fifteen FGFs function in a paracrine manner. The paracrine FGFs includes FGF1-10, FGF16-18, FGF20 and FGF22. These FGFs have heparin/heparan sulphate binding sites. Heparin/heparan sulphate acts as a co-factor that enables stable interaction between FGF and FGFR, and bind to them independently. The binding of FGF ligands to FGFRs leads to the activation of the intracellular tyrosine kinase domain of the FGFR. This triggers the activation of multiple intracellular signaling pathways, including the phosphatidylinositide 3-kinase/Akt, rat sarcoma protein/mitogen-activated protein kinase, signal transducer and activator of transcription, and the phospholipase Cγ pathways (**Itoh, 2016, Maddaluno et al., 2017**).

Aberrations of FGF signaling through mutations or amplification of genes encoding FGFRs cause congenital anomalies and can lead to progression of various types of cancer (**Ornitz and Itoh 2015**).

1.3 Tooth development

The tooth consists of epithelial and mesenchymal components. In mammals, the epithelial enamel organ is derived from the ectoderm. The dental ectomesenchyme originates from cranial neural crest cells of the first branchial arch and frontonasal process (**Jussila and Thesleff 2012**). Tooth development is controlled by epithelial-mesenchymal interactions mediated by numerous factors, including signaling molecules belonging to the Bone morphogenetic protein, Ectodysplasin, SHH, Transforming growth factor β and Wnt pathways (**Thesleff, 2014**).

Tooth formation is initiated by appearance of an epithelial thickening (dental placode), which in the mouse is visible at embryonic day 12.5 (E12.5). Proliferation and invagination of the dental placode into the underlying mesenchyme generates a tooth bud (E13-E13.5 in mice). Tooth development is classified into 3 different stages according to the morphology of the enamel organ (dental epithelium). These are the bud, cap, and bell stages. At the cap stage (E14.5-E15 in mice) the enamel organ surrounds an ectomesenchymal

condensation known as the dental papilla, whereas the entire tooth primordium is wrapped by ectomesenchyme forming the dental sac. The dental papilla gives rise to the dental pulp and predentin/dentin-forming odontoblasts. Cusp morphogenesis initiates at the early bell stage (E16 in mice), and different components of the enamel organ become histologically visible at this stage. These include the inner dental epithelium, the stratum intermedium, the stellate reticulum, and the outer dental epithelium. The inner dental epithelium is a cell layer made of proliferating cells which gives rise to proliferating pre-ameloblasts that differentiate into secretory ameloblasts, cells that produce enamel matrix. During tooth formation, the three-layered stratum intermedium is juxtaposed with the inner dental epithelium, preameloblasts and secretory ameloblasts. The stellate reticulum is located between the stratum intermedium and outer dental epithelium.

During tooth development, in addition to the dental placodes, primary and secondary enamel knots, which appear at the cap and early bell stages, respectively, act as signaling centers, as they express several signaling molecules, including SHH, and drive tooth growth and morphogenesis. Formation of these signaling centers is controlled by epithelial-mesenchymal interactions (**Catón and Tucker, 2009; Thesleff, 2014**). At the late bell stage, the tooth shows predentin/dentin layers and enamel matrix as a result of functional cytodifferentiation of odontoblasts and ameloblasts, respectively [1-11 days post-partum (dpp) in mice]. After secreting enamel matrix, secretory ameloblasts undergo a transition stage during which they lose their Tomes' processes and decrease their height. Subsequently, transition-stage ameloblasts differentiate into maturation-stage ameloblasts (MA; 12 dpp in mice) involved in enamel maturation. MA undergoes cyclical morphological changes into ruffle-ended and smooth-ended MA (**Frank and Nalbandian, 1967; Reith and Boyde, 1981; Lacruz, 2017; Lacruz et al., 2017**). At the maturation stage, the outer dental epithelium, stratum intermedium and stellate reticulum form the papillary layer (PL), a structure also involved in enamel maturation (**Reith and Boyde, 1981; Lacruz et al., 2017**).

In molars, root formation starts after completion of crown growth and morphogenesis (≈10 dpp in mice) (**Huang et al., 2009; Li et al., 2017**). The outer dental epithelium and the inner dental epithelium form a double epithelial structure known as Hertwig´s epithelial root sheath. This structure induces the differentiation of odontoblasts from peripheral cells of the dental papilla. When root odontoblasts form predentin/dentin, Hertwig´s epithelial root sheath disintegrates partially, allowing contact between the dental sac and root dentine. This leads to differentiation of cementoblasts that lays down the cementum over root dentine. The dental sac also gives rise to the fibroblasts and osteoblasts that form the periodontal ligament and the alveolar bone, respectively (**Jussila and Thesleff, 2012**). Remnants of Hertwig's root sheeth form a network of epithelial cells known as epithelial rests of Malassez (ERM) (**Huang et al., 2009; Listgarten, 1975**).

In contrast to murine molars which have a limited growth period, the rodent incisor is a continuously growing tooth, owing to the presence of epithelial (**Smith and Warshawsky, 1975; Harada et al., 1999; Wang et al., 2007; Kuang-Hsien et al., 2014; Yang et al., 2015**) and mesenchymal (**Zhao et al., 2014; An et al., 2018**) stem cells at its posterior end. The rodent incisor also differs from molars by its tissue organisation along its labio-lingual axis. Enamel develops only in the labial side of the incisor as the labial inner dental epithelium gives rise to ameloblasts, whereas the lingual inner dental epithelium is unable to do so. Dentin in the lingual part of the rodent incisor is covered by cementum. Therefore, the lingual side and the labial side of the rodent incisor are considered as a root-analog and a crown-analog, respectively (**Smith and Warshawsky, 1975; Beertsen and Niehof, 1986; Ahmad et al, 2011; Li et al., 2017**).

Like other developing organs, tooth development is regulated by numerous factors from initiation to completion (**Jussila and Thesleff, 2012**), and SHH signaling plays a crucial role during odontogenesis (**Seppala et al., 2017**). In the absence of SHH or SMO, ameloblasts fail to differentiate and produce enamel, and growth and morphogenesis of teeth is abnormal (**Dassule et al., 2000; Gritli-Linde et al., 2002**). Furthermore, loss of SHH signaling leads to fusion of molars (**Gritli-Linde et al., 2002; Seppala et al., 2017**), whereas activation of SHH signaling leads to formation of supernumarary teeth (**Seppala et al., 2017**). SHH signaling is also involved in maintenance of dental stem cells in mouse incisors (**Seppala et al., 2017**).

1.4 Tongue development

The tongue is a muscular organ that is important for mastication, speech and taste. Taste is an essential sense that allows the discrimination between nutritious and toxic substances.

In mice and humans, the dorsal surface of the mature tongue is covered by a mucosa made of epithelium and mesenchyme. The dorsal surface of the oral tongue (anterior two thirds of the tongue) contains gustatory (contains taste buds) and non-gustatory (do not harbor taste buds) papillae. There are three kinds of gustatory papillae: (1) fungiform papillae (FuP) distributed in a specific manner over the oral tongue, (2) several (in humans) or a single (in mice) circumvallate papilla(e) (CV) located at the junction between the oral tongue and the pharyngeal tongue (posterior third of the tongue), and (3) foliate papillae, situated at the lateral edges of the posterior part of the oral tongue. The non-gustatory filiform papillae are distributed among the FuP. Serous glands, known as von-Ebner glands, associated with the CV secrete their content in the trenches of the CV. Other glands, the posterior lingual sero-mucous glands, develop in the pharyngeal tongue (**Hamosh and Scow, 1973; Jitpukdeebodintra et al., 2002; Barlow, 2015**). Thus, the tongue shows differences along its anterior-

posterior axis, with glands present only at the anterior-posterior junction and in the posterior segment.

Taste buds have both epithelial and neuron-like properties, as they can respond to taste stimuli by producing electrochemical signals. Similar to other epithelial cells, taste bud cells regenerate continuously (**Farbman, 1980; Roper, 1992; Finger et al., 2005**). Taste bud cells have a limited life span of 10-14 days, but this could vary since subsets of taste bud cells can survive for up to 45 days (**Beidler and Smallman 1965; Perea-Martinez et al., 2013; Gaillard et al., 2017**). Cell lineage tracing studies identified Keratin 5- and Keratin 14-expressing cells as basally-located epithelial progenitors (situated outside the taste bud) responsible for renewal of taste bud cells and non-taste lingual epithelium (**Thirumangalathu et al., 2009; Liu et al., 2013; Perea-Martinez et al., 2013; Barlow, 2015**).

Taste bud cells are classified into three types (**Yee et al., 2001**). Type I cells have supportive functions and express membrane-bound ATPase (**Miura et al., 2014**), and in mice Type I cells seem to be required for the perception of salt (**Calvo and Egan, 2015**). Type II cells express G-protein-coupled receptors mediating sweet, bitter and umami perception. These cells also express phospholipase Cβ2, which is activated upon binding of tastants to their specific receptors. Type III cells are presynaptic cells that form synapses with afferent gustatory nerve fibers. Upon depolarization, type III cells release serotonin, acetylcholine, norepinephrine and γ -aminobutyric acid. These cells sense sour tastants through polycystic kidney disease-like protein channels (**Calvo and Egan, 2015**). Taste buds contain another type of cells, previously known as type IV cells. These cells are located at the base of taste buds and express *Shh* soon after their final mitosis, and lineage tracing showed that these cells are post-mitotic cells that directly differentiate into the other three cell types within taste buds (**Calvo and Egan, 2015; Barlow 2015**).

In mice the tongue primordium is visible at E10.5. FuP formation is preceded with development at E12.5 of fungiform placodes (FPs), localized epithelial structures made of elongated post-mitotic cells that will eventually differentiate into taste buds. Like the rest of the lingual epithelium (LE), FPs are overlaid with flat cells that form the periderm. During the active prenatal growth phase of the tongue, new FPs form until up to E14. In mice taste bud cells differentiate and are functional after birth (**Kaufman, 1992; Mistretta and Liu, 2006**). Based on gene expression patterns and/or studies in mice, and in rodent organ cultures, it has been shown that tongue development is controlled by coordinated epithelial-mesenchymal interactions mediated by several factors (**Beites et al., 2009; Liu et al., 2013**).

Several signaling molecules and transcription factors have been suggested or shown to play roles during tongue development and patterning of taste papillae. These include SHH (**Hall et al., 2003; Mistretta et al., 2003; Liu et al., 2004**),

bone morphogenetic proteins (**Zhou et al., 2006)**, Wnts **(Liu et al., 2007; Iwatsuki et al, 2007**), FGFs (**Jung et al., 1999**), epidermal growth factors (**Liu et al., 2008)** and SRY (sex determning region Y)-box2 (SOX2) (**Okubo et al, 2006**).

1.4.1 The retinoic acid pathway in the developing tongue

The role of the RA pathway during tongue development is hitherto unknown despite evidence showing expression of members of the RA pathway in the developing tongue (**Dollé et al., 1990; 1994; Ruberte et al., 1990; 1992; Niederreither et al., 1997; 2002; Mollard et al., 2000**). Nevertheless, overactivation of this pathway in animal models have been shown to lead to tongue defects, including agenesis and/or reduced size of the tongue and abnormal adhesions of the LE with oral epithelia (**Kalter, 1960; Kalter and Warkany, 1961; Shenefelt, 1972; Padmanabhan and Ahmed, 1997**), indicating that the tongue is able to respond to RA inputs.

1.4.2 The SHH signaling pathway in the developing and mature tongue

Shh is expressed during the different stages of murine tongue development. *Shh* is expressed in the entire LE from E10.5 to E11.5. From E12.5 to E14, *Shh* expression is restricted to developing FPs (**Hall et al., 1999; Jung et al., 1999**). *Ptch1* expression in the LE overlaps with that of *Shh* at E12, thereafter *Ptch1* expression gradually becomes confined to areas that surround the developing FuP. In contrast to *Shh* that is expressed only in the LE, *Ptch1* is expressed in both the LE and the underlying lingual mesenchyme (LM) (**Hall et al., 1999**). *Gli1* expression parallels that of *Ptch1* in the developing tongue. As *Ptch1* and *Gli1* are SHH targets (**McMahon et al., 2003**), their expression in the LE and LM indicate that these tissues respond to SHH signaling (**Hall et al., 1999**). *Shh* is a well-established marker for taste placodes (**Iwatsuki et al., 2007; Liu et al, 2004, 2013**).

Previous studies using pharmacological manipulation of the SHH pathway in embryonic rodent tongues cultivated *in vitro* suggested that SHH signaling plays a role during tongue growth (**Liu et al., 2004**) and patterning of FuP (**Hall et al., 2003; Mistretta et al., 2003; Liu et al., 2004; Iwatsuki et al., 2007**). Interruption of SHH signaling leads to FuP patterning defects, including formation of abnormally enlarged FuP and increased numbers of these structures, suggesting that SHH signaling inhibits FuP formation (**Hall et al., 2003; Mistretta et al., 2003; Liu et al., 2004**). Experiments in embryonic rat tongue explants showed that defects in FuP patterning and tongue development as a result of inhibition of SHH signaling are stage-dependent (**Liu et al., 2004**): abrogation of SHH signaling at E12 (this stage is equivalent to E10 in mouse embryos) causes severe reduction of tongue size, while SHH signaling loss at

E13 engenders tongue anomalies, including formation of a bifurcated tongue harboring supernumerary FuP. FuP patterning defects were also observed upon inhibition of SHH signaling at E14, but not at E16 onwards (**Liu et al., 2004**)

While the role of SHH signaling in the developing tongue has hitherto been studied only in tongue explants cultivated *in vitro*, the involvement of this pathway in homeostasis of the postnatal, mature (adult) tongue has been addressed *in vivo*. Gain-of-function studies in mice overexpressing *GLI2* (**Liu et al., 2013**) and *Shh* (**Castillo et al., 2014**) in the epithelium of the adult tongue, gave however different outcomes. Overexpression of *GLI2* caused loss of integrity of the LE, failure of maintenance of FuP and taste buds, loss of the typical morphology of filiform papillae, and led the LE to undergo atypical suprabasal proliferation (**Liu et al., 2013**). By contrast, forced expression of SHH in the LE resulted in formation of numerous ectopic taste buds outside of FuP; however, some these taste buds showed only sensory innervation (**Castillo et al., 2014**).

On the other hand conditional removal of GLI activity from the LE in postnatal mice resulted in disruption of the morphology of FuP and CV as well as in gradual loss of taste buds in these papillae, and many of these structures were regenerated upon recovery of Hedgehog signaling (**Ermilov et al., 2016**).

Recent evidence in postnatal mice showed that SHH protein emanating from the LE and/or nerves is required for taste bud maintenance and regeneration (**Castillo-Azofeifa et al., 2017; Lu et al., 2018**), and that exogenous Hh agonists promote regeneration of taste bud cells after loss of these cells caused by pharmacological inhibition of SHH signaling (**Lu et al., 2018**). These findings provide insights into the mechanisms leading to loss of taste perception in cancer patients treated with antagonists of the Hh pathway (**Castillo-Azofeifa et al., 2017; Lu et al., 2018**).

Altogether, these findings indicate that in the adult tongue, homeostasis of the LE, taste papillae and taste buds requires appropriate spatio-temporal activity of Hh signaling, as both loss and overactivation of this pathway impinge upon maintenance and integrity of these structures.

1.4.3 The Wnt signaling pathway in the developing and mature tongue

Canonical Wnt signaling is a potent regulator of FuP patterning. Expression of *Wnt10b* encoding a Wnt ligand parallels that of *Shh* during tongue formation from E12.5 to E14.5 (**Iwatsuki et al., 2007**). Thus, *Shh* is expressed in the LE at earlier stages as compared to *Wnt10b*. Genetic loss of Wnt/β-catenin signaling in mice overexpressing *Dickkopf1*, a gene encoding a Wnt inhibitor, or upon deletion of *Wnt10b, Lef1* or epithelial β-catenin leads to diminished number and reduced size of FuP (**Iwatsuki et al., 2007; Liu et al., 2007**). By contrast

activation of Wnt/β-catenin signaling at E12 causes overproduction and enlargement of FuP (**Liu et al., 2007**). Furthermore, findings in *Wnt10b* and *Lef1* null embryos as well as pharmacological modulation of SHH and Wnt signaling in tongue organ cultures *in vitro* suggest that Wnt and SHH signalings interact during patterning of FuP, where canonical Wnt signaling is required for *Shh* expression, whereas SHH inhibits canonical Wnt signaling (**Iwatsuki et al., 2007**). While these data suggest that canonical Wnt signaling promotes FuP induction, a recent study showed that the effects of Wnt/β-catenin signaling on FuP formation is time-dependent, as genetic activation of canonical Wnt signaling at E11.5 leads to loss of FuP in mouse embryos (**Thirumangalathu and Barlow, 2015**).

Genetic studies in human patients and mice show that Wnt10a, another Wnt ligand (**Xu et al., 2017**) is crucial for differentiation (**Adaimy et al., 2007; Xu et al., 2017**) and maintenance (**Xu et al., 2017**) of several epithelia and ectodermal appendages, including the LE, FuP and filiform papillae (**Adaimy et al., 2007; Xu et al., 2017**). In mice *Wnt10a* is expressed in both the embryonic and post-natal LE (**Iwatsuki et al., 2007; Xu et al., 2017**). Loss of *WNT10A* function in humans causes defects in the LE. Affected patients develop a smooth LE lacking FuP (**Adaimy et al., 2007; Xu et al., 2017**).

Wnt10a ablation in mouse embryos did not affect patterning and differentiation of the LE, suggesting functional redundancy amongst Wnt ligands, for example Wnt10b (**Xu et al., 2017**). By contrast, postnatal mice lacking the function of *Wnt10a* displayed diminished canonical Wnt signaling activity in the LE, and *Wnt10a* loss caused progressive anomalies in the LE, including development of abnormally small taste buds, a defect similar to that in mutants with postnatal loss of β-catenin (**Xu et al., 2017**). Furthermore, it was found that loss of Wnt10a/β-catenin signaling leads to loss of filiform papillae, FuP and taste bud cells, suggesting that this pathway is crucial for maintenance of filiform papillae, FuP and taste bud cells (**Xu et al., 2017**).

In contrast to forced activation of β-catenin in the LE of postnatal mice, which has been shown to favor induction of Type I taste bud cells (**Gaillard et al., 2017**), loss of genes encoding Wnt10a or β-catenin in postnatal mice leads to loss of molecular markers for all types of taste bud cells (**Xu et al., 2017**).

Wnt5a is a ligand belonging to the Wnt family that functions through the non-canonical Wnt pathway (**Liu et al., 2012; Shi et al., 2017**). Wnt5a can also activate or inhibit the canonical Wnt pathway, depending on the Wnt receptor (**Mikels and Nusse, 2006; van Amerongen et al., 2012**). In the embryonic murine tongue *Wnt5a* is expressed in the LM, and loss of *Wnt5a* in mice leads to ankyloglossia (adhesion of the tongue to the floor of the oral cavity) and to development of an abnormally small tongue. However, patterning of the LE and FuP occurs normally in the *Wnt5a*-deficient embryos (**Liu et al., 2012**). By contrast treatment of embryonic tongues *in vitro* with Wnt5a protein seems to

lead to reduced number of FuP and to decreased canonical Wnt signaling (**Liu et al., 2012**).

Taken together, these data suggest that the Wnt signaling pathway, and particularly the canonical Wnt pathway, is a key player during tongue formation and homeostasis of the LE and its appendages, including lingual papillae and taste buds. In view of the existence of interactions between the canonical Wnt pathway and SHH signaling in the developing tongue, it would be interesting to see whether the pathways interact to maintain lingual structures in the postnatal mature tongue.

1.4.4 The FGF pathway in the developing tongue

Previous work showed that *Fgf8* is expressed at low levels in mouse tongue at E10.5 in both the LE and LM. Subsequently, *Fgf8* expression shows a transient upregulation at E11, but it is downregulated at E12 (**Jung et al., 1999**). Another study in mouse embryos revealed that from E12 to E14, the developmental stages studied, *Fgfr2b* is expressed in the LE, whereas *Fgf10* and *Fgf7* are produced in the LM (**Rice et al., 2004**).

A recent comprehensive study of the patterns and levels of expression of all 22 members of the *Fgf* family in the developing murine tongue between E11.5 and E14.5 showed that *Fgf18, Fgf16, Fgf15, Fgf13, Fgf10, Fgf9, Fgf7, Fgf6* and *Fgf5* were all expressed in the LM, but with various strengths of hybridization signals. By contrast, *Fgf2* and *Fgf1* were detected in both the LE and LM. These data suggests a role for FGF signaling in epithelial-mesenchymal interactions during early stages of tongue development (**Du et al., 2016**).

Minor defects were reported to occur in the developing tongue of mice lacking *Fgf10* and *Fgfr2b* mice. In *Fgf10* and *Fgfr2b* null embryos the tongue and the floor of the oral cavity are fused. In addition, *Fgf10* null embryos develop abnormal, thick epithelial patches over the dorsal surface of the tongue (**Rice et al., 2004**). Furthermore, the CV fails to form in mouse embryos lacking *Fgf10* (**Petersen et al., 2011**).

Spry2 is a member of the *Sprouty* family of genes encoding intracellular negative regulators of FGF signaling. $Spry2^{n/n}$ mouse embryos have been reported to exhibit taste papilla defects, including duplication of the CV and reduced number of FuP, whereas compound null mutants for *Spry1* and *Spry2* develop several CV (**Petersen et al., 2011**). However, a recent study showed that in $Spry2^{n/n}$ tongues FuP exhibit reduced size, but their number was unaltered (**Prochazkova et al., 2017**).

These findings suggest that FGF signaling regulates the development of the CV, and that FGF activity is required for normal differentiation of the LE.

1.5 Carbonic anhydrases

Carbonic anhydrases (CAs) are zinc metalloenzymes first discovered in 1933. They catalyze the reversible hydration of CO_2 in the presence of water into HCO3- with the production of a proton. *CA* genes are grouped into 6 classes, with the α-*CA* gene family primarily found in vertebrates. In mammalians, the α-CA family comprises 16 CA isoforms that differ in their enzymatic activities, sites of expression and amino acid sequences (**Imtaiyaz Hassan et al., 2013; Mboge et al., 2018**). CAs are classified according to their subcellular distribution into cytosolic (CA I, CA II, CA III, CA VII, and CA XIII), membrane-bound (CA IV, CA IX, CA XII and CA XIV), mitochondrial (CA VA and CA VB) and secreted (CA VI) types. There are 3 non-catalytic CAs that lack enzymatic activity, and these are known as carbonic anhydrase-related proteins (CARP VIII, CARP X and CARP XI) (**Mboge et al., 2018**).

The α-CAs regulate numerous physiological processes, including pH regulation, respiration, bone resorption, calcification, gluconeogenesis, lipogenesis and ureagenesis. As they are involved in many metabolic processes altered in several disorders such as glaucoma, obesity and pain, CAs are targeted with drugs. Accumulating evidence shows that CA IX and CA XII have roles in tumorigenesis, tumor progression, acidification of the tumor environment, and metastasis, making them attractive anti-cancer targets (**Mboge et al., 2018**).

The cytosolic CAs are widely distributed in human tissues and have diverse functions. They are expressed in red blood cells, skeletal muscles, kidneys, brain, liver and adipose tissues. These CAs have been shown to interact with transporters, forming a “metabolon” to facilitate HCO3-/proton flux. Compared to other cytosolic CAs, CA II is the most widely expressed (**Imtaiyaz Hassan et al., 2013**). CA II is crucial for bone resorption and osteoclast differentiation, and is involved in controlling fluid production in the anterior chamber of the eye. Defects in CA II function cause CA II deficiency syndrome characterized by occurrence of renal tubular acidosis, osteopetrosis, glaucoma, cerebral calcification and growth retardation (**Imtaiyaz Hassan et al., 2013; Mboge et al., 2018**).

CA III is produced in the adipose tissue and skeletal muscles, and is expressed at high levels in osteocytes. Relative to other CA isoforms, CA III has the slowest catalytic activity. CA III has been shown to play a role in adipogenesis. Patients suffering from myasthenia gravis show deficiency in CA III (**Imtaiyaz Hassan et al., 2013**).

CA XIII is expressed in several tissues, including the kidney, brain, gastrointestinal tract (GIT), as well as in male and female reproductive organs. It has been suggested that CA XIII plays a role in maintenance of proper conditions that are required for fertilization in reproductive organs (**Imtaiyaz Hassan et al., 2013; Mboge et al., 2018**).

Secreted CA VI is expressed mainly in mammary and salivary glands, and in other secretory glands such as nasal and lacrimal glands (**Imtaiyaz Hassan et al., 2013**). It has been suggested that CAVI plays various roles, including pH regulation in saliva, protection of the stomach and eosophagus, and promotion of taste perception. Inhibition of CA VI may cause complete loss of taste perception (**Imtaiyaz Hassan et al., 2013, Mboge et al., 2018**).

The membrane-associated CAs have variable roles and expression patterns. CA IV is expressed abundantly in the bone marrow, liver and GIT. CA IV has been shown to be involved in pH regulation in the retina and retinal pigment epithelium. In addition, CA IV has been suggested to have a role in wound healing. Mutations of the gene encoding CA IV have been associated with retinitis pigmentosa characterized by degeneration of rods and cones (**Mboge et al., 2018**). Studies in mice showed that the gene encoding CA IV, *Car4*, is expressed in subsets of taste bud cells, and that CA IV is required for CO_2 sensing (**Imtaiyaz Hassan et al., 2013**).

CA XIV is expressed strongly in brain, muscles and retina. CA XIV has been implicated in the regulation of the acid-base balance in erythrocytes and muscle, and in the modulation of extracellular and intracellular pH and volume (**Imtaiyaz Hassan et al., 2013**). CA IV and CA XIV have been suggested to have overlapping enzymatic functions (**Mboge et al., 2018**) such as in pH regulation, as evidenced in studies using *Car4/Car14* double mutants (**Imtaiyaz Hassan et al., 2013**).

Compared to other CA isoforms, CA IX has limited expression patterns. CA IX is found in hair follicles and the GIT, and is detectable in the epidermis during wound healing (**Mboge et al., 2018**). CA IX has the highest enzymatic activity (**Neri and Supuran, 2011**). Previous work suggested that CA IX is involved in several biological processes, including regulation of the acid-base balance, signal transduction and bicarbonate transport. The gene encoding CA IX in humans (*CAR9*) is upregulated in many aggressive cancers, including tumors of the lung, uterine cervix, ovary and endometrium (**Imtaiyaz Hassan et al., 2013**), and its overexpression is associated with poor prognosis.

CA XII is expressed in various normal tissues, with high expression levels found in the kidney, intestine, pancreas, colon and rectum. In addition to facilitating bicarbonate transport, CA XII is important for normal kidney function. Similar to CA IX, CA XII has been incriminated in tumor development (**Mboge et al., 2018**).

CA-related proteins CARP VIII, CARP X and CARP XI are widely expressed in diverse tissues. These isoforms are expressed at high levels in the central nervous system and lungs. The exact functions CARPs are unknown, they have, however, been suggested to play a role during development of the central nervous system (**Imtaiyaz Hassan et al., 2013**).

1.5.1 Carbonic anhydrases in dental tissues

Several previous studies in rodents explored whether CAs are produced by dental tissues, with focus mainly on the secretory and maturation stages of amelogenesis. Work using histochemistry to detect CA activity indicated presence of CA activity in all epithelia of the enamel organ as well as in preodontoblasts (**Dogterom and Bronckers, 1983; Sugimoto et al., 1988**). RT-PCR assays in extracts from the enamel organ showed that genes encoding each of the 16 CA isoforms, except for the *Car5a* gene, were expressed at the secretory stage of amelogenesis in mice, with *Car2, Car6, Car9* and *Car13* exhibiting the highest expression levels (**Lacruz et al., 2010a**). CAVI and its encoding gene *Car6*, were found to be expressed in the enamel organ at the maturation stage, and it has been suggested that CA VI has role in caries prevention. In this scenario, CA VI may be incorporated into the enamel pellicle of the erupted teeth, where it could neutralize the acid released by cariogenic bacteria (**Kivela et al., 1999; Smith et al., 2006**). CA II/*Car2* have been detected in transition-stage and maturation-stage ameloblasts (**Lin et al., 1994; Toyosawa et al., 1996; Lacruz et al., 2010a; Smith et al., 2006**). However, the question of whether CA II or *Car2* are expressed in secretory ameloblasts remained open, since previous work showed that secretory ameloblasts showed neither CA activity (**Sugimoto et al., 1988**) nor immunostaining for CAII (**Toyosawa et al., 1996**), whereas *Car2* mRNA has been detected in extracts of the enamel organ at the secretory stage of tooth formation (**Smith et al., 2006; Lacruz et al., 2010a**). It has been proposed that CA II plays a role in enamel maturation by creating pH conditions that enable activation of hydrolytic enzymes involved in degradation of enamel matrix proteins (**Lin et al., 1994; Toyosawa et al., 1996**). Patients with CA II deficiency may display dental abnormalities such as enamel hypoplasia and malformed teeth (**Strisciuglio et al., 1990; Nagai et al., 1997; Awad et al., 2002**), suggesting involvement of CAII during odontogenesis.

While the above findings showing presence of CAs or their encoding genes in dental tissues are important, it remained unclear which epithelial dental cells express CAs and which CA isoforms are expressed in a given dental epithelial cell. Furthermore, the expression patterns of CAs in the different dental cell types during the different stages of odontogenesis are hitherto unknown.

1.6 The *Cre/LoxP* system

The mouse is a valuable tool for deciphering the etiopathogenesis of congenital malformations and diseases. Gene function can be studied by disabling genes through the conventional gene knockout approach in mice, leading to genetic loss in the germline and abrogation of gene function in all cells and tissues. This however, can lead to early embryonic lethality, or to severe systemic effects, hampering studies aiming at delineating gene function in a given developing organ. One way to overcome these hurdles is the use of the so-called conditional

gene targeting method, which enables control of gene deletion in space and time (in a tissue-specific and time-controlled manner). One such a method is the *Cre/LoxP* system (**Lobe and Nagy, 1998**). In this method, a site-specific recombinase recognizes specific DNA sequences (recognition sites) and recombines the DNA between them. Depending on the orientation and position of the recognition sites, DNA recombination induced by the recombinase leads to DNA deletions, insertions, inversions or translocations. One system, known as the *Cre/LoxP* system uses the DNA recombinase CRE (Cyclization recombination), a 38 kDa protein of bacteriophage P1. CRE recognizes a 34 bp DNA sequence called *LoxP* site (locus of crossing-over of P1). This system does not require co-factors and acts on wide range of cells (differentiated and undifferentiated cells) both *in vivo* and *in vitro* (**Metzger and Feil, 1999; Kwan, 2002**).

Generation of mutant mice through CRE-mediated deactivation of target genes (**Fig. 1A**) requires a series of crosses between two mouse lines. In the first cross a male carrying either a CRE transgene controlled by a strong tissue-specific promotor or enhancer, or carrying a knock-in allele, in which *Cre* is knocked into a specific locus, is crossed with a female carrying floxed alleles of the targeted gene, i.e. crucial sequences of the targeted genes are flanked by two *LoxP* sites (floxed alleles). Examples of *Cre* transgenes, include the *Wnt1-Cre* and the *K14-Cre* transgenes in which *Cre* is expressed in cells that express or have expressed *Wnt1* or the gene encoding Keratin 14, respectively. Subsequent mouse crosses lead to generation of mutants (homozygous mice) that carry both *Cre* and two floxed alleles of the targeted gene only in cells that express *Cre* and their progeny. Mice that do not carry the *Cre* gene or the floxed alleles of the targeted gene have intact gene function, and mice carrying the *Cre* gene and only one floxed allele of the targeted gene are heterozygous.

Artificial ligand-induced CRE-mediated gene targeting enables abrogation of gene function in a temporally controlled manner in the tissues/cells of choice. One example is the tamoxifen-inducible *Cre/loxP* system. In this system (**Fig. 1B**) the *Cre* gene is fused to a gene encoding a mutant form of estrogen receptor (ER) carrying a mutant ligand-binding domain unable to bind endogenous estrogens. By contrast, the mutant ER can bind 4-hydroxy-tamoxifen (4-OH-TAM), the active form of tamoxifen (TAM). In the absence of 4-OH-TAM, heat shock protein 90 (HSP90) sequesters the CreER fusion protein in the cytoplasm, thus mice or *in vitro*-cultivated cells/organs that express the tamoxifen-inducible Cre and a floxed gene have intact gene function. Exposure of mice or *in vitro*-cultivated cells/organs to 4-OH-TAM leads to dissociation of HSP90 from the CreER fusion protein, the latter translocates into the nucleus where Cre protein induces silencing of the floxed gene. Mice are most usually given TAM either by intraperitoneal injections or via oral gavage. TAM is metabolised into 4-OH-TAM in the liver.

The efficiency and specificity of CRE-mediated recombination is assessed by crossing two mouse lines. A male expressing *Cre* and a female carrying a reporter gene such as the *LacZ* gene. The *LacZ* gene encodes *E. Coli* β-galactosidase. *LacZ* is placed under the control of the ubiquitous, active promotor ROSA26. In addition, within the gene construct, the *LacZ* gene is preceded by floxed STOP sequences, preventing its expression in the absence of CRE. Offsprings carrying both the *Cre* and the *LacZ* genes display *LacZ* activity (β-galacosidase activity) only in cells that express or have expressed *Cre* (as the STOP sequences have been excised by CRE), and the sites of *LacZ* activity indicate cells/tissues in which the gene of interest is deleted (**Nagy, 2000; Kwan, 2002**).

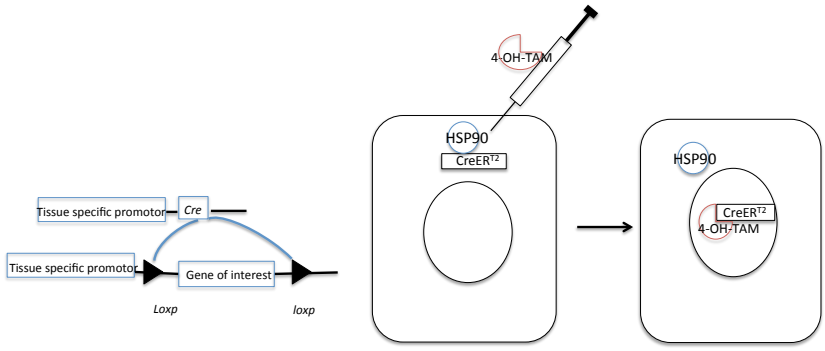

A. *Cre/loxP* systems

B. Inducible *Cre/loxP* systems

Fig. 1 Schematic showing the *Cre/loxP* and inducible *Cre/loxP* systems. (A) Important sequences of the targeted gene are floxed. Upon expression of CRE, the floxed gene sequences are excised and the gene is inactivated. (B) The *Cre* gene is fused to a gene encoding a mutant form of the ligand-binding domain of estrogen receptor (*CreER^{T2}*). In the absence of 4-hydroxy-tamoxifen (4-OH-TAM), CRE protein is sequestered in the cytoplasm by heat shock protein 90 (HSP90). Upon exposure to 4-OH-TAM, this drug binds to the mutant ligand-binding domain of ER. This leads to dissociation of HSP90 from the complex, enabling the CreER^{T2} fusion protein to ranslocate into the nucleus, where it induces recombination events that culminate in silencing of the targeted gene.

2. Aims

This work aimed at deciphering the molecular control of organogenesis, cell type specification and cell differentiation, with special focus on the following goals:

1. Providing a throrough description of the expression patterns of Carbonic anhydrases during mouse tooth development.

2. Deciphering the *in vivo* role of Sonic hedgehog signaling during tongue development, and the mechanisms by which this pathway controls the various processes inherent to the developing tongue.

3. Exploring whether the Sonic hedgehog and retinoic acid cell signaling pathways interact in various developing tissues and organs, and characterizing the nature of their relationships.

3. Materials and Methods

To reach our aims, we used an *in vivo* genetic approach by generating and studying a series of genetically modified mouse lines as well as control mice, and experimental approaches in organ cultures *in vitro*, combined with molecular and morphological analyses.

The use of mice in this work received ethical approval as stated in the articles related to studies I, II and III.

3.1 Mouse models

Mutant and control mice were genotyped using PCR as described in previous studies (cited below) that first reported the creation of mouse lines enabling generation of the various mutants and their control littermates. For staging of mouse embryos, noon of the day of discovery of a vaginal plug was considered as embryonic (E) day 0.5 (E0.5). The various mouse lines used in this work (listed below) were of a mixed genetic background (B6/129S/Swiss black).

3.1.1 Wild-type mice (study I)

For study I, with the exception of the *K14-CRE/R26R* reporter mice and their control littermates, the mice used were not genetically modified, and were of a mixed genetic background (B6/129S/Swiss black).

3.1.2 The *K14-CRE/R26R* reporter mice and controls (studies I and II).

The *K14-CRE/R26R* reporter embryos and postnatal mice were generated by crossing males harboring the *K14-CRE* (*K14-CRE/*$^{+}$*)* transgene and females carrying the *R26R* reporter gene (**Soriano, 1999**) (*R26R/R26R or R26R/*$^{+}$) as described previously (**Dassule et al., 2000; Vaziri Sani et al., 2005; Gritli-Linde et al., 2007**). These mice enable visualization of Keratin 14- (*K14/Krt14*) expressing epithelial cells and their progeny; they also allow for the visualization of CRE activity, indicating the sites of gene deletion. In the *K14-CRE/R26R* reporter mice, CRE activity and the K14-expressing lineage can be visualized in whole-mount organs or in tissue sections by histochemistry for β-galactosidase (activity of the *LacZ* gene product). Embryos and postnatal mice not carrying the *K14-CRE* transgene and/or the *R26R* reporter gene were used as controls.

3.1.3 The *Shh*$^{n/n}$ mutants and controls (study III)

The *Shh*$^{n/n}$ mutants (*ShhGFPCRE/ShhGFPCRE*) were generated by crossing *ShhGFPCRE* males and *ShhGFPCRE* females (**Harfe et al., 2004**). In the *Shh*$^{n/n}$ mutants the *Shh* gene is deactivated in all cells of the embryo. Heterozygous (*ShhGFPCRE/*$^{+}$) embryos and embryos not carrying the *ShhGFPCRE* allele were used as controls.

3.1.4 The *ShhGFPCRE/Smo*$^{f/f}$ mutants and controls (studies II and III)

The *ShhGFPCRE/Smo*$^{f/f}$ mutants were generated through two mouse crosses. First *ShhGFPCRE/*$^{+}$ males (**Harfe et al., 2004**) were mated with *Smo*$^{f/f}$ (**Long et al., 2001; Gritli-Linde et al., 2002; 2007**) females to generate heterozygotes (*ShhGFPCRE/Smo*$^{+/f}$). Heterozygous males were thereafter mated with *Smo*$^{f/f}$ females to generate control and *ShhGFPCRE/Smo*$^{f/f}$ mutant embryos. Embryos not carrying the *ShhGFPCRE* and/or the *Smo* floxed alleles, as well as heterozygotes were used as controls. In the *ShhGFPCRE/Smo*$^{f/f}$ mutants, cells that express *Shh* and their descendants are unable to respond to Hedgehog signaling as they lack SMO function (**Fig. 2B**). Since the *ShhGFPCRE* allele contains a gene encoding Green fluorescent protein (GFP) fused to the *Cre* gene and knocked into the *Shh* locus, sites expressing *Shh* in tissues from controls (*ShhGFPCRE/*$^{+}$*)* and mutant (*ShhGFPCRE/Smo*$^{f/f}$) embryos can be visualized with fluorescence microscopy.

3.1.5 The *ShhGFPCRE/R26R* embryos and controls (study II)

The *ShhGFPCRE/R26R* embryos enable visualisation of cells that express *Shh* and their descendents as well as the sites of CRE activity. This is achieved by the use of β-galactosidase histochemistry in whole-mount organs or in tissue sections derived from these embryos. The *ShhGFPCRE/R26R* embryos were generated by crossing *ShhGFPCRE/*$^{+}$ males with *R26R/R26R* or *R26R/*$^{+}$ females. Embryos not harboring the *ShhGFPCRE* allele and/or the *R26R* reporter gene were used as controls.

3.1.6 The *K14-CRE/Smo*$^{f/f}$ mutants and controls (study II)

Mutants and controls were generated by a series of two mouse crosses (**Gritli-Linde et al., 2007**). First *K14-CRE*$^{/+}$ males were mated with *Smo*$^{f/f}$ females to generate heterozygotes (*K14-CRE/Smo*$^{+/f}$). Thereafter, heterozygous males were mated with *Smo*$^{f/f}$ females to generate mutants *(K14-CRE/Smo*$^{f/f}$). In the mutants, the *Smo* gene is deleted in *K14*-expressing epithelial cells as well as in their progeny. Postnatal mice and embryos lacking the *K14-CRE* transgene and/or the *Smo* floxed alleles, as well as heterozygotes (*K14-CRE/Smo*$^{+/f}$) were used as controls.

3.1.7 The *K14-CRE/Shh$^{f/f}$* mutants and controls (study III)

These mice were generated as described previously (**Dassule et al., 2000; Lewis et al., 2004; Gritli-Linde et al., 2007**). *K14-CRE/Shh$^{+/f}$* heterozygous males (generated by crosses between *K14-CRE/$^{+}$* males and *Shh$^{f/f}$* females) were mated with *Shh$^{f/f}$* females to generate controls and *K14-CRE/Shh$^{f/f}$* mutants. Postnatal mice and embryos lacking the *K14-CRE* transgene and/or the *Shh* floxed alleles, as well as heterozygotes were used as controls. In the *K14-CRE/Shh$^{f/f}$* mutants, the *Shh* gene is disabled in cells that express or have expressed *K14*.

3.1.8 The *Wnt1-CRE/Smo$^{f/f}$* mutants and controls (study II)

The mutants and controls were obtained after a series of two mouse crosses as described previously (**Jeong et al., 2004**). *Wnt1-CRE/Smo$^{+/f}$* heterozygous males were obtained after crosses between *Wnt1-CRE/$^{+}$* males and *Smo$^{f/f}$* females, and the *Wnt1-CRE/Smo$^{f/f}$* mutants as well as controls were generated by mating *Wnt1-CRE/Smo$^{+/f}$* males with *Smo$^{f/f}$* females. In the mutant embryos the *Smo* gene is deleted in neural crest-derived mesenchymal cells; i.e. cells that express *Wnt1* and their progeny (**Fig. 2C**). Heterozygous embryos (*Wnt1-CRE/Smo$^{+/f}$*) as well as embryos lacking the *Wnt1-CRE* transgene and/or the *Smo* floxed alleles were used as controls.

3.1.9 The tamoxifen-inducible *ShhCreER^{T2}/Shh^{f}* and *ShhCreER^{T2}/Smo$^{f/f}$* mutants and control embryos (studies II and III)

These mice were generated through mouse crosses between females carrying the *Shh* or the *Smo* floxed alleles as described above, and males carrying the *ShhCreER^{T2}* knockin allele (**Harfe et al., 2004**). The *ShhCreER^{T2}/Shh^{f}* mutant embryos and control embryos were obtained by mating *ShhCreER$^{T2/+}$* males with *Shh$^{f/f}$* females (studies II and III). To generate *ShhCreER^{T2}/Smo$^{f/f}$* mutants and control embryos (study II), we first generated *ShhCreER^{T2}/Smo$^{+/f}$* heterozygous males through crosses between *ShhCreER$^{T2/+}$* males and *Smo$^{f/f}$* females. Thereafter *ShhCreER^{T2}/Smo$^{+/f}$* heterozygous males were mated with *Smo$^{f/f}$* females. In the absence of tamoxifen (TAM), the *ShhCreER^{T2}/Shh^{f}* and *ShhCreER^{T2}/Smo$^{f/f}$* mutants have intact *Shh* or *Smo* gene function, respectively. Upon TAM treatment of pregnant females the *ShhCreER^{T2}/Shh^{f}* and *ShhCreER^{T2}/Smo$^{f/f}$* mutants lose *Shh* (**Fig. 2D**) or *Smo* gene function, respectively, in cells that express *Shh* and their descendants as a result of *CRE*-mediated gene deletion elicited by 4-OH-tamoxifen, the active metabolite of TAM (**Fig. 1B**). Embryos lacking the *ShhCreER^{T2}* allele and/or the floxed *Shh* or *Smo* alleles were used as controls. Control and mutant embryos were exposed to TAM *in utero* following intraperitoneal injections of pregnant females with TAM (10 mg/ml) every other day, excluding the day of embryo harvest. The first injection consisted of 200 µl of TAM, and the other injections consisted of 100 µl TAM.

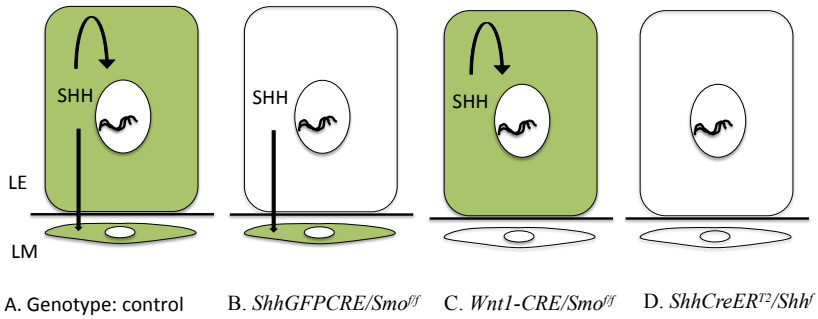

Fig. 2 Schematic showing SHH-responding and SHH-non-responding cells in organs made of an epithelium and a mesenchyme from control and some of the mutants used in this study. (A-D) The developing tongue is used as an example. (A) In the tongue of control embryos Sonic hedgehog protein (SHH) is produced in the lingual epithelium (LE) and acts in both LE and lingual mesenchyme (LM). (B) In *ShhGFPCRE/Smo$^{f/f}$* mutants, because *Smoothened* (*Smo*), the transducer of SHH signaling, is deactivated in the LE, this tissue is non-responsive to SHH signaling, whereas the LM remains responsive to SHH protein emanating from the LE. (C) By contrast in *Wnt1-CRE/Smo$^{f/f}$* mutants, the LM lose responsiveness to SHH as a result of *Smo* removal, whereas the LE has intact SHH signaling. (D) Tamoxifen-induced ablation of *Shh* in the LE of tongues of *ShhCreER^{T2}/Shh^{f}* mutants leads to loss of SHH signaling in both the LE and LM. The green color indicates cells that respond to SHH signaling, and the non-colored cells are those that are un-responsive to SHH signaling. In the *K14-CRE/Smo$^{f/f}$* and TAM-induced *ShhCreER^{T2}/Smo$^{f/f}$* mutant tongues only the LE loses SHH responsiveness (not shown).

3.1.10 The *RAREhsp68LacZ* mice (studies II and III)

Mice carrying the *RAREhsp68LacZ* transgene also known as *RARE-LacZ* or *RAREhspLacZ* (**Rossant et al., 1991**) enable visualization of cells and tissues that respond to retinoic acid (RA) signaling. However, accumulating evidence (**Mendelsohn et al., 1991; Reynolds et al., 1991; Balkan et al., 1992; Colbert et al., 1993**) indicates that the transgene is not active in all tissues and cells in which RA signaling is activated. To generate controls and *ShhGFPCRE/Smo$^{f/f}$* mutants carrying the *RAREhsp68LacZ* transgene, we first generated *ShhGFPCRE/Smo$^{+/f}$* heterozygous males (as described above) carrying the

transgene (*ShhGFPCRE/Smo$^{+/f}$/RAREhsp68LacZ*) through crosses between *ShhGFPCRE/Smo$^{+/f}$* males and *RAREhsp68LacZ* females. The *ShhGFPCRE/Smo$^{+/f}$/RAREhsp68LacZ* males were thereafter mated with *Smo$^{f/f}$* females. Embryos lacking the *RAREhsp68LacZ* transgene, the *ShhGFPCRE* knockin allele and/or the *Smo* floxed alleles as well as heterozygotes were used as controls. The sites of RA activity were visualized by histochemistry for β-galactosidase (activity of the *LacZ* gene product) in tissue sections (study II) or in whole mounts (study III).

3.2 Histology, immunohistochemistry and immunofluorescence (studies I, II and III)

Heads and other soft organs from embryos and postnatal mice (studies I, II and III) as well as organs cultivated *in vitro* (studies II and III) were fixed overnight at 4°C in either 4% paraformaldehyde (PFA) in phosphate-buffered saline (PBS) or in 95% ethanol containing 1% glacial acetic acid (ETOH-acac). The ETOH-acac-fixed specimens were subsequently post-fixed for 5 days in a solution consisting of 4% PFA, 10% glacial acetic acid and 0.85% NaCl. Following anesthesia twelve days post-partum (12 dpp) mice (study I) were fixed with 4% PFA in PBS by perfusion through the left heart ventricle after a brief (two minutes) perfusion with PBS. The heads were post-fixed overnight at 4°C in 4% PFA in PBS. Other heads from 12 dpp mice (study I) were dissected and fixed by immersion overnight at 4°C in ETOH-acac. After fixation, the specimens were demineralized in two ways: (1) the PFA-fixed specimens were demineralized in a solution consisting of 2.5% PFA in PBS and 12 % ethylene diamine tetra-acetic acid (EDTA), pH 7.4 for 4-6 weeks at 4°C with several changes, and (2) the ETOH-acac-fixed specimens were demineralized for 5 days at 4°C in a mixture consisting of 4% PFA, 10% glacial acetic acid and 0.85% NaCl. The fixed specimens as well as the decalcified heads were washed to eliminate the fixatives and the decalcifying agents, and processed for paraffin embedding and sectioning.

For histology, sections were stained with alcian blue van Gieson (studies II and III).

After antigen unmasking in either 1 mM EDTA, pH 8, or in 10 mM citrate buffer, pH 6, dewaxed sections were processed for immunohistochemistry or immunofluorescence as described in detail in study I. Following immunohistochemistry sections were counterstained with methyl green. Immunofluorescence signals are either green or red, as a result of use of the Alexa Fluor 488-tyramide conjugate or the Streptavidin-Alexa Fluor 594 conjugate, respectively. Controls for immunostaining included negative controls generated by omission of the primary antibodies and/or replacement of the primary antibodies by pre-immune sera, as well as positive controls generated by

assessment of protein distributions in sections of organs in which the expression of genes and/or their protein products has been reported in earlier studies. Immunostaining of tissues that are not targeted for gene deletion are used as internal controls. Tissues processed for histology, immunohistochemistry and immunofluorescence were viewed and imaged under bright-field illumination with a Nikon (Eclipse E600) microscope equipped with a camera.

The primary antibodies used, their dilutions and their sources are described in **Table 1**

3.3 *In situ* hybridization (studies I, II and III)

For *in situ* hybridization (ISH), embryos and postnatal mice up to 1 dpp were fixed in 4% PFA in PBS. For ISH in teeth from 12 dpp mice (study I), jaws from mice perfused with 4% PFA in PBS were demineralized in a solution consisting of 2.5% PFA in PBS and 12 % EDTA, pH 7.4 for 4-6 weeks at 4 °C.

ISH was performed in either whole-mount organs or in tissue sections. Whole-mount ISH was performed using Digoxigenin (Dig)-labelled riboprobes, and transcripts were detected by an alkaline phosphatase-labelled anti-Dig antibody (made in sheep) as described previously (**Wilkinson, 1992**). For ISH in tissue sections, dewaxed sections were hybridized with ^{35}S-UTP-labelled riboprobes and the transcripts were detected by autoradiography as described previously (**Angerer and Angerer. 1992**). Riboprobes (antisense probes) were generated by *in vitro* transcription of sequences within coding regions of genes after linearization of plasmids. Depending on the construct, SP6, T7 or T3 RNA polymerases were used to generate antisense riboprobes. The transcription reaction mixture contained Dig-UTP or ^{35}S-UTP to generate Dig-labelled or ^{35}S-UTP-labelled riboprobes, respectively. Tissue section ISH was also performed with oligonucleotide probes, and transcripts were detected using histochemistry for horseradish peroxidase as suggested by the manufacturer (Advanced Cell Diagnostics). After ISH with riboprobes or oligonucleotide probes, sections were counterstained with Richardson's Azur II-methylene blue. Specimens processed for whole-mount ISH were viewed and imaged with a Leica M165FC stereomicroscope equipped with a camera. Tissue sections processed with oligonucleotide probes or with radioactive riboprobes were viewed and imaged under bright-field or bright- and dark-field illuminations, respectively, with a Nikon (Eclipse E600) microscope equipped with a camera.

The probes used for ISH were as described in studies I, II and III. The dig-labelled and/or ^{35}S-UTP-labelled riboprobes are specific to: *Shh*, *Shh*/exon2, *Ptch1, Gli1, Cyp26a1, Cyp26b1, Cyp26c1, RARg, RARb, Car2 and Car 6*. The oligonucleotide probes are specific to: *Ptch1, Gli1, Cyp26a1, Cyp26b1*, *Cyp26c1*, *RARg* and *Wnt10b*.

3.4 Histochemistry (studies I, II and III)

Histochemistry enabling detection of β-galactosidase activity in whole-mount organs (studies II and III) or in tissue sections of organs that do not require decalcification (study II) was performed as described previously (**Vaziri Sani et al., 2005; Gritli-Linde et al., 2007**), and the reaction buffer is described below. For detection of β-galactosidase activity in jaws/teeth from 12 dpp mice, the specimens were fixed overnight at 4°C in 2% PFA in PBS. After fixation the tissues were demineralized in 10% EDTA pH 7.3 for several weeks. Following several washes in PBS containing 0.01% sodium deoxycholate, 0.02% NP40 and 2 mM $MgCl_2$, pH7.5, the jaws were incubated overnight at 4°C in PBS containing 30% sucrose. The following day the specimens were embedded in OCT compound, frozen on dry ice and stored at -70°C. Twelve µm-thick cryostat sections were processed for histochemistry. Cryostat tissue sections (on histological glass slides) were re-hydrated in PBS and incubated overnight at 37°C in staining jars containing 50 ml β-galactosidase reaction buffer. The reaction buffer consisted of 0.1 M Phosphate buffer, pH 7.4 containing 1mg/ml X-gal (dissolved in dimethylformamide), 0.01 % sodium deoxycholate, 0.02% NP-40, 2 mM MgCl2, 5 mM potassium ferricyanide, 5 mM potassium ferrocyanide, 20 mM Tris-HCL pH 7.3. The specimens were then rinsed in PBS, post-fixed in formalin, washed in PBS and processed for mounting after counterstaining with nuclear fast red. Organs processed for whole-mount β-galactosidase activity were processed in the reaction buffer in sealed tubes overnight at 37°C.

For histochemical detection of Carbonic anhydrase activity (study I), sections of PFA-fixed and demineralized jaws/teeth of 12 dpp mice were prepared and processed as described previously (**Sugimoto et al., 1988**). The sections were first preincubated for 20 minutes in 0.1 M phosphate buffer, pH 6.0, thereafter the sections were incubated at room temperature for a total period of 7-30 minutes in Hansson´s medium, pH 5.8-5.9. The medium consisted of 5.3×10^{-2} H_2SO_4, 1.57×10^{-1} M $NaHCO_3$, 3.5×10^{-3}M $CoSO_4$, 1.17×10^{-2} M KH_2PO_4. The slides were repeatedly immersed in and removed from Hansson´s solution. Specifically, the incubation was done by immersing the slides every 10 seconds during the first minute and every 20 seconds afterwards. Thereafter, the slides were rinsed two times in 0.1 M phosphate buffer, pH 6.0 for 20 seconds each. The reaction sites were visualized by immersing the slides in 1% $(NH_4)_2S$ for 30 seconds. After that the slides were rinsed in dH2O and mounted.

A camera-equipped Leica M165FC stereomicroscope and a camera-equipped Nikon (Eclipse E600) microscope were used to capture images of the whole-mount organs and tissue sections, respectively, under bright-field illumination.

3.5 Green fluorescent protein imaging (study II)

Organs were fixed overnight at 4°C in 1% PFA in PBS. After several washes in PBS at 4°C, the specimens were viewed and imaged under UV illumination and a filter for Green fluorescent protein with a Leica M165FC fluorescence stereomicroscope equipped with camera.

3.6 Reverse transcription quantitative polymerase chain reaction (studies II and III)

For reverse transcription quanatitative polymerase chain reaction (RT-qPCR), organs were dissected under RNAase-free conditions and stored for less than a week at 4°C in RNAlater^{TM} (InVitrogen) before RNA extraction and reverse transcription. RT-qPCR and primer sets used were as described in studies II and III. Student's t-test was used for statistical analyses.

3.7 Quantifications (studies II and III)

The number of taste buds in tongues from control and mutant embryos (study II) were determined in tongue whole-mounts after ISH for *Shh*. Quantification of Keratin 8-expressing cellular aggregates (taste buds or parts of taste buds) was performed after immunohistochemistry in all sections of tongues from control and mutant fetuses as described in study II. The number ectopic Merkel cells as well as the number of taste buds and ectopic Merkel cells that are innervated by gustatory nerve fibers (study II) was assessed in tongue sections from control and mutant mice after double immunofluerescence for various specific markers as described in study II.

The number of apoptotic cells in tails from control and mutant embryos (study III) was determined in tissue sections processed for cleaved lamin A/C immunohistochemistry as described in study III.

Statistical analyses of all the above quantifications were done with Student's t-test.

3.8 Organ cultures *in vitro* (studies II and III)

Mandibular arch/tongues (study II) and pelvic girdles/tails (study III) were harvested from embryos in sterile bacterial 10 cm-diameter plastic Petri dishes (Corning) containing sterile, ice-cold Hank's balanced salt solution (without

Ca++ and without Mg++; Thermo Fisher) under a stereomicroscope (Nikon). The culture system consisted of sterile 35 mm-diameter plastic cell culture dishes (Corning) containing home-made stainless steel grids (≈ 20 mm diameter and ≈ 3 mm height). Millipore filter papers (45 µm pore-size) were placed on top of the grids. The filter papers, the grids as well as tools for dissection were sterilized by autoclaving. The specimens were placed and cultivated on top of the filter papers at the air-culture medium interface. The culture conditions and the various treatments were as described in studies II and III. The specimens were processed for immunohistochemistry, histochemistry or ISH as described above.

Table1. Antibodies and dilutions used in the three studies

Antibody	**Dilution**	**Source**	**Study**
Chicken anti-200 kD Neurofilament heavy (NF200)	1:4,000	Abcam	II
Chicken anti-keratin 15	1:10,000	Covance, Berkeley, CA, USA	II
Goat anti-ALDH1A2	1:400	Santa Cruz Biotech-nology	II, III
Goat anti-CA IV; anti-gen affinity-purified	1:1,000	R&D Systems	I
Goat anti-CA IX; anti-gen affinity-purified	1:3,000	R&D Systems	I
Goat anti-CAXIII (K-16), antigen affinity-purified	(1:500) without tyramide; (1:1500, 1:2000) with tyramide amplification	Santa Cruz Biotechnology	I
Goat anti-CA XIV (N-19); antigen affinity-purified	1:200	Santa Cruz Biotech-nology	I
Goat anti-SHH	1:200	R&D Systems	II
Goat anti-SOX2	1:3,500	Santa Cruz Biotech-	II

		nology	
Rabbit anti-ALDH1A1, monoclonal	1:400	Sigma	II, III
Rabbit anti-ALDH1A3	1:400	Sigma life Science	II,III
Rabbit anti- Brachyury, monoclonal	1:5000	Abcam	III
Rabbit anti-CA II (H-70)	1:750; 1:1,000	Santa Cruz Biotechnology	I
Rabbit anti-CA III; antigen afinity-purified	1:200; 1:1,000	Proteintech	I
Rabbit anti-CA VI (1-18-R; antigen affinity purified)	1:2,000; 1:3000	Santa Cruz Biotechnology	I
Rabbit anti-CA IX (M-100)	1:250	Santa Cruz Biotechnology	I
Rabbit anti-CARP XI (H-50)	1:600; 1:1,000	Santa Cruz Biotechnology	I
Rabbit anti-cleaved lamin A, small subunit	1:1000	Cell Signaling Technology, Beverly, MA, USA	III
Rabbit anti- FOXA1, monoclonal	1:5000	Abcam	III
Rabbit anti-Homer 1	1:3,000	Proteintech	II
Rabbit anti-keratin 6	1:10,000	Covance, Berkeley, CA, USA	II
Rabbit anti-P2X2	1:200	Us Biological Life Sciences	II
Rabbit anti-Rab3c	1:1,000	Proteintech	II
Rabbit anti-RARγ	1:3,000	LifeSpan Bioscience	II

Rabbit anti-SHH (AB80)	1:800	(**Bumcrot et al., 1995; Gritli-Linde et al., 2001**)	II, III
Rabbit anti-mouse CA XIII antiserum	1:4,000	S.Parkkila (**Lehtonen et al., 2004**)	I
Rabbit anti-mouse CA XIVantiserum	1:8,000	A.Waheed/W.S. Sly (**Ochrietor et al., 2005**)	I
Rat anti-keratin 8 (Troma-1), monoclonal	1:3000	Developmental Studies Hybridoma Bank, University of Iowa	II, III
Rat anti-LAMP-1 (clone 1D4B), monoclonal	1:40,000; 1:50,000	Santa Cruz Biotechnology	I
Rat anti-LAMP-2 (clone 6A430), monoclonal	1:1,000	Santa Cruz Biotechnology	I

4. Results

The main findings in the three studies are summarized below.

4.1 Study I

Although previous studies showed presence of carbonic anhydrase (CA) activity (**Dogterom and Bronckers, 1983; Sugimoto et al., 1988**) and CA II protein (**Toyosawa et al., 1996**) in rodent tooth sections, as well as expression of transcripts encoding various CAs in tissue extracts from developing rodent teeth (**Lin et al., 1994; Smith et al., 2006; Lacruz et al., 2010a; Simmer et al., 2010**), the expression patterns of CAs during the different stages of odontogenesis and the identity of the dental cells that express CAs remained largely unknown. To determine where and when CAs are expressed during tooth development, we studied the distribution patterns of eight CAs (CA II/*Car2*, CA II, CA IV, CA VI/*Car6*, CA IX, CARP XI, CA XIII and CA XIV) in mouse teeth during different stages of tooth formation.

Antibodies against the CAs studied are described in Table 1 shown above as well as in study I. The specificities of the antibodies have been tested by the manufacturers and/or in previous studies. We further tested anti-CA specificities in non-dental tissues that have been previously shown to express CAs (**Fig. S1**) as well as by omitting the primary antibodies or by substituting the primary antibodies with pre-immune sera (**Fig. S2**). Furthermore, two different antibodies targeting CAIX, CA XIII or CA XIV were used.

We found that at embryonic stage 12.5 (E12.5), when the embryonic tooth is at the placodal stage, CA XIII was the only CA isoenzyme detectable in both the dental epithelium and the dental mesenchyme (**Fig. 1** and **Table S1**). At E13.5, when the tooth is at the bud stage, in addition to CA XIII, the dental epithelium and the condensed dental mesenchyme also displayed CA II and CA VI immunostaining (**Fig. 1** and **Table S1**). CA II, CA VI and CA XIII, were the only CA isoenzymes detectable at the cap stage (E14.5) of odontogenesis. At this stage, strong and weak hybridization signals of CA II (*Car2*) and CA VI (*Car6*) transcripts, respectively, were detectable in both the dental epithelium and the dental mesenchyme (**Fig. 3**). At the early bell stage, *Car2* hybridization signals underwent an increase in the dental papilla mesenchyme, and *Car6* transcripts were also detectable in both the dental epithelium and dental papilla mesenchyme (**Fig. 1**).

Sections across molar teeth at the differentiation stage (bell stage in molars) as well as sections across different anterior-posterior levels of incisor teeth enable analyses of differentiated ameloblasts and odontoblasts that secreted enamel and predentin/dentin matrices, respectively, as well as newly differentiated odontoblasts and the non-differentiated, proliferating precursors of ameloblasts and odontoblasts (preameloblasts and preodontoblasts). Immunostaining revealed expression of several CA isoenzymes in different dental cells at the cytodifferentiation stage. In the epithelial enamel organ, preameloblasts facing predentin secreted by newly differentiated odontoblasts displayed weak immunostaining for CA II, CA III, CA VI, CA IX, CARP XI and CA XVI, and strong immunoreactivity for CA XIII (**Fig. 2** and **Table S1**). Secretory ameloblasts expressed all eight CAs but with varying staining intensities, and *in situ* hybridization revealed that these cells express *Car2* and *Car6* (**Fig. S3** and **Table S1**). Other cells of the epithelial enamel organ, including cells of the stratum intermedium, stellate reticulum, inner dental epithelium and outer dental epithelium showed weak immunostaining for some CA isoenzymes, and the stratum intermedium was strongly labelled with anti-CA IX (**Fig. 2, Fig. S3** and **Table S1**). All cells of the epithelial enamel organ were positive for CA XIII, and the inner dental epithelium, preameloblasts and secretory ameloblasts exhibited the strongest CA XIII immunostaining (**Fig. 2** and **Table S1**).

Preodontoblasts and cells of the dental papilla mesenchyme showed immunoreactivities for CA II, CA VI and CA XIII, and CA XIII staining was stronger in preodontoblasts than in dental papilla cells (**Fig. 2** and **Table S1**). Newly differentiated odontoblasts that secreted predentin displayed robust CA II, CA XIII and CA XIV immunostaining, moderate immunoreactivities for CA VI and CARP XI, and weak CA IX staining (**Fig. 2** and **Table S1**). Interestingly, in incisor teeth, newly differentiated odontoblasts and odontoblasts (cells that secrete both predentin and dentin components) in the root analog of the tooth expressed CA III, whereas these cell types in the crown analog of the tooth were CA III-negative (**Fig 2, Fig S2** and **Table S1**). Furthermore, in molar teeth at advanced stages of development (12 dpp), while odontoblasts within the tooth's crown were CA III-negative, odontoblasts within the roots were strongly labelled with CA III antibody (**Fig. 3, Fig. S2** and **Table S1**). Compared to newly differentiated odontoblasts, odontoblasts expressed all eight CA isoenzymes (except crown/crown analog odontoblasts that were CA III-negative), and immunoreactivities for CA II, CA III, CA VI, CA XIII and CA XIV were the strongest (**Fig. 3, Fig. 4, Fig. S2** and **Table S1**). In addition these cells displayed strong and moderate hybridization signals for *Car2* and *Car6*, respectively (**Fig. S3**).

At 12 dpp, secretory ameloblasts in the main cusps of the first and second molars cease enamel secretion, and after a transition stage during which some ameloblasts undergo apoptosis while the remaining ones lose their Tomes' processes and exhibit a patent decrease in size, these cells undergo cytological and functional changes that enable them to carry out functions crucial for enamel

maturation; these cells are known as maturation-stage ameloblasts (MA). At the maturation stage of amelogenesis, cells of the stratum intermedium, stellate reticulum and outer dental epithelium form the papillary layer adjacent to MA.

Transition-stage ameloblasts expressed all eight CAs with varying intensities of immunolabelling (**Fig. 3, Fig. 4** and **Table S1**). These cells were also *Car2*- and *Car6*-positive (**Fig. S3**). Remarkably, while MA showed moderate CA IV immunostaining, they exhibited robust immunolabelling with antibodies targeting the other CAs tested (**Fig. 3, Fig. 4** and **Table S1**). In addition, MA exhibited high levels of *Car2* and *Car6* expression (**Fig. S3**). A closer look, revealed differences in the subcellular distributions of CA IV, CA IX and CARP XI between the ruffle-ended (RMA) and smooth-ended (SMA) MA. While these CAs displayed homogeneous distributions in SMA, they were apparently confined to the ruffled border of RMA (**Fig. 3** and **Fig. 4**). At the maturation stage, the papillary layer (PL) abutting MA exhibited intense CA II and CA XIII immunostaining and was stained weakly with antibodies targeting CA VI, CA IX, CARP XI and CA XIV. CA III immunolabeling was readily detectable in the PL abutting the RMA but was virtually absent in the PL adjacent to SMA (**Fig. 3** and **Table S1**).

Interestingly, the epithelial rests of Malassez (ERM) displayed high levels of CA II/*Car2* expression and moderate staining for CA XIII (**Fig. 5** and **Table S1**), and these cells, together with other epithelial and mesenchymal cells of teeth, displayed CA activity as revealed by histochemistry (**Fig. 5**).

Importantly from tooth initiation to advanced postnatal stages, CA XIII protein detected with two different antibodies was consistently found to be confined mainly to intracytoplasmic punctae in all dental cells (**Figs. 1, Fig. 2, Fig. 4** and **Fig. S4**), and this staining pattern mimicked that of the lysosomal proteins LAMP1 and LAMP2 (**Fig. 6** and **Fig. S4**). Furthermore, punctate patterns of CA XIII staining were also readily visible in sections from non-dental tissues, including the kidney and various cephalic structures (**Fig. S1** and **data not shown**).

While assessing the expression patterns of CAs during tooth development, we discovered several novel sites previously not known to express CAs. These include the notochord and nucleus pulposus which, at E12.5 exhibited high CAII /*Car2* expression levels and CA VI immunostaining.

4.2 Study II

The role of SHH signaling in the developing tongue *in vivo* is, to a large extent, unclear. Previous work in embryonic rodent tongues cultivated *in vitro* showed that SHH signaling inhibits fungiform papilla development (**Hall et al., 2003, Liu et al., 2004; Mistretta el al., 2003**). However, it is unclear whether the SHH signaling inhibitors used in those experiments inhibit SHH signaling in the lingual epithelium (LE), in the lingual mesenchyme (LM) or in both tissues. Ablation of SHH signaling in the LM through Wnt1-CRE-mediated deletion of the *Smo* gene in *Wnt1-CRE/Smo$^{n/f}$* mutant mice has been shown to lead to development of an abnormally small and cleft tongue (**Jeong et al., 2004**). However, it is unclear whether in these mutants the tongue forms taste buds. To shed light on the role of SHH signaling during tongue development *in vivo*, we studied mutant mice in which SHH signaling is ablated in the LE, LM or in both the LE and the LM. We also complemented our *in vivo* genetic analyses by *in vitro* approaches in tongue organ cultures.

SHH signaling in the LE controls anterior-posterior patterning, cell fate specification and epithelial differentiation, and SHH signaling in the LM regulates tongue growth and morphogenesis

We generated mutant mice (*ShhGFPCRE/Smo$^{f/f}$*) lacking SHH signaling specifically in the LE through ablation of the *Smo* gene in SHH expressing cells and their progeny as described in Materials & Methods. We showed that *Cre* activity, visualized by β-galactosidase histochemistry, is robust and that it is confined to the LE (**Fig. S1**). Thus *Smo* gene removal in the *ShhGFPCRE/Smo$^{f/f}$* mutant tongues is expected to occur in the LE. In the *ShhGFPCRE/Smo$^{f/f}$* mutant mice the LE continues to express *Shh*, however, it is unable to respond to SHH signals, whereas the LM continues to receive SHH signaling from SHH emanating from the LE. We confirmed loss of SHH signaling in the LE of the mutants by *in situ* hybridization (ISH) for *Ptch1* and *Gli1* as well as by RT-qPCR for *Ptch1* (**Fig. S1**), as expression of these genes indicate cells that respond to Hedgehog signaling (**McMahon et al., 2003**). Furthermore, in the *ShhGFPCRE/Smo$^{f/f}$* mutants the LM expressed *Ptch1* and *Gli1*, confirming intact SHH signaling in this tissue (**Fig. 1**).

To determine the impact of loss of SHH signaling in the LE of the *ShhGFPCRE/Smo$^{f/f}$* mutants on tongue development, we assessed tongue sections after histological staining (alcian blue van Gieson), immunohistochemistry and ISH. We found that while the *ShhGFPCRE/Smo$^{f/f}$* mutant tongues were of normal size, they displayed severe histological changes in the LE. These include loss of filiform papillae and development of abnormal foci made of a thickened epithelium that lost expression of Keratin 8, Keratin 6 and Keratin 15 (**Fig. 1**)

The tongue in humans and mice normally harbors minor salivary glands in its posterior part (**Fig. 1; Hamosh and Scow, 1973; Jitpukdeebodintra et al., 2002**): (1) the serous type von Ebner's glands, which develop from the epithelium of the circumvallate papilla at the border between the anterior and posterior parts of the tongue, and (2) the sero-mucous type posterior lingual glands that form in the posterior segment of the tongue (pharyngeal tongue). Surprinsingly, we found that the *ShhGFPCRE/Smo$^{f/f}$* mutant tongues formed heterotopic sero-mucous glands in the anterior tongue (oral tongue), indicating glandular metaplasia of the LE. Furthermore, in the *ShhGFPCRE/Smo$^{f/f}$* mutant tongues von Ebners glands were not only overgrown, they also transformed into a sero-mucous type, as indicated by presence of cells stained with alcian blue (**Fig. 1**). Alcian blue is known to stain mucous cells (for example cells that contain mucopolysaccharides) (**Bancroft and Stevens, 1990**). Despite the severe alterations of the LE of the *ShhGFPCRE/Smo$^{f/f}$* mutants, taste buds, identified by immunostaining for Keratin 8 (K8) and SOX2 (**Knapp et al., 1995; Okubo et al., 2006**), were readily visible (**Fig. 2**). These findings indicate that loss of SHH signaling in the LE causes abnormal anterior-posterior patterning of the LE, and leads to disrupted cell fate specification in the LE and to altered epithelial differentiation.

Next, we ablated the *Shh* gene using the tamoxifen (TAM)-inducible *ShhCreER^{T2}* knockin allele as described in Materials & Methods. Exposure of embryos to TAM *in utero* is expected to lead to ablation of the *Shh* gene in the *ShhCreER^{T2}/Shh^{f}* mutants. As *Shh* is expressed in the LE and SHH protein signals in the LE and to the LM (**Hall et al., 1999; Jeong et al., 2004; Jung et al., 1999; Xavier et al., 2016**), loss of *Shh* in the *ShhCreER^{T2}/Shh^{f}* mutants is expected to cause loss of SHH signaling in both the LE and LM. Indeed, ISH showed that in *ShhCreER^{T2}/Shh^{f}* mutant embryos that were first exposed to TAM at E10.5 (E10.5 TAM-exposed or E10.5 TAM-induced embryos/tongues), the tongue displayed severe downregulation of *Gli1* in the LE and LM, and these mutants lost SHH protein in the LE (**Fig. 4**). Loss of SHH signaling in the *ShhCreER^{T2}/Shh^{f}* mutant tongues was also confirmed by RT-qPCR for *Ptch1* (**Fig 4**).

Comparison between tongues from E10.5 TAM-exposed control and *ShhCreER^{T2}/Shh^{f}* mutant embryos revealed that the mutant tongues were severely reduced in size and were cleft in their anterior part (bifid tongue) (**Fig. 4**). However, the LE of these mutant tongues formed taste buds as revealed by ISH with a *Shh* probe that recognizes both the deleted (*exon2*) and the non-deleted alleles of the *Shh* gene, as well as by immunostaining for K8 (**Fig. 4**).

The *Wnt1-CRE/Smo$^{n/f}$* mutants in which SHH signaling is lost specifically in the LM also display bifid tongues that are severely decreased in size (**Jeong et al., 2004**). We found that like the E10.5 TAM-induced *ShhCreER^{T2}/Shh^{f}* mutant tongues, the *Wnt1-CRE/Smo$^{f/f}$* mutant tongues formed taste buds visualized by K8 immunostaining (**Fig. S2**). These data indicate that the E10.5 TAM-induced

ShhCreER^{T2}/Shh^{f} mutant embryos and the *Wnt1-CRE/Smo$^{f/f}$* mutants display overlapping tongue anomalies.

We also found that taste buds develop in tongues from *ShhCreER^{T2}/Shh^{f}* mutant embryos that were first exposed to TAM at E11.5. In tongues from these mutants, we confirmed ablation of *Shh* in the LE by ISH for for *Shh* (the *Shh* probe used targets *exon2* of the *Shh* gene, the deleted allele in the mutants). As expected, in these mutants, SHH signaling is lost in both the LE and the LM, and this was evidenced by ISH for *Gli1* (**Fig. 5**). The taste buds in the E11.5 TAM-induced *ShhCreER^{T2}/Shh^{f}* mutant and control tongues were revealed by ISH with a probe targeting both the deleted and non-deleted alleles of the *Shh* gene, as well as by immunostaining for K8 and for SOX2. In contrast to the E10.5 TAM-induced *ShhCreER^{T2}/Shh^{f}* mutant embryos, the E11.5 TAM-induced *ShhCreER^{T2}/Shh^{f}* mutants developed tongues of normal size and shape (**Fig. 5**).

Taken together, these data demonstrate that SHH signaling within the LM is required for normal growth and morphogenesis of the tongue and that taste bud formation is not dependent on SHH signaling in the LM.

To determine whether in the *ShhGFPCRE/Smo$^{f/f}$* mutant tongues as well as in the E10.5 or E11.5 TAM-induced *ShhCreER^{T2}/Shh^{f}* mutant tongues taste buds were innervated by gustatory nerves, we processed tongue sections for K8/P2X2 double immunostaining. We found that in all the above mutants taste buds were innervated by P2X2-positive neurites, indicating that loss of SHH signaling has no effects on taste bud innervation by nerves transducing taste stimuli (**Fig. 3, Fig. 4, Fig. 5, Table S1 and Table S2**).

In contrast to the *ShhGFPCRE/Smo$^{f/f}$* mutant tongues, the E10.5 or E11.5 TAM-induced *ShhCreER^{T2}/Shh^{f}* mutant tongues did not exhibit glandular metaplasia (**Fig. 4** and **Fig. 5**). These findings suggest that development of the heterotopic glands requires influences from the LM that are dependent on SHH signaling in this tissue.

SHH signaling in the LE is required to prevent epithelial cells from adopting a Merkel cell fate

While assessing development of taste buds in the *ShhGFPCRE/Smo$^{f/f}$* mutant tongues using K8 and SOX2 staining, we detected numerous K8-positive and SOX2-postive single cells in the basal layer of the LE (**Fig. 2**). These cells could be either taste bud cells or Merkel cells, since both cell types share several molecular markers, including K8 and SOX2. To distinguish between the two cell types, we carried out double immunofluorescence staining for K8 together with markers that are specific to taste bud cells (SHH) or Merkel cells (Rab3c). We also identified Homer1, a scaffolding protein (**Shiraishi et al., 2004**), as a new marker for taste bud cells; we thus used Homer1 immunostaining as well. Our analyses showed that the single cells in the basal layer of the LE of the mutants

were Merkel cells and not taste bud cells (**Fig. 2 and Table S1**), and that these ectopic Merkel cells were innervated by non-gustatory neurites (**Fig. 2 and Table S1**). We also detected Merkel cells in the LE of the E10.5 TAM-induced mutant tongues (**Fig. 4**). Thus loss of SHH signaling in the LE causes epithelial progenitors to adopt a Merkel cell identity, leading to Merkel cell metaplasia in the LE.

SHH signaling in the LE controls cell fate specification and patterning of the LE by preventing epithelial cells to form taste placodes

In vitro manipulation of the SHH pathway in rodent tongues showed that SHH signaling inhibits fungiform placode (FP) formation (**Hall et al., 2003; Mistretta et al., 2003; Iwatsuki et al., 2007; Liu et al., 2004**). It remained however, unclear whether SHH signaling in the LE, LM or in both these lingual tissues is behind inhibition of FPs. Furthermore, the mechanisms by which SHH inhibit FP formation are not fully elucidated. FPs are localized epithelial thickenings in the embryonic tongue, and are made of progenitors of taste buds (**Mistretta and Liu, 2006**)). To determine the *in vivo* role of SHH signaling during FP patterning and identify the tissue in which SHH signaling operate to control FP formation, we assessed tongues from control and mutant mice after ISH for *Shh* (and SHH immunostaining) and *Wnt10b*, well-established taste placode markers (**Barlow and Klein; 2015**), as well as after immunostaining for the taste bud markers SOX2 and/or K8. We also used ISH and immunostaining to detect taste buds, as these structures are known to express *Shh* transcripts and SHH protein (**Barlow and Klein; 2015**).

We found that the *ShhGFPCRE/Smo$^{f/f}$* mutant tongues (**Fig. 3**) and the E11.5 TAM-induced *ShhCreER^{T2}/Shh^{f}* mutant tongues (**Fig. 5**) displayed large areas harboring numerous FPs and taste buds, and formed abnormally enlarged FPs and taste buds. This was in contrast to the control tongues which displayed the expected spacing and arrangement of FPs and taste buds (**Fig. 3 and Fig. 5**). Quantification of *Shh*-positive spots that represent FPs or taste buds in whole-mount tongues from *ShhGFPCRE/Smo$^{f/f}$* mutants and from E11.5 TAM-induced *ShhCreER^{T2}/Shh^{f}* mutants, as well as from their respective control littermates, revealed that the mutant tongues exhibit increased numbers of *Shh*-positive spots. Furthermore, quantification of the number of K8-positive cell clusters representing taste buds or part of taste buds in fungiform papillae of E18.5 tongues, revealed that the tongues from E11.5 TAM-induced *ShhCreER^{T2}/Shh^{f}* mutant embryos display an increased number of K8-positive cell clusters per section as compared to tongues from control embryos. These data show that loss of SHH signaling leads to an increase in the number and size of FPs and taste buds.

In the murine embryonic tongue, FP formation normally occurs between E12.5 and E14 (**Mistretta and Liu, 2006**). Thus, after E14.5 no new FPs are formed.

Surprisingly, we found that tongues from *ShhGFPCRE/Smo$^{f/f}$* mutants, as well as tongues from *ShhCreER^{T2}/Shh^{f}* mutant embryos that have been first exposed to TAM at E10.5 or E11.5, all exhibited taste placodes well after cessation of the normal period of FP formation. This was revealed by ISH for *Shh* and/or by SHH immunostaining, as well as by ISH for *Wnt10b* (**Fig. 6**). These data indicate that loss of SHH signaling leads to *de novo* induction of taste placodes, and that SHH signaling, operating strictly in the LE, controls patterning of FPs and formation of taste buds. Furthermore, our findings show that SHH signaling not only inhibits FP and taste bud formation during the active period of FP paterning, confirming previous findings in tongue organ cultures (**Hall et al., 2003; Mistretta et al., 2003; Iwatsuki et al., 2007; Liu et al., 2004**), but also prevents progenitors in the LE to continuously form taste placodes after the period of FP formation has ceased.

SHH signaling is required during a limited period (before E12.5) to control tongue growth and morphogenesis and patterning of the LE and cell fate specification in this tissue

We took advantage of the TAM-inducible *ShhCreER^{T2}* allele to determine the period during which SHH signaling is necessary for normal tongue development. We found that in contrast to tongues from *ShhCreER^{T2}/Shh^{f}* embryos that have been first exposed to TAM at E10.5 or at E11.5 and tongues from *ShhGFPCRE/Smo$^{f/f}$* mutant embryos, tongues from *ShhCreER^{T2}/Smo$^{f/f}$* mutant (TAM-induced removal of the *Smo* gene in the LE) embryos as well as tongues from *ShhCreER^{T2}/Shh^{f}* mutant embryos that have been first exposed to TAM at E12.5 were of normal size and shape, and formed a normally patterned and differentiated epithelium **(Fig. S2)**. Similarly, we observed normal development of tongues from *K14-CRE/Smo$^{f/f}$* mutants in which the *Smo* gene is deleted in the LE (in Keratin-14-expressing cells and their progeny). In the *K14-CRE/Smo$^{f/f}$* mutant tongues, *Smo* gene ablation in the LE occurs at ≈ E13.5, since robust CRE activity, revealed by β-galactosidase histochemistry, was observed at E13.5 **(Fig. S2)**. These findings show that proper tongue growth and morphogenesis, as well as normal patterning of the LE and cell fate specification in this tissue necessitate SHH signaling before E12.5.

SHH signaling controls tongue development by antagoniszing retinoic acid (RA) signaling through the RA-catabolizing enzymes CYP26s

Altogether, our findings show that SHH signaling controls various steps of tongue development, from growth and morphogenesis to patterning of the LE and cell fate specification in the LE. The question that arises is: by which mechanisms does SHH fulfill these functions? We posited that retinoic acid (RA) signaling may be involved in the generation of the tongue anomalies caused by loss of SHH signaling in our mutants. Several lines of evidence point

to involvement of RA. (1) RA (or its precursor vitamin A) is known to be a potent inducer of sero-mucous glandular metaplasia in several epithelia (**Fell & Mellanby, 1953; Lawrence & Bern, 1960; Lawrence et al., 1960; Hardy, 1968; Covant & Hardy, 1988; Blanchet et al., 1998**), and in the *ShhGFPCRE/Smo$^{f/f}$* mutant tongues, the LE underwent sero-mucous glandular metaplasia. (2) Exposure of rodent embryos to excess RA generates tongue anomalies (**Padmanabhan and Ahmed, 1997; Abe et al., 2008; Shenefelt, 1972**) similar to those caused by loss of SHH signaling in *Shh$^{n/n}$* mutants (**Chiang et al., 1996**) as well as in the mutants analysed in this study. These tongue anomalies are aglossia (agenesis of the tongue) as observed in the *Shh$^{n/n}$* mutants, microglossia (decreased size of the tongue) and bifid tongue as observed in *ShhCreER^{T2}/Shh^{f}* mutant embryos that were first exposed to TAM at E10.5 as well as in the *Wnt1-CRE/Smo$^{f/f}$* mutant embryos. (3) Transcripts encoding components of the RA signaling pathway, including the RA receptors (RARs) as well as the RA-synthesizing (RALDHs) and the RA-catabolizing (CYP26) enzymes, have been previously shown to be expressed in the embryonic tongue (**Dollé et al., 1990; 1994; Ruberte et al., 1992; Niederreither et al., 1997; 2002**).

To explore the likelihood of involvement of RA signaling in the generation of tongue anomalies in our mutants, we first assessed the expression patterns and levels of *RARb* and *RARg* (*RARb* and *RARg* encode the RA receptors RARβ and RARγ, respectively), two well-established direct transcriptional targets of RA signaling (**Blomhoff and Blomhoff; 2006)**. Thus, enhanced *RARb* and *RARg* levels indicate enhanced RA signaling in a given tissue. Using ISH in tongues from *ShhGFPCRE/Smo$^{f/f}$* mutants and TAM-induced *ShhCreER^{T2}/Shh^{f}* mutants, we found enhanced *RARb* and *RARg* hybridization signals in the LE of the mutant tongues. In addition, RT-qPCR showed that tongues from the mutants displayed enhanced *RARb* and *RARg* expression levels (**Fig. 7 and Fig. S3**). Furthermore, immunostaining showed that the LE of the *ShhGFPCRE/Smo$^{f/f}$* mutant tongues displayed increased RARγ immunoreactivity, except in epithelial foci which also displayed weak *RARg* hybridization signals (**Fig 7 and Fig. S4**). These data indicate enhanced RA signaling in the LE upon loss of SHH signaling in the mutant tongues. We also found that taste buds expressed *RARg*/RARγ transcripts and protein (**Fig S4**), and that the orthotopic and heterotopic lingual glands in the control and *ShhGFPCRE/Smo$^{f/f}$* mutant tongues, respectively, expressed RARγ protein (**Fig. S4**).

We next showed that the developing tongue is exposed to RA, since we found that from the earliest stages of tongue formation (E11.5) onwards, the LE and/or the LM produce RALDH1, RALDH2 and/or RALDH3 proteins, and that FPs and taste buds expressed RALDH3 and RALDH1 proteins, respectively. Furthermore, the orthotopic lingual glands in the control and *ShhGFPCRE/Smo$^{f/f}$* mutant tongues, as well as the heterotopic glands in the *ShhGFPCRE/Smo$^{f/f}$* mutant tongues also diplayed RALDH1-3 immunostaining. RALDH1-3

immunostaining also revealed that the distribution patterns of RALDH1-3 were, to a large extent, not disrupted in the *ShhGFPCRE/Smo$^{f/f}$* mutant tongues (**Fig. S5** and **Fig. S6**).

The above findings show that enhanced RA signaling upon loss of SHH signaling in the developing tongue is not caused by enhanced or ectopic RA synthesis by RALDHs. RA signaling is subject to rigid regulation through the activities of RALDHs and the RA-catabolizing enzymes CYP26A1, CYP26B1 and CYP26C1 (**White and Schilling, 2008; Pinnimpede et al., 2010**). *Cyp26a1* and *Cyp26c1* are expressed in the LE (**Abu-Abed et al., 2002; Tahayato et al., 2003; De Roos et al., 1999**), whereas *Cyp26b1* expression is confined to the LM (**Abu-Abed et al., 2002**). We therefore used whole-mount ISH and ISH in tongue sections to analyse the expression patterns of *Cyp26a1* and *Cyp26c1* transcripts in tongues from *ShhGFPCRE/Smo$^{f/f}$* mutants, as well as in tongues from *ShhCreER^{T2}/Shh^{f}* embryos that were first exposed to TAM at E10.5 or at E11.5. These analyses were intended to test the hypothesis that enhanced RA signaling in tongues from mutants with loss of SHH signaling is caused by loss of *Cyp26* expression. Indeed, we found that the LE of the mutants displayed a severe downregulation of *Cyp26a1* and *Cyp26c1* expression, except in epithelial foci (**Fig. 8 and Fig. 9**). Interestingly, in tongues from *ShhCreER^{T2}/Shh^{f}* mutant embryos that were first exposed to TAM at E12.5, expression of *Cyp26a1* and *Cyp26c1* was not altered (**Fig. 9**).

Importantly, during the period of FP patterning (between E12.5 and E14), we found that in tongues from control embryos, *Cyp26a*1 and *Cyp26c1* were expressed in the interplacodal LE, *i.e.* the epithelium between FPs, but these genes were not expressed in FPs. Moreover, *Cyp26a1* and *Cyp26c1* transcripts were excluded from the posterior tongue, where the circumvallate papilla and the posterior lingual glands develop (**Fig. 8 and Fig. 9**). In addition, we found that after E14.5, when FPs are normally no longer induced to form, *Cyp26a1* and *Cyp26c1* expression in the LE started to be downregulated (**Fig. 9**). RT-qPCR analysis of *Cyp26b1* showed no alterations of *Cyp26b1* expression levels in the LM of tongues from the *ShhGFPCRE/Smo$^{f/f}$* mutants and tongues from the E10.5 TAM-induced *ShhCreER^{T2}/Shh^{f}* mutants, whereas in tongues from E11.5 TAM-induced *ShhCreER^{T2}/Shh^{f}* mutants *Cyp26b1* expression levels were increased in the LM (**Fig. 9**).

Exposure *in vitro* of explants from control embryos to SAG, an agonist of SMO, enhanced *Cyp26a1* hybridization signals in the tongue, but failed to induce ectopic *Cyp26a1* expression in other mandibular structures (**Fig. 9**). Thus, SHH signaling does not directly induce *Cyp26a1* expression.

Taken together, these findings show that SHH signaling is required for maintenance and/or reinforcement of the expression of *Cyp26a1* and *Cyp26c1*, and that loss of SHH signaling causes enhanced RA signaling in the LE as a result of loss of *Cyp26a1* and *Cyp26c1* expression.

RA signaling promotes and SHH inhibits lingual gland and taste placode formation, and RA signaling is not the cause of Merkel cell metaplasia upon loss of SHH signaling

To determine whether RA signaling is required for lingual gland formation, and whether enhanced RA signaling in the *ShhGFPCRE/Smo$^{f/f}$* mutant tongues causes glandular metaplasia in the LE, we treated *in vitro*-cultivated tongue/mandible explants from controls and mutant embryos with retinoids or with inhibitors of RA signaling. The retinoids used are *all trans*-RA, the RARγ agonist CD1530, and the RARβ agonist CD2314. The inhibitors of the RA signaling pathway used are BMS493, a pan-RAR antagonist, and DEAB, an inhibitor of RA synthesis. DMSO was used as vehicle control. After cultivation, sections from the tongue/mandible explants were processed for K8 immunohistochemistry.

We found that the retinoids induced development of heterotopic glands in tongue explants from control embryos, and inhibitors of RA signaling inhibited development of heterotopic glands in tongue explants from *ShhGFPCRE/Smo$^{f/f}$* mutant embryos. By contrast, the inhibitors of RA signaling were unable to abrogate formation of the thickened epithelial foci and ectopic Merkel cells in the *ShhGFPCRE/Smo$^{f/f}$* mutant explants (**Fig. S7 and Table S3**). We also found that BMS493 inhibited formation of the orthotopic lingual glands (von Ebner's glands and the posterior lingual glands) in tongue explants from control embryos (**Fig. S7 and Table S3**).

These findings show that enhanced RA signaling causes glandular metaplasia in the LE of the *ShhGFPCRE/Smo$^{f/f}$* mutants, and that RA signaling is necessary for development of the orthotopic lingual glands. In addition, the data indicate that the development of epithelial foci and the occurrence of Merkel cell metaplasia in the *ShhGFPCRE/Smo$^{f/f}$* mutant tongues are not due to enhanced RA signaling.

To determine the impact of RA signaling on taste placode formation, we cultivated tongue explants with retinoids or with RA inhibitors and analysed the explants after whole-mount ISH for *Shh* to detect taste placodes. Interestingly, we found that retinoids promoted development of enlarged *Shh*-positive spots, whereas exposure of explants to BMS493 led to failure of formation of *Shh*-positive spots in large areas of the tongues (**Fig. 10 and Table S4**). We also found that in tongue explants from *ShhGFPCRE/Smo$^{f/f}$* mutant embryos, exposure to BMS493 or to DEAB led to the reduction of areas with *Shh*-positive spots (**Fig. 10 and Table S4**). These data show that RA signaling promotes the formation of taste placodes.

Taken together, all these findings show that RA promotes taste placode and lingual gland formation. Furthermore, given the phenotype engendered by loss of SHH signaling in the developing tongues (glandular metaplasia and/or

overproduction of enlarged taste placodes), it could be concluded that SHH signaling inhibits taste placode and lingual gland formation.

Previous work and our present analyses showed that the developing tongue expresses components of the RA signaling pathway. Furthermore, our findings show that the LE responds to RA signaling (analyses of the mutant tongues *in vivo*) and to retinoids (tongue explants cultivated *in vitro*). However, we found that in tongues from control and *ShhGFPCRE/Smo$^{f/f}$* mutant embryos carrying the *RARE-hsp68-LacZ* (also known as *RAREhsplacZ*) transgene, which enable visualization of RA activity (**Rossant et al., 1991**), the LE as well as the orthotopic and heterotopic lingual glands were devoid of β-galactosidase activity. In addition, retinoid treatment of tongue explants from embryos carrying the *RARE-hsp68-LacZ* transgene was unable to induce activity of the *RARE-hsp68-LacZ* transgene in the LE (**Fig. S8**). These findings suggest that the *RARE-hsp68-LacZ* transgene is not active in the LE. In fact, other transgenes that enable visualization of RA activity also failed to reveal RA activity in the LE **(Reynolds et al., 1991; Mendelsohn et al., 1991; Balkan et al., 1992; Colbert et al., 1993)**. It has been suggested that such transgenes fail to visualize RA activity in several tissues and cells known to respond to RA signaling (**Mendelsohn et al., 1994; Siegenthaler et al., 2009; Dollé et al., 2010**).

5. Discussion

5.1 Study I

Our study revealed dynamic expression patterns of CAs during tooth development. Furthermore, our analyses not only confirmed previous findings (**Dogterom and Bronckers, 1983; Sugimoto et al., 1988**) that MA and the PL exhibit CA activity, they also enabled visualization, in tissue sections, of the patterns and subcellular distributions of CAs in these cells. We showed that secretory ameloblasts expressed CA II/*Car2*, CA VI/*Car6*, CA IX, CA XIII and CA XIV, and that newly differentiated odontoblasts and odontoblasts expressed several CAs. We also revealed that the PL expresses various CAs, including CA II/*Car2*.

Enamel maturation requires intact function of MA. These cells undergo cyclical functional and morphological changes as they modulate between two types: the ruffle-ended MA (RMA) displaying deep folds of the apical plasma membrane, and the smooth-ended MA (SMA) exhibiting a smooth apical plasma membrane. Prior work showed that during the various stages of amelogenesis, the enamel matrix is subject to pH shifts. While during enamel secretion the pH values are neutral, they undergo remarkable changes during the maturation stage, with acidic and alkaline values in areas adjacent to RMA and SMA, respectively (**Lacruz et al., 2010b**). These pH variations require a tight control of extracellular pH, and CAs have been incriminated, together with other proteins, in pH regulation of the enamel matrix (**Lin et al., 1994; Josephsen et al., 2010; Lacruz et al., 2010b; Simmer et al., 2010**). CAs are also involved in the regulation of intracellular pH (**Grinstein et al., 1989, Shrode et al., 1997**) in metabolically active cells that express bicarbonate transporters (**Pastorekova et al., 2004; Harju et al., 2013; Hassan et al., 2013**).

It is therefore not a surprise that several CA isoenzymes were expressed in secretory ameloblasts, newly differentiated odontoblasts, odontoblasts and MA, as these metabolically active cells are known to secrete large amounts of extracellular matrices (secretory ameloblasts, newly differentiated odontoblasts, and odontoblasts) and are actively involved in reabsorption of degraded extracellular proteins (odontoblasts and MA) (**Simmer and Hu 2002; Kawashima and Okiji, 2016**).

Normal enamel formation requires adequate cytodifferentiation and function of secretory ameloblasts and MA, and defects in these processes lead to enamel hypoplasia, abnormal enamel maturation or both (**Simmer et al., 2010; Pham et al., 2017**). That CAs are expressed in secretory and MA suggests that they

perform crucial functions in these cells, and that defects in CA function or their absence may impinge upon enamel formation, generating enamel defects. Indeed, some patients with CA II deficiency syndrome have been reported to display enamel hypoplasia and severe tooth decay (**Strisciuglio et al., 1990; Awad et al., 2002; Bosley et al., 2011**). Recently, it has been shown that epithelial deletion of *Dlx3* in mice generates hypomineralized teeth. *Car6* and *Car12* were found to be significantly downregulated in *Dlx3* mutant teeth, and MA exhibited a significant decrease in CA VI protein levels in the *Dlx3* mutant teeth. By contrast, *Dlx3* deletion did not impinge significantly upon the expression levels of *Car2*, *Car3* and *Car13*. It was also found that the promoter region of human *CA6* responds to DLX3 (**Duverger et al., 2017**).

Secreted CA VI may indirectly influence the integrity of dental hard tissues, since CA VI has been shown to bind to the enamel pellicle and to display catalytic activity (**Leinonen et al., 1999; Kimoto et al., 2006**), and in humans, several polymorphisms in the *CAVI* gene have been shown to be associated with susceptibility to tooth caries (**Li et al., 2015**).

Intriguingly, we found that CAs were not only expressed in dental cells involved in secretion and biomineralization of the dental extracellular matrices (ameloblasts and odontoblasts), but also in differentiating as well as in un-differentiated, proliferating cells of the ameloblast and odontoblast cell lineages. Furthermore, we found that other cells of the epithelial enamel organ and dental mesenchyme expressed CAs. These observations, suggest that CAs are involved in regulation of cell proliferation and differentiation of tooth-forming cells, likely through pH regulation, as optimum pH values are required for normal cell proliferation (**Grinstein et al., 1989, Shrode et al., 1997**) and differentiation (**Alonso-Torre et al., 1993; McAdams et al., 1998**). In line with this, CAII has been shown to play a role in ameloblast differentiation in cultured teeth through lowering the intracellular pH (**Wang et al., 2010**), and also in osteoclast differentiation (**Lehenkari et al., 1998**). In several tumours, CA IX expression is upregulated by hypoxia-inducible factor 1, the latter is activated by low oxygen tension and high cell density (**Wykoff et al., 2000; Supuran, 2017**). CA IX has been shown to be required not only for secretory functions in the stomach but also for the regulation of cell proliferation (**Gut et al., 2002**).

Surprisingly, we found that CAIII was expressed in odontoblasts within the roots of molars and root analog of incisors, and that this isoenzyme was undetectable in odontoblasts within the molar crown and odontoblasts in the crown analog of incisors. Why this asymmetrical pattern of CA III expression in odontoblasts takes place is at present unclear. This could be caused by exposure of crown/crown analog and root/root analog preodontoblasts to different influences emanating from nearby dental epithelial cells, i.e. the inner dental epithelium and the epithelial root sheath, respectively (**Luan et al., 2006**).

Interestingly, our analyses revealed that CAII/*Car2* is expressed at high levels in the epithelial rests of Malassez (ERM) at the surface of roots and root analog of molars and incisors, respectively. These ERM also displayed moderate staining for CA XIII. Importantly, these cells exhibited robust CA activity. While the role of ERM remains largely unclear, previous work showed that ERM may contribute to a subset of cementoblasts, cells that produce cementum, a biomineralized tissue that covers the root/root analog (**Li et al., 2017**). It has also been suggested that ERM maintain the width of the periodontal ligament (**Luan et al., 2006**). It seems that the width of the periodontal ligament is affected by the activity of osteoclasts and osteoblasts. CAII deficiency syndrome in humans is associated with osteopetrosis and cerebral calcifications (**Venta et al, 1991**), and CAII is crucial for the regulation of osteoclast intracellular pH and bone resorption (**Lehenkari et al., 1998**). In addition, in human osteocyte-like cells, it has been shown that *Car2* expression is upregulated by Sclerostin, and findings in these cells suggest involvement of CA II in the regulation of bone mineral homeostasis (**Kogawa et al, 2013**). These observations suggest that CAII may have a role in regulating the width of the periodontal ligament. Whether *Car2*-deficient mice (**Lewis et al., 1988; Margolis et al., 2008**) have abnormal roots/root analog is not known, and it is worth investigating. There could be compensation by other CAs, such as CA XIII that might mitigate a root phenotype in *Car2* mutant mice.

We also uncovered a hitherto unknown subcellular localization of CA XIII not only in all cells of teeth, but also in cells within several non-dental tissues. Analyses with two different antibodies revealed that CA XIII is mainly localized in intracytoplasmic vesicles in cells of all tissues analysed, and CA XIII immunostaining patterns largely overlapped with immunostaining for the lysosomal membrane proteins LAMP1 and LAMP2 in developing teeth. LAMP-1 and LAMP-2 constitute about 50% of the lysosomal membrane proteins (**Ruivo et al., 2009**)

Previous studies reported presence of CA activity and CA proteins in lysosomes of leukocytes (**Rikihisa, 1985**), osteoclasts (**Anderson et al., 1982; Toyosawa et al., 1989**) and liver cells (**Iritani and Wells; 1974**), however the identity of the CAs in lysosomes remained unknown. It is noteworthy that immunostaining with a CA XIII antibody different from the two antibodies we used also revealed staining in intracytoplasmic vesicles in cultured cells (www.proteinatlas.org). Taken together with our findings, these observations suggest that lysosomes harbor CAs, and that within these organelles CAs may be involved in the regulation of pH. Further studies are required to confirm the presence of CA XIII in lysosomes. These would necessitate subcellular fractionations to isolate lysosomes, rigorous testing of the purity of the lysosomal fraction, and advanced assays such as mass spectrometry.

Altogether, our findings are expected to be of value for future work aiming at deciphering the role of CAs during tooth development.

5.2 Study II

In this study, we used an *in vivo* genetic approach and complementary assays in embryonic tongues cultivated *in vitro*. Our investigations enabled us to reveal hitherto unknown roles for SHH signaling during tongue development, and to decipher how SHH works to drive normal tongue development.

SHH signaling in the lingual mesenchyme before E12.5 is required for normal tongue growth and morphogenesis

We showed that loss of SHH signaling in the lingual epithelium (LE) of mutant mice lacking the *Smo* gene (*ShhGFPCRE/Smo$^{f/f}$*) in this tissue leads to abberrations in the LE without affecting tongue growth. By contrast, temporally-controlled ablation of SHH signaling in the LE and in the lingual mesenchyme (LM) by removal of the *Shh* gene in *ShhCreER^{T2}/Shh^{f}* mutant embryos that have been first exposed to tamoxifen (TAM) at E10.5 causes development of an abnormally small and bifid tongue. Similarly, genetic removal of SHH signaling in the LM of *Wnt1-CRE/Smo$^{f/f}$* mutant mice leads to formation of a small and cleft tongue. These findings indicate that SHH, operating mainly in the LM, is required for normal tongue growth and morphogenesis, and are somewhat similar to those reported for the developing secondary palate, where SHH activity in the palatal mesenchyme is necessary for normal growth of the palatal shelves **(Rice et al., 2004; Lan and Jiang, 2009**).

The occurrence of bifid tongue in humans with Ellis-van Creveld syndrome caused by mutations of the *EVC* and *EVC2* genes, the products of which are required for normal Hedgehog signaling (**Nakatomi, 2009; Dorn et al., 2012; Yang et al., 2012; Caparrós-Martín et al., 2013**), and in the E10.5 TAM-induced *ShhCreER^{T2}/Shh^{f}* mutant embryos, strongly suggests that SHH signaling performs similar functions in humans and in mice to drive tongue morphogenesis.

We also showed that SHH signaling is required during a limited period for normal growth and morphogenesis of the tongue. Indeed, we found that loss of SHH signaling in tongues from *ShhCreER^{T2}/Shh^{f}* mutant embryos that have been first exposed to TAM at E11.5 or at E12.5, the tongues were of normal size and shape. Thus, SHH signaling before E12.5 is required for proper growth and morphogenesis of the tongue. Our findings not only confirmed previous work in rodent tongue organ cultures *in vitro* that showed that loss of SHH signaling during early stages of tongue formation causes abnormal growth of the tongue, and that loss of SHH signaling at more advanced stages has no effects on tongue growth (**Liu et al., 2004)**, they also revealed that the LM is the main tissue in which SHH signaling operate to ensure formation of a tongue with adequate size and shape.

We found that the cause of enhanced RA signaling in the developing tongue from *ShhCreER^{T2}/Shh^{f}* mutants that have been first exposed to TAM at E10.5 is due to loss of *Cyp26a1* and *Cyp26c1* expression in the LE. The LM of these mutants did not show significant alterations of *Cyp26b1* expression levels. The decreased degradation of RA in the LE of the mutant tongues led to enhanced RA signaling in this tissue as shown in Figs. 7 and S3. Since RA is a highly diffusible and potent small molecule, we cannot exclude the possibility that in these mutants, due to elevated amounts of RA in the LE, RA may also diffuse to the LM, leading to a slight enhancement of RA signaling (despite unchanged *Cyp26b1* expression levels) in this tissue that is not readily visible by ISH for *RARb* and *RARg*. This may have an impact on the SHH signaling-deficient mesenchyme.

In the *Shh$^{n/n}$* mutant embryos, the tongue fails to form (aglossia) (**Chiang et al., 1996**). Furthermore, the *Wnt1-CRE/Smo$^{f/f}$* mutant embryos develop severe microglossia and tongue clefting. These defects are more severe than those observed in tongues from *ShhCreER^{T2}/Shh^{f}* mutant embryos that have been first exposed to TAM at E10.5. This is expected, since in the *Shh$^{n/n}$* mutants and in the *Wnt1-CRE/Smo$^{f/f}$* mutants, loss of SHH signaling occurs during earlier stages of embryogenesis than in the E10.5 TAM-induced *ShhCreER^{T2}/Shh^{f}* mutant embryos. Indeed *Shh* gene ablation in the *Shh$^{n/n}$* mutant embryos occurs within the germline. This means that all cells that will form the body are devoid of the *Shh* gene. Therefore, cell or tissues that normally express *Shh* in control animals, will be unable to express *Shh* in the *Shh$^{n/n}$* mutant embryos. In oro-facial primordia, *Shh* is normally expressed in epithelia (**Echelard et al., 1993**). In the *Wnt1-CRE/Smo$^{f/f}$* mutants, the *Smo* gene is ablated in neural crest cells that generate cranio-oro-facial primordia, including those that form the tongue mesenchyme.

The severe tongue anomalies in the *Shh$^{n/n}$* and *Wnt1-CRE/Smo$^{f/f}$* mutant embryos are likely due to diminished proliferation and/or to enhanced death (by apoptosis) of the neural crest cell (NCC)-derived mesenchyme of the tongue primordium. Supporting this notion is the fact that SHH signaling is known to be required for survival of NCCs and of NCC-derived cells, including mesenchymal cells in cranio-oro-facial primordia (**McMahon et al., 2003**).

Exposure of mouse embryos to excess RA at E8 causes aglossia or microglossia (**Padmanabhan and Ahmed, 1997**), and mouse embryos exposed to excess RA at E8.5 develop microglossia and bifid tongue (**Abe et al., 2008**). Since at E8 and E8.5 the embryonic tongue is not yet formed in mouse embryos, these findings suggest that the tongue phenotypes generated by overexposure to RA might be a result of the effects of RA on NCCs that form the mesenchyme of the embryonic tongue. This notion is supported by previous findings indicating that genetically-induced enhancement of RA signaling or excess retinoids impinge

upon migration (**Yasuda et al., 1989; Uehara et al., 2007)** and survival (**Melnik, 2017**) of NCCs.

It remains thus to be determined whether the severe tongue anomalies in the *Shh*$^{n/n}$ and *Wnt1-CRE/Smo*$^{f/f}$ mutants are due to enhanced RA as a result of loss of SHH signaling. The oral tongue develops from the first branchial arch (mandibular arch), and the posterior one third of the tongue forms from cells emanating from the second, third and fourth branchial arches **(Sadler, 2015**). Notably, in mouse embryos *Cyp26a1* is expressed in the epithelium of the mandibular arch as well as in branchial pouches (**de Roos et al., 1999**), and *Cyp26c1* is expressed in both the epithelium and mesenchyme of the mandibular arch (**Tahayato et al., 2003**). We showed that RALDH1-3 are expressed in the tongue primordium (**Fig. S5**). *Shh* is expressed in the epithelium of the mandibular arch as well as in the epithelium of branchial pouches (**Jeong et al., 2004**; **Moore-Scott et al., 2005**), and SHH signaling in the epithelium and mesenchyme is crucial for proper development of the branchial arches (**Jeong et al., 2004**; **Moore-Scott et al., 2005**). It has been shown that the *Shh*$^{n/n}$ mutant embryos exhibit atrophy of all branchial arches, agenesis of the first branchial pouch, as well as atrophy of the second, third and fourth branchial pouches (**Moore-Scott et al., 2005**). All these observations indicate that *Cyp26a1* and *Cyp26c1* are expressed in branchial arch structures that respond to SHH signaling. It would thus be interesting to determine whether in the *Shh*$^{n/n}$ mutant embryos, the expression *Cyp26a1* and *Cyp26c1* in the branchial arch apparatus is lost, and whether this leads to enhanced RA signaling. In such a scenario, enhanced RA signaling, due to locally enhanced RA availability, combined with maternally-derived RA, might affect tongue development in the *Shh*$^{n/n}$ mutants. In the *Wnt1-CRE/Smo*$^{f/f}$ mutant embryos, analyses of the expression patterns of *Cyp26a1*, *Cyp26b1* and *Cyp26c1*, as well as the expression levels of *RARb* and *RARg* during early stages of tongue development is a necessary first step to determine whether the tongue phenotype is caused by enhanced RA.

SHH and RA signalings exhibit antagonistic activities and regulate anterior-posterior patterning of the LE and cell fate specification in this tissue

SHH signaling is involved in patterning of a wide range of tissues and organs (**McMahon et al., 2003**). For example, SHH inputs are required for ventralizing the neural tube (**McMahon et al, 2003**), proper anterior-posterior patterning of digits (**Harfe et al., 2004**) and for the regulation of left-right asymmetry during early embryogenesis (**McMahon et al., 2003**). RA is also a powerful molecule involved in embryonic patterning (**Duester, 2008; Niederreither and Dollé 2008; Mark et al., 2009**), including anterior-posterior patterning of the hindbrain (**White and Schilling, 2008**).

Normally, minor salivary glands develop from the LE at the border between the oral tongue and the pharyngeal tongue (von Ebner's glands) and from the LE of the pharyngeal tongue (posterior lingual glands). We showed that SHH signaling, acting strictly in the LE, is required for proper anterior-posterior patterning of the LE and cell fate specification in this tissue. Indeed, the SMO-deficient LE of the *ShhGFPCRE/Smo$^{f/f}$*mutant embryos underwent glandular metaplasia revealed by formation of heterotopic sero-mucous glands in the oral tongue. It is noteworthy that neither humans nor mice form minor salivary glands in the oral tongue. Our molecular analyses in the *ShhGFPCRE/Smo$^{f/f}$* mutant tongues revealed that loss of SHH signaling leads to enhanced RA signaling in the LE as a result of loss of *Cyp26a1* and *Cyp26c1* expression. We also showed that *in vitro* exposure of tongue explants from control embryos to retinoids engenders glandular metaplasia in the oral tongue, whereas inhibitors of RA signaling abrogate development of glandular metaplasia in tongue explants from *ShhGFPCRE/Smo$^{f/f}$* mutant embryos. Furthermore, we showed that *in vitro* inhibition of RA signaling in cultivated tongues from control embryos leads to failure of development of the orthotopic lingual glands. Moreover, our *in situ* hybridization analyses showed that *Cyp26a1* and *Cyp26c1* are not expressed in the posterior part of the tongue, where von Ebner's glands and posterior lingual glands develop. Taken together, these findings show that SHH inhibits, whereas RA promotes the formation of lingual minor salivary glands, and that SHH inhibits minor salivary gland formation in the oral tongue by antagonizing RA signaling through maintenance of *Cyp26a1* and *Cyp26c1* expression. Thus antagonistic SHH and RA activities are involved in anterior-posterior patterning of the LE and in the control of cell fate determination in this tissue.

We also found that in the *ShhGFPCRE/Smo$^{f/f}$* mutant tongues, in addition to being overgrown, von Ebner's glands underwent transformation from a serous type into a sero-mucous type. As we found that the circumvallate papilla from which von Ebner's glands develop does not express *Cyp26a1* and *Cyp26c1* transcripts, we can conclude that mucous metaplasia of von Ebner's glands is caused by supraphysiological levels of RA emanating from the LE of the oral tongue, *i.e.* the epithelium anterior to the circumvallate papilla.

It is well established that retinoids are capable of inducing sero-mucous glandular metaplasia in numerous epithelia, including whisker and feather follicles (**Fell & Mellanby, 1953; Lawrence & Bern, 1960; Lawrence et al., 1960; Hardy, 1968; Covant & Hardy, 1988; Blanchet et al., 1998**). These observations, together with our data, further support our conclusions that enhanced RA signaling is behind the sero-mucous glandular metaplasia that takes place in the epithelium of the *ShhGFPCRE/Smo$^{f/f}$* mutant tongues.

In contrast to the *ShhGFPCRE/Smo$^{f/f}$* mutant tongues, tongues from *ShhCreER^{T2}/Shh^{f}* mutant embryos that have been first exposed to TAM at E10.5 or at E11.5 did not undergo glandular metaplasia. These results suggest that for

glandular metaplasia to occur, SHH signaling should be intact in the LM, and this was the case in the *ShhGFPCRE/Smo$^{f/f}$* mutant tongues. By contrast in the TAM induced *ShhCreER^{T2}/Shh^{f}* mutant tongues, SHH signaling is lost in both the LE and LM. This is reminiscent of the effects of loss of SHH signaling in the developing skin and hair follicles. Glandular metaplasia in the epidermis and epithelium of hair follicles was found to require SHH-dependent mesenchymal inputs, since unlike *K14-CRE/Smo$^{f/f}$* mutant mice which exhibited glandular metaplasia, *K14-CRE/Shh$^{f/f}$* mutants did not develop this anomaly (**Gritli-Linde et al., 2007**).

Our experiments in tongue organ cultures *in vitro* showed that RA signaling is required for lingual gland formation, as inhibition of RA signaling caused failure of formation of von Ebner's glands and posterior lingual glands. Previous work in postnatal mice showed that vitamin A deficiency leads to squamous metaplasia of lingual glands (**Wolbach and Howe, 1925**). Thus, RA signaling is not only required for initial development of lingual glands (our findings), but also for their maintenance. In fact, genetic and/or experimental studies in rodents showed that RA signaling is required for proper development of several glands, including salivary glands and Harderian glands. For example, genetic loss of *Aldh1a3* in mice causes agenesis of the Harderian glands (**Dupé et al., 2003**), and various combined losses of *RARs* in mice cause agenesis or dysplasia of salivary glands and/or agenesis of the Harderian glands (**Mark et al., 2009**). Recent work also showed that RA signaling is required for the formation of salivary glands (**Metzler et al., 2018**). It has also been shown that vitamin A deficiency in rodents causes squamous metaplasia (**Wolbach and Howe, 1925**; **Wolfe and Salter, 1931**) and hypoplasia of salivary glands (**Wolbach and Howe, 1925**).

We also revealed that in addition to controlling anterior-posterior patterning of the LE and cell fate determination in this tissue, SHH signaling within the LE inhibits fungiform placode (FP) and taste bud formation. Thus, SHH signaling also controls the fate of epithelial progenitors of the interplacodal epithelium. This is supported by our findings that tongues from *ShhCreER^{T2}/Shh^{f}* mutant embryos that have been first exposed to TAM at E11.5 as well as tongues from *ShhGFPCRE/Smo$^{f/f}$* mutants formed abnormally enlarged FPs and taste buds, and exhibited increased numbers of *Shh*-expressing spots. The latter likely represent FPs and/or taste buds. Oversized FPs and taste buds also formed in tongues from *ShhCreER^{T2}/Shh^{f}* mutant embryos that have been first exposed to TAM at E10.5. In all these mutants, we found that the LE underwent enhanced RA signaling as a result of loss of expression of *Cyp26a1* and *Cyp26c1*. Our *in vitro* experiments showed that retinoids promote development of taste placodes, whereas inhibitors of RA signaling inhibit taste placode formation. We also showed that the LE expresses RALDH1-3, *RARg* and *RARb*, and that the interplacodal epithelium expresses *Cyp26a1* and *Cyp26c1* transcripts. Importantly, we demonstrated that FPs and taste buds are devoid of *Cyp26a1* and *Cyp26c1* transcripts, and that FPs and taste buds produce RALDH3 and RALDH1 proteins, respectively.

Furthermore, we showed that taste buds express RARγ protein and *RARg* mRNA.

All these findings strongly suggest that RA signaling promotes FP and taste bud formation, and that SHH inhibits formation of these structures, at least in part, through inhibition of RA activity.

Our analyses *in vivo*, which showed that SHH signaling inhibits FP induction during the period of FP patterning, confirm results of previous work in embryonic rodent tongues cultivated *in vitro* (**Hall et al., 2003; Mistretta et al., 2003; Iwatsuki et al., 2007; Liu et al., 2004**). In addition, however, we revealed that SHH performs this function in the LE, and that SHH signaling prevents continuous induction of taste placode formation. The latter function of SHH signaling in the LE is supported by our finding that loss of SHH signaling in tongues from *ShhCreER^{T2}/Shh^{f}* mutant embryos that have been first exposed to TAM at E10.5 or at E11.5 as well as in tongues from *ShhGFPCRE/Smo$^{f/f}$* mutant embryos, the LE continued to form taste placodes (*de novo* taste placode formation) after E14.5, when FPs normally are no longer formed. *de novo* taste placode formation has never been reported previously in other mouse models used to decipher the molecular control of FP patterning and taste bud formation. Notably, the *de novo* formation of taste placodes in the LE upon loss of SHH signaling is reminiscent of *de novo* hair follicle formation in mutant mice lacking SHH signaling in skin and hair follicle epithelia (**Gritli-Linde et al., 2007**).

The conclusion that SHH signaling within the LE, and not in the LM, is required to inhibit FP induction was drawn from our finding that mutants lacking SHH signaling in the LE (*ShhGFPCRE/Smo$^{f/f}$*mutants) and mutants lacking SHH signaling in both the LE and the LM (TAM-induced *ShhCreER^{T2}/Shh^{f}*mutants) formed tongues overproducing enlarged FPs. In addition, we showed that SHH signaling in the LM is not required for taste bud formation, since the *Wnt1-CRE/Smo$^{f/f}$* mutant tongues formed taste buds.

Genetic studies in mice have shown that canonical WNT signaling in the LE controls FP formation (**Barlow; 2015**). It seems also that the SHH and the canonical WNT signaling pathways interact during FP patterning. Indeed, it has been found that upon loss of canonical WNT signaling, the FPs and their associated mesenchyme lose expression of *Shh* and *Ptch1*, respectively, while overactivation of the canonical WNT pathway leads to expansion of *Shh* expression (**Iwatsuki et al., 2007; Liu et al., 2007**). Furthermore, while canonical WNT signaling induces *Shh* expression, SHH inhibits canonical WNT activity in embryonic rodent tongues cultivated *in vitro* (**Iwatsuki et al., 2007**). However, the mechanism by which SHH inhibits canonical WNT signaling in the LE remained unclear. Here, we showed that in mutants lacking SHH signaling (*ShhGFPCRE/Smo$^{f/f}$* and TAM-induced *ShhCreER^{T2}/Shh^{f}* mutants), the LE underwent an ectopic expression of *Wnt10b* well after expression of *Wnt10b* transcripts normally ceases in this tissue. Our findings strongly suggest that one

mechanism by which SHH inhibits canonical WNT activity in the LE is through inhibition of *Wnt10b* expression.

Both the SHH and canonical WNT signaling pathways have been shown to control maintenance of the LE and its derivatives, including taste buds, in postnatal mice. Overexpression of *GLI2* in the LE of adult mice (**Liu et al., 2013**) led to various defects in the LE, including failure of maintenance of fungiform papillae and taste buds. However, forced expression of SHH in the LE of adult mice gave a different outcome: the LE formed supernumerary taste buds outside of fungiform papillae (**Castillo et al., 2014**). These are unexpected, opposite results, the underlying mechanisms of which need further work.

More recent work showed that genetic ablation of GLI activity in the LE of postnatal mice causes formation of abnormal gustatory papillae and a gradual loss of taste buds, and that re-initiation of SHH signaling re-establishes normal formation of these structures (**Ermilov et al., 2016**). It seems also that nerve-derived SHH and SHH derived from the LE are crucial for taste bud homeostasis in postnatal mice (**Castillo-Azofeifa et al., 2017; Lu et al., 2018**). Furthermore, it has been reported that following taste bud cell loss caused by inhibitors of SHH signaling, taste bud cells can be promoted to regenerate by treatment with Hedgehog agonists (**Lu et al., 2018**).

As to the canonical WNT pathway in the tongue of postnatal mice, it has been shown that this pathway uses WNT10a as a ligand. Loss of WNT10a function in mice leads to reduced canonical WNT signaling in the LE and causes several defects in this tissue, including reduced size of taste buds, and this anomaly seems also to occur in postnatal mice genetically lacking β-catenin function (**Xu et al., 2017**). Maintenance of derivatives of the LE, including taste buds as well as fungiform and filiform papillae, has been found to require WNT10a/β-catenin signaling (**Xu et al., 2017**). In addition, it has been reported that the formation of all types of taste bud cells in postnatal mice requires WNT10a/β-catenin signaling, since loss-of-function of WNT10a or β-catenin causes loss of all types of taste bud cells (**Xu et al., 2017**). By contrast, overactivation of β-catenin in the LE of postnatal mice is capable of inducing only type I taste bud cells (**Gaillard et al., 2017**).

We found that adult mice express RALDH1 in taste buds, and that at least up to birth, the LE expresses RARγ protein and *RARg* mRNA. It would be interesting to determine whether RA signaling is involved in maintenance of the LE, lingual papillae and taste buds in the mature tongue. A hint that RA signaling may be involved in taste bud cell homeostasis comes from previous observations in rats subjected to short-term vitamin A deficiency. These rats did not exhibit squamous metaplasia of taste bud cells, yet they were found to have altered sweet taste perception (**Reifen et al., 1998**). Another question worth addressing is whether the RA signaling pathway interacts with the SHH or canonical WNT signaling pathways in the mature tongue. It is unlikely that such interactions, if

they do occur, would involve CYP26 enzymes, since after E16.5 *Cyp26a1* and *Cyp26c1* transcripts are not expressed in the LE (**Abu-Abed et al., 2002; Tahayato et al., 2003**).

Besides patterning defects of FPs and as well as glandular and Mekel cell metaplasiae, loss of SHH signaling during tongue development led to formation of squamous foci made of a thickened epithelium that are conspicuously prominent in the *ShhGFPCRE/Smo$^{f/f}$* mutant tongues. These foci displayed altered expression of Keratin 6, Keratin 8 and Keratin 15. In addition, these foci not only showed decreased *RARg* hybridization signals and RARγ immunostaining, but they also maintained *Cyp26a1* and *Cyp26c1* expression. These data indicate that the squamous foci are unable to respond to RA signaling. In the *ShhGFPCRE/Smo$^{f/f}$* mutant tongue organ cultures the squamous foci were not affected by inhibition of RA signaling. This is somehow expected, as vitamin A deficiency is known to induce squamous metaplasia in epithelia **(Wolbach and Howe, 1925**; **Wolfe and Salter, 1931**). With the exception of taste buds and lingual glands, the lingual epithelium is normally of a squamous type. The mechanisms leading to formation of these foci are at present unclear, however these could have formed from progenitor cells that should have formed filiform papillae.

SHH signaling is required before E12.5 for anterior-posterior patterning of the LE and for cell fate specification in this tissue

As described above, we found that SHH signaling within the LM is required during a restricted period (before ≈E12.5) for adequate growth and morphogenesis of the tongue. We also found that SHH signaling in the LE is necessary before ≈E12.5 for proper anterior-posterior patterning of the LE and for specifying cell types in this tissue. This conclusion is based on several findings. (1) In contrast to the *ShhGFPCRE/Smo$^{f/f}$* mutant tongues, tongues from *ShhCreER^{T2}/Smo$^{f/f}$* embryos that have been first exposed to TAM at E12.5 had a normal LE. Indeed, in these mutants, the LE did not exhibit thickened epithelial foci and was devoid of Merkel cell and glandular metaplasiae. Furthermore, other derivatives of the LE such as taste buds and filiform papillae developed normally in the E12.5 TAM-induced *ShhCreER^{T2}/Smo$^{f/f}$* mutants. (2) In contrast to tongues from *ShhCreER^{T2}/Shh^{f}* mutant embryos that have been first exposed to TAM at E11.5, which exhibited FP and taste bud patterning defects (abnormal size and number of FPs and taste buds), tongues from *ShhCreER^{T2}/Shh^{f}* mutant embryos that have been first exposed to TAM at E12.5 had normally patterned FPs and taste buds. (3) Tongues from *K14-CRE/Smo$^{f/f}$* mutants in which *Smo* is expected to be deleted at ≈E13.5 in the LE, as shown by *lacZ* staining, had no alterations in the LE and its derivatives.

SHH signaling in the LE is required to prevent cells from adopting a Merkel cell fate

Merkel cells ensure light tactile sensations in the skin. These cells originate from the epithelium (**van Keymeulen et al., 2009**), and in the hairy skin they develop from hair follicle placodes (**Nguyen et al., 2018**). Merkel cells are found in touch domes of the hairy skin and in whisker follicles, and they also develop in the glabrous epidermis of finger tips (**Maksimovic et al., 2014**). In adult mice Merkel cell-neurite complexes have also been detected in the epithelium of the hard palate (**Nunzi et al., 2004**). In contrast to other species such as birds (**Toyoshima and Shimamura, 1991**) and frogs (**Toyoshima et al., 1999**), Merkel cells do not form in the lingual epithelium of humans (**Yom et al., 2006**).

We have analysed numerous tongue sections from numerous control mice at different developmental stages (up to birth) after immunostaining for K8, SOX2 and Rab3c, and never detected Merkel cells in the LE, including within taste buds (taste buds were Rab3c-negative). We also analysed tongues from adult mice after K8 immunostaining (our unpublished data), and never detected single, basally located K8+ Merkel cells. Similarly, numerous previous studies, which always use K8 as a marker for taste bud cells in the developing murine tongue as well as in tongues from adult mice never reported the presence K8-expressing cells in the basal layer of the LE. Surprisingly, we found that all the *ShhGFPCRE/Smo$^{f/f}$* mutant tongues assessed consistently displayed numerous ectopic Merkel cells in the basal layer of the LE. Merkel cells also developed in the LE of *ShhCreER^{T2}/Shh^{f}* embryos that have been first exposed to TAM at E10.5. However, these mutants displayed only a few dispersed Merkel cells in the LE as compared to the *ShhGFPCRE/Smo$^{f/f}$* mutants. These data show that in the absence of SHH signaling in the LE, this tissue underwent Merkel cell metaplasia. This is another example of disrupted cell fate specification in the LE as a result of loss of SHH signaling.

Because numerous genes and/or proteins, including Keratin 20, *Krt8*/Keratin 8, *Sox2*/SOX2, Advillin, *Satb2*, *Cpe*, Claudin6, Claudin7, *Mash1, Hes6*, *and Snap25* are expressed in both Merkel cells and taste bud cells (**our data**; **Barlow, 2015; Haeberle et al., 2004; Okubo et al., 2006; Michlig et al., 2007; Hevezi et al., 2009; Seta et al., 2011**), it is tempting to speculate that upon loss of SHH signaling in the LE, epithelial progenitors that are destined to form taste bud cells, instead adopted a Merkel cell fate.

SHH signaling has been shown to be required for Merkel cell specification in the hairy skin, whereas in the glabrous skin (hairless skin), Merkel cells develop independently of SHH inputs (**Perdigoto et al., 2016; Nguyen et al., 2018**). Thus, like in the glabrous skin, the ectopic Merkel cells that formed in the LE of our mutant mice do not depend on SHH signaling for their specification.

Our *in vitro* experiments showed that inhibitors of RA signaling were unable to abrogate Merkel cell metaplasia in the LE of the *ShhGFPCRE/Smo$^{f/f}$* mutant tongues. Thus, this anomaly is not due to increased RA signaling. The identification of the mechanisms reponsible for Merkel cell metaplasia upon loss of SHH signaling in the LE requires further studies. Recently, it has been shown that Merkel cell specification in the hairy skin requires intact function of FGFR2 (**Nguyen et al., 2018**). It would be therefore interesting to explore whether FGF signaling is involved in the specification of Merkel cells upon loss of SHH in the lingual epithelium, while keeping in mind that FGFR2 may not be required for specification of Merkel cells in the glabrous skin. Our findings are expected to be of interest, as the causes of Merkel cell carcinoma of the tongue are to date unknown (**Yom et al., 2006**).

Conclusion

To conclude, we revealed multiple facets of SHH function during tongue formation. We showed that SHH controls cell fate specification in the LE, since in its absence cells in the LE adopt different identities, by forming minor salivary glands or taste placodes (supernumerary and enlarged taste placodes) in the wrong places, while some other cells form epithelial foci with a molecular signature different from that of the normal LE. Other cells of the mutant LE switched to a Merkel cell type. We also showed that SHH inhibits lingual gland formation by inhibiting RA, and that SHH inhibits taste placode formation though inhibition of RA signaling. Finally we showed that RA signaling promotes the formation of taste placodes and lingual minor salivary glands. Our findings are expected to provide valuable information for future research aiming at finding ways to induce regeneration of lost taste buds and salivary glands, and to pave the way for deciphering the etiopathogenesis of lingual Merkel cell carcinoma.

6. Conclusions

The present studies led to the following conclusions:

- Carbonic anhydrases (CAs) display dynamic distribution patterns during tooth development
- In addition to being localized in the cytoplasm, CA XIII very likely localizes in lysosomes.
- In the developing tongue, Sonic Hedgehog (SHH) signaling is required during a restricted period (before 12.5) for: (1) normal tongue growth and morphogenesis, (2) proper patterning of the lingual epithelium (LE), and (3) specification of cell types inherent to the LE.
- In the developing tongue, SHH signaling in the LE is required to attenuate retinoic acid (RA) signaling, and SHH inhibits the expression of *Wnt10b*.
- In the developing tongue, SHH inhibits and RA promotes taste placode and lingual minor salivary gland formation.
- In the developing tongue, SHH inhibits taste placode formation through inhibition of RA signaling, and one mechanism by which SHH signaling inhibits canonical Wnt signaling is through inhibition of *Wnt10b* expression.
- In the developing tongue, SHH signaling is required to prevent Merkel cell specification in the LE.
- Normal embryogenesis and organogenesis require a tight control of RA and Hedgehog activities.

7. Future Perspectives

- Mouse models with tissue-specific loss-of-function of more than one carbonic anhydrase would shed light on the *in vivo* role of Carbonic anhydrases during tooth development.
- Identification of the mechanisms behind Merkel cell formation upon loss of SHH signaling in the lingual epithelium would require advanced technologies such as RNA sequencing and complementary assays in control and mutant tongues with loss of SHH signaling in the lingual epithelium.
- It would be interesting to determine whether in the developing tongue, the RA and canonical Wnt signaling pathways interact. This would require the use, for example, of mouse models with loss-of-function of the canonical Wnt pathway.
- Future studies are required to determine whether RA signaling has a role in maintenance of the lingual epithelium and taste bud cells in the mature tongue, and mouse models with tissue-specific ablation of two or three *RARs* in compound mutants would be useful to address this issue.
- The nature of interactions between the Hedgehog and RA signaling pathways during embryogenesis and organogenesis remains largely unexplored. There exist numerous mouse models with deregulation of the Hedgehog or the RA pathways that can be used to determine whether and how the two pathways interact in a given developing organ or tissue.

Acknowledgement

I would like to express my deep appreciation to my dear supervisor Amel Gritli-Linde. You have been so supportive and generous. Thank you for giving me the opportunity to be your student and for your supervision and guidance. Thank you for supporting me at both the personal and educational levels. Thank you for always correcting my pronounciation and teaching me new words and things in life. “When there is a will, there is a way and never give up”, that is you and your way in life, which you have induced in the entire lab. Deep from my heart, THANK YOU.

Professor Anders Linde, thank you for being kind and always helping me no matter what or how much I have asked you. Your kindess is an integral part of your personality. I am so glad to have you as a head of our department. Thank you for always correcting my English and Swedish, TACK SÅ MYCKET. Thank you also for allowing me to teach part of your lectures and to have the patience to listen and to correct my way of presentation.

Amel and Anders, I am so appreciating for the parental care that you have offered to my family and me. Love will always persist for both of you.

Kristina Hallberg, Katarina Nobelius and Claes-Göran Reibring, thank you for your presence in the lab and for being helpful every time I have contacted you. I am so grateful for your cooperation at work and your advice and precious information about life in Sweden. Thank you also for helping me to improve my Swedish language, TACK TACK.

Yu Fang, thank you for being a nice classmate in the Introductory Course. I hope you enjoy your presence next to your daughter in China.

My deep thanks go to my kind and beloved parents, my caring brothers; Mohamed, Nail and Nader and my brothers’ wives and children. Your continuous support has been one of the driving forces that always push me forward.

My beloved brother Nail, grandmother and grandfather, my thanks go to you wherever you are. You are always in my heart and your belief in my abilities was one reason for my success and achievemnts.

Uncle Essam, aunt Helena and children, thank you for your kind support during my stay in Sweden.

Dalal and Tahany, thank you for your kindness and for encouraging me to finish my thesis.

My big family in Egypt and my friends in Egypt and Sweden, thank you all for your continuous support.

Last but absolutely not least, my heartfelt thanks to my small family: my kind husband Mohamed; beloved children Ahmed, Hana and Nora. Your massive support has made this work possible and allowed me to bypass problems. Your presence lightens my life and your smile nourishes my heart. I am glad to have you next to me in all the nice and hard times in our life. I wish you all happiness in your life and progress in your career. I will always love you.

References

Abe, M., Maeda, T. & Wakisaka, S. (2008) Retinoic acid affects craniofacial patterning by changing Fgf8 expression in the pharyngeal ectoderm. Dev Growth Differ. 50: 717-729.

Abu-Abed, S., MacLean, G., Fraulob, V., Chambon, P., Petkovitch, M. & Dollé, P. (2002) Differential expression of the retinoic acid-metabolizing enzymes CYP26A1 and CYP26B1 during murine organogenesis. Mech Dev, 110, 173-177.

Acebron, S.P. & Niehrs, C. (2016) β-Catenin-Independent Roles of Wnt/LRP6. Signaling Trends Cell Biol, 26(12), 956-967.

Adaimy, L., Chouery, E., Megarbane, H., Mroueh, S., Delague, V., Nicolas, E., Belguith, H., de Mazancourt, P. & Megarbane, A. (2007) Mutation in WNT10A is associated with an autosomal recessive ectodermal dysplasia: the odonto-onycho-dermal dysplasia. Am J Hum Genet, 81(4), 821-828.

Ahmad, M., Iseki, H., Abduweli, D., Baba, O., Tabata, M.J. & Takano, Y. (2011) Ultrastructural and histochemical evaluation of appositional mineralization of circumpulpal dentin at the crown- and root-analog portions of rat incisors. J Electron Microsc (Tokyo), 60(1), 79-87.

Alonso, S., Hernandez, D., Chang, Y-T., Gocke, C.B., McCray, M., Varadham, R., Matsui, W.H., Jones, R.J. & Ghiaur, G. (2016) Hedgehog and retinoic acid signaling alters multiple myeloma microenvironment and generates bortezomib resistance. J Clin Invest, 126, 4460-4468.

Alonso-Torre, S.R., Alvarez, J., Montero, M., Sanchez, A. & Garcia-Sancho, J. (1993) Control of Ca2+ entry into HL60 and U937 human leukaemia cells by the filling state of the intracellular Ca2+ stores. Biochem J, 289, 761–766.

Al Tanoury, Z., Piskunov, A. & Rochette-Egly, C. (2013) Vitamin A and retinoid signaling: genomic and nongenomic effects. J Lipid Res, 54(7), 1761-1775.

An, Z., Akily, B., Sabalic, M., Zong, G., Chai, Y. & Sharpe, P.T. (2018) Regulation of Mesenchymal Stem to Transit-Amplifying Cell Transition in the Continuously Growing Mouse Incisor. Cell Rep, 5;23(10), 3102-3111.

Anderson, R.E., Schraer, H. & Gay, C.V. (1982) Ultrastructural immunocytochemical localization of carbonic anhydrase in normal and calcitonin-treated chick osteoclasts. Anat Rec, 204, 9–20.

Angerer, L.M. & Angerer, R.C. (1992) In situ hybridization to cellular RNA with radiolabelled RNA probes. In: Wilkinson, D.G. (Ed.). In situ Hybridization. A Practical Approach. Oxford University Press, Oxford, UK.

Awad, M., Al-Ashwal, A.A., Sakati, N., Al-Abbad, A.A. & Bin-Abbas, B.S. (2002) Long-term follow up of carbonic anhydrase II deficiency syndrome. Saudi Med J, 23, 25-29.

Balkan, W., Colbert, M., Bock, C, & Linney, E. (1992) Transgenic indicator mice for studying activated retinoic acid receptors during development. Proc Natl Acad Sci USA, 89, 3347–3351.

Bancroft, J.D. & Stevens, A. (1990) Theory and Practice of histological technique. 3rd edition, New York, NY, Churchill Livingston, 192-195.

Barlow, L.A. (2015) Progress and renewal in gustation: new insights into taste bud development. Development, 142, 3620–3629.

Barlow, L.A. & Klein, O.D. (2015) Developing and regenerating a sense of taste. Curr Top Dev Biol. 111: 401–419.

Beertsen, W. & Niehof, A (1986) Root-analogue versus crown analogue dentin: a radioautographic and ultrastructural investigation of the mouse incisor. Anat Rec, 215, 106-118.

Beidler, L.M. & Smallman, R.L. (1965) Renewal of cells within taste buds. J Cell Biol, 27(2), 263-272.

Beites, C.L., Hollenbeck, P.L., Kim, J., Lovell-Badge, R., Lander, A.D. & Calof, A.L., (2009) Follistatin modulates a BMP autoregulatory loop to control the size and patterning of sensory domains in the developing tongue. Development, 136(13), 2187-2197.

Blanchet, S., Favier, B., Chevalier, G., Kastner, P. & Michaille, J-J., Chambon, P., Dhouailly, D. (1998) Both retinoic acid receptors α (RARα) and γ (RARγ) are able to initiate mouse upper-lip skin glandular metaplasia. J Invest Dermatol. 111: 206-212.

Blomhoff, R. & Blomhoff, H.K. (2006) Overview of retinoid metabolism and function. J Neurobiol. 66: 606–630.

Bosley, T.M., Salih, M.A., Alorainy, I.A., Islam, Z., Oystreck, D.T., Suliman, O.S., al Malki, S., Suhaibani, A.H., Khiari, H., Beckers, S., van Wesenbeeck, L., Perdu, B., AlDrees, A., Elmalik, S.A., Van Hul, W. & Abu-Amero, K.K. (2011) The neurology of carbonic anhydrase type II deficiency syndrome. Brain, 134, 3502–3515.

Brewer, J.R., Mazot, P. & Soriano, P. 2016 Genetic insights into the mechanisms of Fgf signaling. Genes Dev, 1;30(7), 751-71.

Briscoe, J. & Thérond, P.P. (2013) The mechanisms of Hedgehog signaling and its roles in development and disease. Nat Rev Mol Cell Biol, 14(7), 416-429.

Bumcrot, D. A., Takada, R. & McMahon, A. P. (1995) Proteolytic processing yields two secreted forms of sonic hedgehog. Mol Cell Biol, 15,2294 -2303.

Calvo, S.S. & Egan, J.M. (2015) The endocrinology of taste receptors. Nat Rev Endocrinol, 11(4), 213-227.

Caparrós-Martín, J.A., Valencia, M., Reytor, E., Pacheco, M., Fernandez, M., Perez-Aytes, A., Gean, E., Lapunzina, P., Peters, H., Goodship, J.A. & Ruiz-Perez, V.L. (2013) The ciliary Evc/Evc2 complex interacts with Smo and controls Hedgehog pathway activity in chondrocytes by regulating Sufu/Gli3 dissociation and Gli3 trafficking in primary cilia. Hum Mol Genet. 22:124–139.

Castillo-Azofeifa, D., Losacco, J.T., Salcedo, E., Golden, E.J., Finger, T.E. & Barlow, L.A. (2017) Sonic hedgehog from both nerves and epithelium is a key trophic factor for taste bud maintenance. Development, 144(17), 3054-3065.

Castillo, D., Seidel, K., Salcedo, E., Ahn, C., de Sauvage, F.J., Klein, O.D. & Barlow, L.A. (2014) Induction of ectopic taste buds by SHH reveals the competency and plasticity of adult lingual epithelium. Development, 141(15), 2993-3002.

Catón, J. & Tucker, A.S. (2009) Current knowledge of tooth development: patterning and mineralization of the murine dentition. J Anat, 214(4), 502-515.

Chiang, C., Litingtun, Y., Lee, E., Young, K.E., Corden, J.L., Westphal, H. & Beachy, P.A. (1996) Cyclopia and defective axial patterning in mice lacking Sonic Hedgehog gene function. Nature, 383: 407-413.

Chuong, C.M., Patel, N., Lin, J., Jung, H.S. & Widelitz, R.B. (2000) Sonic hedgehog signaling pathway in vertebrate epithelial appendage morphogenesis: perspectives in development and evolution. Cell Mol Life Sci, 57(12), 1672-1681.

Colbert, M., Linney, E. & LaMantia, A- S. (1993) Local sources of retinoic acid coincide with retinoid-mediated transgene activity during embryonic development. Proc Natl Acad Sci USA, 90, 6572–6576.

Covant, H.A. & Hardy, M.H. (1988) Stability of the glandular morphogenesis produced by retinoids in the newborn hamster cheek pouch in vitro. J Exp Zool, 246: 139-149.

Cunningham, T.J. & Duester, G. (2015) Mechanisms of retinoic acid signaling and its roles in organ and limb development. Nat Rev Mol Cell Biol, 16(2),110-123.

Dassule, H., Lewis, P., Bei, M. & McMahon, A.P. (2000) Sonic hedgehog regulates growth and morphogenesis of the tooth. Development, 127, 4775–4785.

De Roos, K., Sonneveld, E., Compaan, B., ten Berge, D., Durston, A.J. & van der Saag, P.T. (1999) Expression of retinoic acid 4-hydroxylase (CYP26) during mouse and Xenopus laevis embryogenesis. Mech Dev, 82: 205–211.

Dijksterhuis, J.P., Petersen, J. & Schulte, G. (2014) WNT/Frizzled signaling: receptor-ligand selectivity with focus on FZD-G protein signaling and its physiological relevance: IUPHAR Review 3. Br J Pharmacol, 171(5), 1195-1209.

Dogterom, A.A. & Bronckers, A.L.J.J. (1983) Carbonic anhydrase in developing hamster molars. J Dent Res, 62, 789–791.

Doldo, E., Costanza, G., Agostinelli, S. & Tarquini, C., Ferlosio, A., Arcuri, G., Passeri, D., Scioli, M.G. & Orlandi, A. (2015). Vitamin A, cancer treatment and prevention: the new role of cellular retinol binding proteins. Biomed Res Int, 2015, 624627.

Dollé, P., Ruberte, E., Leroy, P., Morris-Kay, G. & Chambon, P. (1990) Retinoic acid receptors and cellular retinoid binding proteins. I. A systematic study of their differential patterns of transcription during mouse organogenesis. Development, 110, 1133-1151.

Dollé, P., Fraulob, V., Kastner, P. & Chambon, P. (1994) Developmental expression of murine retinoid X receptor (RXR) genes. Mech Dev, 45(2), 91-104.

Dollé, P., Fraulob, V., Gallego-Llamas, J., Vermot, J. & Niederreither, V. (2010) Fate of retinoic acid-activated embryonic cell lineages. Dev Dyn, 239: 3260–3274.

Dorn, K.V., Hughes, C.E. & Rohatgi, R. A. (2012) Smoothened-Evc2 complex transduces the hedgehog signal at primary cilia. Dev Cell, 23: 823–835.

Du, W., Prochazka, J., Prochazkova, M. & Klein, O.D. (2016) Expression of FGFs during early mouse tongue development. Gene Expr Patterns, 20(2), 81-87.

Duester, G. (2008) Retinoic acid synthesis and signaling during early organogenesis. Cell, 19, 134(6), 921-931.

Duester, G. (2013) Retinoid signaling in control of progenitor cell differentiation during mouse development. Semin Cell Dev Biol, 24(10-12), 694-700.

Dupé, V., Matt, N., Garnier, J.M., Chambon, P., Mark, M. & Ghyselinck, N.B. (2003) A newborn lethal defect due to inactivation of retinaldehyde dehydrogenase type 3 is prevented by maternal retinoic acid treatment. Proc Natl Acad Sci USA, 100, 14036–14041.

Duverger, O., Ohara, T., Bible, P.W., Zah, A. & Morasso, M.I. (2017) DLX3-Dependent Regulation of Ion Transporters and Carbonic Anhydrases is Crucial for Enamel Mineralization. J Bone Miner Res, 32(3), 641-653.

Elmazar, M.M.A., Reichert, B., Scroot, B. & Nau, H. (1996) Patterns of retinoid-induced teratogenenic effects: Possible relationships with relative selectivity

for nuclear retinoid receptors RARa, RARb and RARg. Teratology, 53, 158-167.

Echelard, Y., Epstein, D.J., St-Kacques, B., Shen, L., Mohler, J., McMahon, J.A. & McMahon, A.P. (1993) Sonic hedgehog, a member of a family of putative signaling molecules, is implicated in the regulation of CNS polarity. Cell, 75, 1417-1430.

Ermilov, A.N., Kumari, A., Li, L., Joiner, A.M., Grachtchouk, M.A., Allen, B.L., Dlugosz, A.A. & Mistretta, C.M. (2016) Maintenance of Taste Organs Is Strictly Dependent on Epithelial Hedgehog/GLI Signaling. PLoS Genet, 28, 12(11).

Farbman, A.I. (1980) Renewal of taste bud cells in rat circumvallate papillae. Cell Tissue Kinet, 13, 349–357.

Farzan, S. F., Singh, S., Schilling, N. S. & Robbins, D. J. (2008) The Adventures of Sonic Hedgehog in Development and Repair. III. Hedgehog processing and biological activity. Am. J. Physiol. Gastrointest. Liver Physiol, 294(4), G844-G849.

Fell, H.B., Mellanby, E. (1953) Metaplasia produced in cultures of chick ectoderm by high vitamin A. J Physiol, 119, 470-488.

Finger, T.E., Danilova, V., Barrows, J., Bartel, D.L., Vigers, A.J., Stone, L., Hellekant, G., & Kinnamon, S.C. (2005) ATP signaling is crucial for communication from taste buds to gustatory nerves. Science, 310, 1495-1499.

Frank, R.M. & Nalbandian, J. (1967) Ultrastructure of amelogenesis. In Structural and Chemical Organization of Teeth, vol I (ed. A. E. W. Miles), New York, Academic Press.

Gaillard, D., Bowles, S.G., Salcedo, E., Xu, M., Millar, S.E. & Barlow, L.A. (2017) β-catenin is required for taste bud cell renewal and behavioral taste perception in adult mice. PLoS Genet, 28;13(8), e1006990.

Geelen, J.A.G. & Peters, P.W.J. (1979) Hypervitaminosis A-induced teratogenesis. CRC Critical Rev Toxicol, 6, 351-375.

Grinstein, S., Rotin, D. & Mason, M.J. (1989) Na+/H+ exchange and growth factor-induced cytosolic pH changes. Role in cellular proliferation. Biochim Biophys Acta, 988, 73–97.

Gritli-Linde, A., Lewis, P., McMahon, A.P. & Linde, A. (2001) The whereabouts of a morphogen: Direct evidence for short- and long-range activity of Hedgehog signaling peptides. Dev Biol, 236, 364-386.

Gritli-Linde, A., Bei, M., Maas, R., Zhang, X.M., Linde, A. & McMahon, A.P. (2002) Shh signaling within the dental epithelium is necessary for cell proliferation, growth and polarization. Development, 129(23), 5323-37.

Gritli-Linde A. (2007) Molecular control of secondary palate development. Dev Biol, 301, 309-326.

Gritli-Linde, A., Hallberg, K., Harfe, B.D., Reyahi, A., Kannius-Janson, M., Nilsson, J., Cobourne, M.T., Sharpe, P.T., McMahon, A.P. & Linde, A. (2007) Abnormal hair development and apparent follicular transformation to mammary gland in the absence of hedgehog signaling. Dev Cell, 12(1), 99-112.

Gritli-Linde, A. (2008) The etiopathogenesis of cleft lip and cleft palate: usefulness and caveats of mouse models. Curr Top Dev Biol, 84, 37-138.

Gritli-Linde, A. (2010) p63 and IRF6: brothers in arms against cleft palate. J Clin Invest, 120(5), 1386-1389.

Gut, O.M., Parkkila, S., Vernerovà, Z., Rohde, E., Závada, J., Höcker, M., Pastorek, J., Karttunen, T., Gibadulinová, A., Závadová, Z., Knobeloch, K.P., Wiedenmann, B., Svoboda, J., Horak, I. & Pastoreková, S. (2002) Gastric hyperplasia in mice with targeted disruption of the carbonic anhydrase gene Car9. Gastroenterology, 123, 1889–1903.

Haeberle, H., Fujiwara, M., Chuang, J., Medina, M.M., Panditrao, M.V., Bechsted, S., Howard, J. & Lumpkin, E.A. (2004) Molecular profiling reveals synaptic release machinery in Merckel cells. Proc Natl Acad Sci USA, 101, 14503–14508.

Hall, J.M., Hooper, J.E. & Finger, T.E., (1999) Expression of Sonic hedgehog, Patched, and Gli1 in developing taste papillae of the mouse. J. Comp. Neurol, 406, 143–155.

Hall, J.M.H., Bell, M.L. & Finger, T.E. (2003) Disruption of Sonic hedgehog signaling alters growth and patterning of lingual taste papillae. Dev Biol, 255, 263-277.

Hamosh, M. & Scow, R.O. (1973) Lingual lipase and its role in the digestion of dietary lipid. J Clin Invest, 52, 88–95.

Harada, H., Kettunen, P., Jung, H.-S., Mustonen, T., Wang, Y. A. & Thesleff, I. (1999) Localization of putative stem cells in dental epithelium and their association with Notch and FGF signaling. J. Cell Biol, 147,105 -120.

Hardy, M.H. (1968) Glandular metaplasia of hair follicles and other responses to vitamin A excess in cultures of rodent skin. J Embryol Exp Morph, 19, 157-180.

Harfe, B.D., Scherz, P.J., Nissim, S., Tian, H., McMahon, A.P. & Tabin, C. (2004) Evidence for expansion-based temporal Shh gradient in specifying vertebrate digit identities. Cell, 118, 517–528.

Harju, A–K., Bootorabib, F., Kuuslahti, M., Supuran, C.T. & Parkkila, S. (2013) Carbonic anhydrase III: a neglected isoenzyme is stepping into the limelight. J Enz Inhib Med Chem, 28, 231–239.

Hassan, I.M., Shajee, B., Waheed, A., Ahmad, F. & Sly, W.S. (2013) Structure, function and applications of carbonic anhydrase isozymes. Bioorg Med Chem, 21, 1570–1582.

Henning, P., Conaway, H.H. & Lerner, U.H. (2015) Retinoid receptors in bone and their role in bone remodeling. Front Endocrinol (Lausanne) 11, 6:31.

Hevezi, P., Moyer, B.D., Lu, M., Gao., N., White, E., Echeverri, F., Kalabat, D., Soto, H., Laita, B., Li, C., Yeh, S.A., Zoller, M., Zlotnik, A. (2009) Genome-wide analysis of gene expression in primate taste buds reveals links to diverse processes. PLoS ONE, 4, e6395.

Huang, X., Bringas, P. Jr., Slavkin, H.C. & Chai, Y. (2009) Fate of HERS during tooth development. Dev Biol, 334, 22–30.

Hui, C-C. & Angers, S. (2011) Gli proteins in development and disease. Annu Rev Cell Dev Biol, 27, 513-537.

Imtaiyaz Hassan, M., Shajee, B., Waheed, A., Ahmad, F. & Sly, W.S. (2013) Structure, function and applications of carbonic anhydrase isozymes. Bioorg Med Chem, 15; 21(6), 1570-1582.

Iritani, N. & Wells, W.W. (1974) Studies on a HCO3− -stimulated ATPase and carbonic anhydrase system in rat liver lysosomes. Arch Biochem Biophys 164: 357–366.

Itoh, N. (2016) FGF10: A multifunctional mesenchymal-epithelial signaling growth factor in development, health, and disease. Cytokine Growth Factor Rev, 28, 63-69.

Iwatsuki, K., Liu, H-X., Grunder, A., Singer, M.A., Lane, T.F., Grosschedl, R., Mistretta, C.M. & Margolskee, R.F. (2007) Wnt signaling interacts with Shh to regulate taste papilla development. Proc Natl Acad Sci USA, 104, 2253–2258.

Jeong, J., Mao, J., Tenzen, T., Kottman, A.H. & McMahon, A.P. (2004) Hedgehog signaling in the neural crest cells regulates the patterning and growth of facial primordia. Genes Dev, 18, 937–951.

Jeong, J. & McMahon, A.P. (2005) Growth and pattern of the mammalian neural tube are governed by partially overlapping feedback activities of the hedgehog antagonists patched 1 and Hhip1. Development, 132, 143–154.

Jiang, J. & Hui, C-C. (2008) Hedgehog signaling in development and cancer. Dev Cell, 15, 801-812.

Jitpukdeebodintra, S., Chai, Y. & Snead, M.L. (2002) Developmental patterning of the circumvallate papilla. Int J Dev Biol, 46, 755–763.

Josephsen, K., Takano, Y., Frische, S., Praetorius, J., Nielsen, S., Aoba, T., & Fejerskov, O. (2010) Ion transporters in secretory and cyclically modulating ameloblasts: a new hypothesis for cellular control of

preeruptive enamel maturation. Am J Physiol Cell Physiol, 299, C1299–C1307.

Jung, H-S., Oropeza, V. & Thesleff, I. (1999) Shh, Bmp-2, Bmp-4 and Fgf-8 are associated with initiation and atterning of mouse tongue papillae. Mech Dev, 81, 179–182.

Jussila, M. & Thesleff, I. (2012) Signaling networks regulating tooth organogenesis and regeneration, and the specification of dental mesenchymal and epithelial cell lineages. Cold Spring Harb Perspect Biol, 1;4(4), a008425.

Kalter, H. (1960) The teratogenic effects of hypervitaminosis A upon the face and mouth of inbred mice. Ann NY Acad Sci.; 85: 42–55.

Kalter, H. & Warkany, J. (1961) Experimental production of congenital malformations in strains of inbred mice by maternal treatment with hypervitaminosis A. Am J Pathol, 38, 1–21.

Kaufman, M.H. (1992) Atlas of Mouse Development. Academic Press, San Diego, USA.

Kawashima, N. & Okiji, T. (2016) Odontoblasts: Specialized hard-tissue-forming cells in the dentin-pulp complex. Congenit Anom (Kyoto), 56(4), 144-153.

Kimoto, M., Kishino, M., Yura, Y. & Ogawa, Y. (2006) A role of salivary carbonic anhydrase VI in dental plaque. Arch Oral Biol, 51, 117-122.

Kivela, J., Parkkila, S., Parkkila, A.K., Leinonen, J. & Rajaniemi, H. (1999) Salivary carbonic anhydrase isoenzyme. VI J Physiol, 520 (Pt 2), 315-320.

Knapp, L., Lawton, A., Oakley, B., Wong, L. & Zhang, C. (1995) Keratins as markers of differentiated taste cells of the rat. Differentiation, 58(5): 341–349.

Kogawa, M., Wijenayaka, A.R., Ormsby, R.T., Thomas, G.P., Anderson, P.H., Bonewald, L.F., Findlay, D.M. & Atkins, G.J. (2013) Sclerostin regulates release of bone mineral by osteocytes by induction of carbonic anhydrase 2. J Bone Miner Res, 28(12), 2436-2448.

Kuang-Hsien, Hu. J., Mushegyan, V. & Klein, O. D. (2014) On the cutting edge of organ renewal: identification, regulation, and evolution of incisor stem cells. Genesis, 52, 79-92.

Kwan, K.M. (2002) Conditional alleles in mice: practical considerations for tissue-specific knockouts. Genesis, 32, 49-62.

Lacruz, R.S., Hilvo, M., Kurtz, I. & Paine, M.L. (2010a) A survey of carbonic anhydrase mRNA expression in enamel cells. Biochem Biophys Res Commun, 19; 393(4), 883-887.

Lacruz, R.S., Nanci, A., Kurtz, I., Wright, J.T. & Paine, M.L. (2010b) Regulation of pH during amelogenesis. Calcif Tissue Int, 86, 91–103.

Lacruz, R.S. (2017) Enamel: Molecular identity of its transepithelial ion transport system. Cell Calcium, 65, 1-7.

Lacruz, R.S., Habelitz, S., Wright, J.T. & Paine, M.L. (2017) Dental enamel formation and implications for oral health and disease. Physiol Rev, 1;97(3), 939-993.

Lan, Y. & Jiang, R. (2009) Sonic Hedgehog signaling regulates reciprocal epithelial-mesenchymal interactions controlling palatal growth. Development, 136, 1387-1396.

Lan, Y., Xu, J. & Jiang, R. (2015) Cellular and molecular mechanisms of palatogenesis. Curr Top Dev Biol, 115, 59-84.

Lawrence, D.J. & Bern, H.A. (1960) Mucous gland formation in keratinized adult epithelium in situ treated with vitamin A. Exp Cell Res, 21, 443-446.

Lawrence, D.J., Bern, H.A. & Steadman, M.G. (1960) Vitamin A and keratinization. Studies on the hamster cheek pouch. Ann Otol Rhinol Laryngol, 69, 645-661.

Lee, R.T., Zhao, Z. & Ingham, P.W. (2016) Hedgehog signalling. Development, 1;143(3), 367-372.

Lehenkari, P., Hentunen, T.A., Laitala-Leinonen, T., Tuukkanen, J. & Vaananen, H.K. (1998) Carbonic anhydrase II plays a major role in osteoclast differentiation and bone resorption by effecting the steady state intracellular pH and Ca2+. Exp Cell Res, 242(1), 128–137.

Lehtonen, J., Shen, B., Vihinen, M., Casini, A., Scozzafava, A. Supuran, C.T., Parkkila, A.K., Saarnio, J., Kivelä, A.J., Waheed, A., Sly, W.S. & Parkkila, S. (2004) Characterization of CAXIII, a novel member of the carbonic anhydrase isoenzyme family. J Biol Chem, 279, 2719–2727.

Leinonen, J., Kivelä, J., Parkkila, S., Parkkila, A.K. & Rajaniemi, H. (1999) Salivary carbonic anhydrase isoenzyme VI is located in the human enamel pellicle. Caries Res, 33, 185-190.

Lewis, P.M., Gritli-Linde, A., Smeyne, R. Kottmann, A. & McMahon, A.P. (2004) Sonic hedgehog signaling is required for expansion and patterning of the mouse cerebellum. Dev Biol, 270, 393-410.

Lewis, S.E., Erickson, R.P., Barnett, L.B., Venta, P.J. & Tashian, R.E. (1988) N-Ethyl-N-nitrosourea induced null mutation at the car-2 locus-an animal model for human carbonic anhydrase II deficiency syndrome. Proc Natl Acad Sci USA, 85, 1962–1966.

Li, J., Parada, C. & Chai, Y. (2017) Cellular and molecular mechanisms of tooth root development. Development, 1;144(3), 374-384.

Li, Z.Q., Hu, X.P., Zhou, J.Y., Xie, X.D. & Zhang, J.M. (2015) Genetic polymorphisms in the carbonic anhydrase VI gene and dental caries susceptibility. Genet Mol Res, 14(2), 5986–5993.

Lin, H.M., Nakamura, H., Noda, T. & Ozawa, H. (1994) Localization of H(+) - ATPase and carbonic anhydrase II in ameloblasts at maturation. Calcif Tissue Int, 55(1), 38-45.

Liu, F., Thirumangalathu, S., Gallant, N.M., Yang, S.H., Stoick-Cooper, C.L., Reddy, S.T., Andl, T., Taketo, M.M., Dlugosz, A.A., Moon, R.T., Barlow, L.A., & Millar, S.E. (2007) Wnt β-catenin signaling initiates taste papilla development. Nature genetics, 39, 106-112.

Liu, H.X., Maccallum, D.K., Edwards, C., Gaffield, W. & Mistretta, C.M. (2004) Sonic hedgehog exerts distinct, stage-specific effects on tongue and taste papilla development. Dev Biol, 276, 280-300.

Liu, H.X., Henson, B.S., Zhou, Y., D'Silva, N.J. & Mistretta, C.M. (2008) Fungiform papilla pattern: EGF regulates inter-papilla lingual epithelium and decreases papilla number by means of PI3K/Akt, MEK/ERK, and p38 MAPK signaling. Dev Dyn, 237(9), 2378-2393.

Liu, H.X., Grosse, A.S., Iwatsuki, K., Mishina, Y., Gumucio, D.L. & Mistretta, C.M. (2012) Separate and distinctive roles for Wnt5a in tongue, lingual tissue and taste papilla development. Dev Biol, 1;361(1), 39-56.

Liu, H.X., Ermilov, A., Grachtchouk, M., Li, L., Gumucio, D.L., Dlugosz, A.A. & Mistretta, C.M. (2013) Multiple Shh signaling centers participate in fungiform papilla and taste bud formation and maintenance. Dev Biol, 1;382(1), 82-97.

Listgarten, M.A. (1975) Cell rests in the periodontal ligament of mouse molars. J Periodontal Res, 10, 197–202.

Lobe, C.G. & Nagy, A. (1998) Conditional genome alteration in mice. Bioessays 20, 200–208.

Long, F., Zhang, X. M., Karp, S., Yang, Y. & McMahon, A. P. (2001) Genetic manipulation of hedgehog signaling in the endochondral skeleton reveals a direct role in the regulation of chondrocyte proliferation. Development, 128,5099 -5108.

Lu, W.J., Mann, R.K., Nguyen, A., Bi, T., Silverstein, M., Tang, J.Y., Chen, X. & Beachy, P.A. (2018) Neuronal delivery of Hedgehog directs spatial patterning of taste organ regeneration. Proc Natl Acad Sci U S A, 9;115(2), E200-E209.

Luan, X., Ito, Y. & Diekwish, T.G.H. (2006) Evolution and development of Hertwig's epithelial root sheath. Dev Dyn, 235, 1167–1180.

Maddaluno, L., Urwyler, C. & Werner, S. (2017) Fibroblast growth factors: key players in regeneration and tissue repair. Development, 144(22), 4047-4060.

Maksimovic, S., Nakatani, M., Baba, Y., Nelson, A.M., Marshall, K.L., Wellnitz, S.A., Firozi, P., Woo, S.H., Ranade, S., Patapoutian, A. & *Lumpkin, E.A.*

(2014) Epidermal Merkel cells are mechanosensory cells that tune mammalian touch receptors. Nature, 29, 509(7502), 617-621.

Margolis, D.S., Szivek, J., Lai, L–W. & Lien, Y-H. (2008) Phenotypic characteristics of bone in carbonic anhydrase II-deficient mice. Calcif Tissue Int, 82, 66–76.

Mark, M., Ghyselinck, N.B. & Chambon, P. (2009) Function of retinoic acid receptors during embryonic development. Nucl Recept Signal, 7, e002.

Mboge, M.Y., Mahon, B.P., McKenna, R. & Frost, S.C. (2018) Carbonic Anhydrases: Role in pH Control and Cancer. Metabolites, 28, 8(1).

*McAdams, T.A., Miller, W.M. & Papoutsakis, E.T. (*1998*)* pH is a potent modulator of erythroid differentiation*. Br J Haematol,* 103*, 317–325.*

McMahon, A.P., Ingham, P.W. & Tabin, C.J. (2003) Developmental roles and clinical significance of hedgehog signaling. Curr Top Dev Biol, 53, 1-114.

Melnik, B.C. (2017) Apoptosis May Explain the Pharmacological Mode of Action and Adverse Effects of Isotretinoin, Including Teratogenicity. Acta Derm Venereol, 8,97(2), 173-181.

Mendelsohn, C., Ruberte, E., LeMeur, M., Morriss-Kay, G. & Chambon, P. (1991) Developmental analysis of the retinoic acid-inducible RAR-beta2 promoter in transgenic animals. Development, 113, 723–734.

Mendelsohn, C., Larkin, S., Mark, M., LeMeur, M., Clifford, J., Zelent, A. & Chambon, P. (1994) RARb isoforms: distinct transcriptional control by retinoic acid and specific spatial patterns of promoter activity during mouse embryonic development. Mech Dev, 45, 227–241.

Metzger, D. & Feil, R. (1999) Engineering the mouse genome by site-specific recombination. Curr. Opin. Biotechnol. 10, 470–476.

Metzler, M.A., Raja, S., Elliott, K.H., Friedl, R.M., Tran, N.Q.H., Brugmann, S.A., Larsen, M. & Sandell, L.L. (2018) Correction: RDH10-mediated retinol metabolism and RARα-mediated retinoic acid signaling are required for submandibular salivary gland initiation. Development, 30,145(17).

Michlig, S., Damak, S., & Le Coutre, J. (2007) Claudin-based permeability barrier in taste buds. J Comp Neurol, 502, 1003–1011.

Mikels, A.J. & Nusse, R. (2006) Purified Wnt5a protein activates or inhibits beta-catenin-TCF signaling depending on receptor context. PLoS Biol, 4(4), e115.

Mistretta, C.M., Liu, H.X., Gaffield, W. & MacCallum, D.K. (2003) Cyclopamine and jervine in embryonic rat tongue cultures demonstrate a role for Shh signaling in taste papilla development and patterning: fungiform papillae double in number and form in novel locations in dorsal lingual epithelium. Dev Biol, 254, 1-18.

Mistretta, C.M. & Liu, H.X. (2006) Development of fungiform papillae: patterned lingual gustatory organs. Arch Histol Cytol, 69(4), 199-208.

Miura. H., Scott, J.K., Harada, S. & Barlow, L.A. (2014) Sonic hedgehog-expressing basal cells are general post-mitotic precursors of functional taste receptor cells. Dev Dyn, 243(10).1286-1297.

Mollard, R., Viville, S., Ward, S.J., Décimo, D., Chambon, P. & Dollé, P. (2000) Tissue-specific expression of retinoic acid receptor isoform transcripts in the mouse embryo. Mech Dev, 94, 223-232.

Moore-Scott, B.A. & Manley, N.R. (2005) Differential expression of Sonic hedgehog along the anterior-posterior axis regulates patterning of pharyngeal pouch endoderm and pharyngeal endoderm-derived organs. Dev Biol, 15, 278(2), 323-35.

Nagai, R., Kooh, S.W., Balfe, J.W., Fenton, T. & Halperin, M.L. (1997) Renal tubular acidosis and osteopetrosis with carbonic anhydrase II deficiency: pathogenesis of impaired acidification Pediatr. Nephrol, 11, 633-636.

Nagase, T., Nagase, M., Machida, M. & Yamagishi, M., (2007) Hedgehog signaling: a biophysical or biomechanical modulator in embryonic development? Ann N Y Acad Sci, 1101, 412-438.

Nagy,A., (2000) Cre recombinase: the universal reagent for genome tailoring. Genesis ,26, 99-109.

Nakatomi, M. (2009) Ellis-van Creveld (EVC) syndrome: unusual oral defects in humans and Evc mutant mice. J Oral Biosci, 51, 151–157.

Neri, D. & Supuran, C.T. (2011) Interfering with pH regulation in tumours as a therapeutic strategy. Nat Rev Drug Discov, 16; 10 (10),767-777.

Nguyen, M.B., Cohen, I., Kumar, V., Xu, Z., Bar, C., Dauber-Decker, K.L., Tsai, P.C., Marangoni, P., Klein, O.D., Hsu, Y.C., Chen, T., Mikkola, M.L. & Ezhkova, E. (2018) FGF signalling controls the specification of hair placode-derived SOX9 positive progenitors to Merkel cells. Nat Commun, 13,9(1), 2333.

Niederreither, K., McCaffery, P., Dräager, U.C., Chambon, P. & Dollé, P. (1997) Restricted expression and retinoic acid-induced downregulation of the retinaldehyde dehydrogenenase type 2 (RALDH-2) gene during mouse development. Mech Dev, 62, 67-78.

Niederreither, K., Fraulob, V., Garnier, J-M., Chambon, P. & Dollé, P. (2002) Differential expression of retinoic acid-synthesizing (RALDH) enzymes during fetal development and organ differentiation in the mouse. Mech Dev, 110, 167-171.

Niederreither, K. & Dollé, P. (2008) Retinoic acid in development: towards an integrated view. Nat Rev Genet, 9, 541-553.

Nunzi, M.G., Pisarek, A. & Mugnaini, E. (2004) Merkel cells, corpuscular nerve endings and free nerve endings in the mouse palatine mucosa express three subtypes of vesicular glutamate transporters. J Neurocytol, 33(3), 359-76.

Nusse, R. & Clevers, H. (2017) Wnt/β-Catenin Signaling, Disease, and Emerging Therapeutic Modalities. Cell, 1;169(6), 985-999.

Ochrietor, J.D., Clamp, M.F., Moroz, T.P., Grubb, J.H., Shah, G.N., Waheed, A., Sly, W.S. & Linser, P.J. (2005) Carbonic anhydrase XIV identified as the membrane CA in mouse retina: strong expression in Müller cells and the RPE. Exp Eye Res, 81, 492–500.

Okubo, T., Pevny, L.H. & Hogan, B.L. (2006) Sox2 is required for development of taste bud sensory cells. Genes Dev, 20, 2654–2659.

Ornitz, D. M. & Itoh, N. (2015) The Fibroblast Growth Factor signaling pathway. Wiley Interdiscip. Rev Dev Biol, 4, 215-266.

Osanai, M., Takasawa, A., Takasawa, K., Murata, M. & Sawada, N. (2018) Retinoic acid-metabolizing enzyme cytochrome P450 26A1 promotes skin carcinogenesis induced by 7,12-dimethylbenz[a]anthracene. Oncol Lett, 15(6), 9987-9993.

Padmanabhan, R. & Ahmed, I. (1997) Retinoic acid-induced asymmetric craniofacial growth and cleft palate in the mouse fetus. Reprod Toxicol, 11, 843–860.

Padmanabhan, R. (1998) Retinoic-acid-induced caudal regression syndrome in the mouse fetus. Reprod Toxicol, 12, 139-151.

Pastorekova, S., Parkkila, S., Pastorek, J. & Supuran, C.T. (2004) Carbonic anhydrases: Current state of the art, therapeutic applications and future prospects. J Enz Inhib Med Chem, 19, 199–229.

Perdigoto, C.N., Dauber, K.L., Bar, C., Tsai, P-C., Valdes, V.J., Cohen, I., Santoriello, F.J., Zhao, D., Zheng, D., Hsu, Y.C. & Ezhkova, E . (2016) Polycomb-mediated repression and Sonic Hedgehog signaling interact to regulate Merkel cell specification during skin development. PLoS Genet, 12, e1006151.

Perea-Martinez, I., Nagai, T. & Chaudhari, N. (2013) Functional cell types in taste buds have distinct longevities. PLoS ONE, 8 (1), e53399.

Petersen, C.I., Jheon, A.H., Mostowfi, P., Charles, C., Ching, S., Thirumangalathu, S., Barlow, L.A. & Klein, O.D. (2011) FGF signaling regulates the number of posterior taste papillae by controlling progenitor field size. PLoS Genet, 7(6), e1002098.

Pham, C.D., Smith, C.E., Hu, Y., Hu, J.C., Simmer, J.P. & Chun, Y.P. (2017) Endocytosis and Enamel Formation. Front Physiol. Jul 31;8:529.

Pinnimpede, T., Cameron, D.A., MacLean, G.A., Li, H., Abu-Abed, S. & Petkovitch, M. (2010) The role of CYP26 enzymes in defining appropriate

retinoic acid exposure during embryogenesis. Birth Defects Res (PartA), 88, 883–894.

Prochazkova, M., Häkkinen, T.J., Prochazka, J., Spoutil, F., Jheon, A.H., Ahn, Y., Krumlauf, R., Jernvall, J. & Klein, O.D. (2017) FGF signaling refines Wnt gradients to regulate the patterning of taste papillae. Development, 144(12), 2212-2221.

Reifen, R., Agami, O., Weiser, H., Biesalski, H. & Naim, M. (1998) Impaired responses to sweet taste in vitamin A-deficient rats. Metabolism, 47(1), 1-2.

Reith, E.J. & Boyde, A. (1981) The arrangement of ameloblasts on the surface of maturing enamel of the rat incisor tooth. J Anat 133: 381–388.

Reynolds, K., Mezey, E. & Zimmer A. (1991) Activity of the beta-retinoic acid receptor promoter in transgenic mice. Mech Dev, 36, 15–29.

Rice, R., Spencer-Dene, B., Connor, E.C., Gritli-Linde, A., McMahon, A.P., Dickson, C., Thesleff, I. & Rice, D.P. (2004) Disruption of Fgf10/Fgfr2b-coordinated epithelial-mesenchymal interactions causes cleft palate. J Clin Invest, 113(12),1692-1700.

Rikihisa, Y. (1985) Ultrastructural localization of carbonic anhydrase in lysosomes. Ant Rec, 211, 1–8.

Rishikaysh, P., Dev, K., Diaz, D., Qureshi, W.M., Filip, S. & Mokry, J. (2014) Signaling involved in hair follicle morphogenesis and development. Int J Mol Sci, 22;15(1), 1647-1670.

Rohatgi, R., Milenkovic, L. & Scott, M.P. (2007) Patched1 regulates hedgehog signaling at the primary cilium. Science, 317, 372–376.

Roper, S., (1992) The microphysiology of peripheral taste organs. J Neurosci, 12, 1127–1134.

Rossant, J., Zirngibl, R., Cado, D., Shago, M. & Giguère, V. (1991) Expression of a retinoic acid response element-hsplacZ transgene defines specific domains of transcriptional activity during mouse embryogenesis. Genes Dev, 5, 1333–1344.

Ruberte, E., Dollé, P., Krust, A., Zelent, A., Morris-Kay, G. & Chambon, P. (1990) Specific spacial and temporal distribution of retinoic acid receptor gama transcripts during mouse embryogenesis. Development, 108, 213-222.

Ruberte, E., Friederich, V., Morriss-Kay, G. & Chambon, P. (1992) Differential distribution patterns of CRABP I and CRABP II transcripts during mouse embryogenesis. Development, 115(4), 973-987.

Ruivo, R., Anne, C., Sagné, C. & Gasnier, B. (2009) Molecular and cellular basis of lysosomal transmembrane protein dysfunction. Biochim Biophys Acta, 1793(4), 636-649.

Sadler, T.W. (2015) Langman´s medical embryology (11th ed.). Wolters Kluwer, Hong Kong.

Seppala, M., Xavier, G.M., Fan, C-M. & Cobourne, M.T. (2014) Boc modifies the spectrum of holoprosencephaly in the absence of Gas1 function. Biol Open, 728-740.

Seppala, M., Fraser, G.J., Birjandi, A.A., Xavier, G.M. & Cobourne, M.T. (2017) Sonic Hedgehog Signaling and Development of the Dentition. J Dev Biol, 31, 5(2).

Seta, Y., Oda, M., Kataoka, S., Toyono, T. & Toyoshima, K. (2011) Mash1 is required for the differentiation of AADC-positive type III cells in mouse taste buds. Dev Dyn, 240, 775–784.

Shenefelt, R.E . (1972) Morphogenesis of malformations in hamsters caused by retinoic acid: Relation to dose and stage at treatment. Teratology, 5, 103-118.

Shi, Y.N., Zhu, N., Liu, C., Wu, H.T., Gui, Y., Liao, D.F., Qin, L. (2017) Wnt5a and its signaling pathway in angiogenesis. Clin Chim Acta, 471, 263-269.

Shiraishi, Y., Mizutani, A., Yuasa, S., Mikoshiba, K. & Furuichi, T. (2004) Differential expression of Homer family proteins in the developing mouse brain. J Comp Neurobiol, 473, 582–599.

Shrode, L.D., Rubie, E.A., Woodgett, J.R. & Grinstein, S. (1997) Cytosolic alkalinization increases stress-activated protein kinase/c-Jun NH2-terminal kinase (SAPK/JNK) activity and p38 mitogen-activated protein kinase activity by a calcium-independent mechanism. J Biol Chem, 272, 13653–13659.

Siegenthaler, J.A., Ashique, A.M., Kostantino, Z., Patterson, K.P., Hecht, J.H., Kane, M.A., Folias, A.E., Choe, Y., May, S.R., Kume, T., Napoli, J.L., Peterson, A.S. & Pleasure, S.J. (2009) Retinoic acid from the meninges regulates cortical neuron generation. Cell, 139, 597–609.

Simmer, J.P. & Hu, J.C. (2002) Expression, structure, and function of enamel proteinases. Connect Tissue Res, 43(2-3), 441-449.

Simmer, J.P., Papagerakis, P., Smith, C.E., Fisher, D.C., Rountrey, A.N., Zheng, L., & Hu, J.C. (2010) Regulation of dental enamel shape and hardness. J Dent Res, 89, 1024–1038.

Simpson, F., Kerr, M.C. & Wicking, C., (2009) Trafficking, development and hedgehog. Mech Dev, 126, 279–288.

Smith, C. E. & Warshawsky, H. (1975) Cellular renewal in the enamel organ and the odontoblast layer of the rat incisor as followed by radioautography using 3H-thymidine. Anat Rec, 183,523-562.

Smith, C.E., Nanci, A. & Moffatt, P. (2006) Evidence by signal peptide trap technology for the expression of carbonic anhydrase 6 in rat incisor enamel organs. Eur J Oral Sci, 114 Suppl 1, 147-153.

Soriano, P. (1999) Generalized lacZ expression with the ROSA26 Cre reporter strain. Nat Genet, 21, 70–71.

Strigini, M. & Cohen, S. M. (1997) A Hedgehog activity gradient contributes to AP axial patterning of the Drosophila wing. Development 124, 4697 -4705.

Strisciuglio, P., Sartorio, R., Pecoraro, C., Lotito, F. & Sly, W.S. (1990) Variable clinical presentation of carbonic anhydrase deficiency: evidence for heterogeneity? Eur J Pediatr, 149, 337-340.

Sugimoto, T., Ogawa, Y., Kuwahara, H., Shimazaki, M., Yagi, T. & Sakai, A. (1988) Histochemical demonstration of carbonic anhydrase activity in the odontogenic cells of the rat incisor. J Dent Res, 67 (10), 1271-4.

Supuran, C.T. (2017) Carbonic Anhydrase Inhibition and the Management of Hypoxic Tumors. Metabolites, 16;7(3), pii: E48.

Tahayato, A., Dollé, P. & Petkovitch, M. (2003) Cyp26c1 encodes a novel retinoic acid-metabolizing enzyme expressed in the hindbrain, inner ear, first brachial arch and tooth buds during murine development. Gene Exp Patterns, 3, 449-454.

Thesleff, I. (2014) Current understanding of the process of tooth formation: transfer from the laboratory to the clinic. Aust Dent J, 59 Suppl 1, 48-54.

Thirumangalathu, S., Harlow, D.E., Driskell, A.L., Krimm, R.F. & Barlow, L.A. (2009) Fate mapping of mammalian embryonic taste bud progenitors. Development,136(9), 1519-1528.

Thirumangalathu, S. & Barlow, L.A. (2015) β-Catenin signaling regulates temporally discrete phases of anterior taste bud development. Development, 15;142(24),4309-4317.

Tickle, C. (2006) Making digit patterns in the vertebrate limb. Nat Rev Mol Cell Biol, 7(1),45-53.

Torroja, C., Gorfinkiel, N. & Guerrero, I. (2005) Mechanisms of Hedgehog gradient formation and interpretation. J Neurobiol, 64, 334–356.

Toyosawa, S., Ogawa, Y., Chang, C.K., Soga, S.I., Hong, S.S. & Yagi, T. (1989) Ultrastructural histochemistry of carbonic anhydrase in rat osteoclasts. J Osaka Univ Dent Sch 29, 72–80.

Toyosawa, S., Ogawa, Y., Inagaki, T. & Ijuhin, N. (1996) Immunohistochemical localization of carbonic anhydrase isozyme II in rat incisor epithelial cells at various stages of amelogenesis. Cell Tissue Res, 285(2), 217-225.

Toyoshima, K. & Shimamura, A. (1991) Uranaffin reaction of Merkel corpuscles in the lingual mucosa of the finch, Lonchula striata var. domestica. J Anat, 179, 197-201.

Toyoshima, K., Seta, Y., Toyono, T. & Takeda, S. (1999) Merkel cells are responsible for the initiation of taste organ morphogenesis in the frog. J Comp Neurol, 29, 406(1), 129-40.

Uehara, M., Yashiro, K., Mamiya, S., Nishino, J., Chambon, P., Dollé, P. & Sakai, Y. (2007) CYP26A1 and CYP26C1 cooperatively regulate anterior-posterior patterning of the developing brain and the production of migratory neural crest cells in the mouse. Dev Biol, 302, 399-411.

van Amerongen, R., Fuerer, C., Mizutani, M. & Nusse, R. (2012) Wnt5a can both activate and repress Wnt/β-catenin signaling during mouse embryonic development. Dev Biol, 1;369(1),101-114.

Van Keymeulen, A., Mascre, G., Youseff, K.K., Harel. I., Michaux, C., De Geest, N., Szpalski, C., Achouri, Y., Bloch, W., Hassan, B.A. & Blanpain, C. (2009) Epidermal progenitors give rise to Merkel cells during embryonic development and adult homeostasis. J Cell Biol, 5,187(1), 91-100.

Vaziri Sani, F., Hallberg, K., Harfe, B.D., McMahon, A.P., Linde, A. & Gritli-Linde. A. (2005) Fate-mapping of the epithelial seam during palatal fusion rules out epithelial-mesenchymal transformation. Dev Biol, 15;285(2), 490-495.

Venta, P.J., Welty, R.J., Johnson, T.M., Sly, W.S. & Tashian, R.E. (1991) Carbonic anhydrase II deficiency syndrome in a Belgian family is caused by a point mutation at an invariant histidine residue (107 His----Tyr): complete structure of the normal human CA II gene. Am J Hum Genet, 49(5), 1082–1090.

Wang, X., Suzawa, T., Ohtsuka, H., Zhao, B., Miyamoto, Y., Miyauchi, T., Nishimura, R., Inoue, T., Nakamura, M., Baba, K. & Kamijo, R. (2010) Carbonic anhydrase II regulates differentiation of ameloblasts via intracellular pH-dependent JNK signaling pathway. J Cell Physiol, 225(3), 709-719.

Wang, X.P., Suomalainen, M., Felszeghy, S., Zelarayan, L.C., Alonso, M.T., Plikus, M.V., Maas, R.L., Chuong, C.M., Schimmang, T. & Thesleff, I. (2007) An integrated gene regulatory network controls stem cell proliferation in teeth. PLoS Biol, 5(6), e159.

White, R.J. & Schilling, T.F. (2008) How degrading: Cyp26s in hindbrain development. Dev Dyn, 237, 2775–2790.

Wiese, K.E., Nusse, R. & van Amerongen, R. (2018) Wnt signalling: conquering complexity. Development, 26, 145(12).

Wilkinson, D.G. (1992) Whole-mount in situ hybridization of vertebrate embryos. In: Wilkinson D.G. (Ed.). In situ Hybridization. A Practical approach. Oxford University Press, Oxford, UK.

Wolbach, S.B. & Howe, P.R. (1925) Tissue changes following deprivation of fat-soluble A vitamin. J Exp Med, 42, 753-777.

Wolfe, J.M. & Salter, H.P. (1931) Vitamin A deficiency in the albino mouse. J Nutr, 4, 185-192.

Wykoff, C.C., Beasley, N.J., Watson, P.H., Turner, K.J., Pastorek, J., Sibtain, A., Wilson, G.D., Turley, H., Talks, K.L., Maxwell, P.H., Pugh, C.W., Ratcliffe, P.J., & Harris, A.L. (2000) Hypoxia-inducible expression of tumor-associated carbonic anhydrases. Cancer Res, 60, 7075–7083.

Xavier, M.G., Seppala, M., Barrell, W., Birjandi, A.A., Geoghegan, F. & Cobourne, M. (2016) Hedgehog receptor function during craniofacial development. Dev Biol, 415, 198–215.

Xu, M., Horrell, J., Snitow, M., Cui, J., Gochnauer, H., Syrett, C.M., Kallish, S., Seykora, J.T., Liu, F., Gaillard, D., Katz, J.P., Kaestner, K.H., Levin, B., Mansfield, C., Douglas, J.E., Cowart, B.J., Tordoff, M., Liu, F., Zhu, X., Barlow, L.A., Rubin, A.I., McGrath, J.A., Morrisey, E.E., Chu, E.Y. & Millar, S.E. (2017) WNT10A mutation causes ectodermal dysplasia by impairing progenitor cell proliferation and KLF4-mediated differentiation. Nat Commun, 7;8, 15397.

Yang C, Chen W, Chen Y, Jiang J. Smoothened transduces hedgehog signal by forming a complex with Evc/Evc2. Cell Res. 2012; 11: 1593–1604. Yang, Z., Balic, A., Michon, F., Juuri, E. & Thesleff, I. (2015) Mesenchymal Wnt/β-Catenin Signaling Controls Epithelial Stem Cell Homeostasis in Teeth by Inhibiting the Antiapoptotic Effect of Fgf10. Stem Cells, 33(5), 1670-81.

Yang, Z., Balic, A., Michon, F., Juuri, E., Thesleff, I. (2015) Mesenchymal Wnt/β-Catenin Signaling Controls Epithelial Stem Cell Homeostasis in Teeth by Inhibiting the Antiapoptotic Effect of Fgf10. Stem Cells, 33(5),1670-81.

Yasuda, Y., Okamoto, M., Konishi, H., Matsuo, T., Kihara, T. & Tanimura, T. (1986) Developmental anomalies induced by all-trans retinoic acid in fetal mice: I. Macroscopic findings. Teratology, 34(1), 37-49.

Yasuda, Y., Itoh, K., Mizuno, N., Konishi, H. & Tanimura, T. (1989) Alterations in migrating cranial neural crest cells in embryos of mice fed retinoic acid. Anal Cell Pathol, 2(1), 23-40.

Yee, C., Yang, R., Böttger, B., Finger, T.E. & Kinnamon, J.C. (2001) "Type III" cells of rat taste buds: immunohistochemical and ultrastructural studies of neuron specific enolase, protein gene product 9.5 and serotonin. J Comp Neurol, 440, 97-108.

Yom, S.S., Rosenthal, D.I., El-Naggar, A.K., Kies, M.S. & Hessel, A.C. (2006) Merkel cell carcinoma of the tongue and head and neck oral mucosal sites. Oral Surg Oral Med Oral Pathol Oral Radiol Endod, 101, 761–768.

Young, D.L., Schneider, R.A., Hu, D. & Helms, J.A. (2000) Genetic and teratogenic approaches to craniofacial development. Crit Rev Oral Biol Med, 11(3),304-17.

Zhan, T., Rindtorff, N. & Boutros, M. (2017) Wnt signaling in cancer. Oncogene, 36(11), 1461-1473.

Zhao, H., Feng, J., Seidel, K., Shi, S., Klein, O., Sharpe, P. & Chai, Y. (2014) Secretion of Shh by a neurovascular bundle niche supports mesenchymal stem cell homeostasis in the adult mouse incisor. Cell Stem Cell 14, 160-173.

Zhou, Y., Liu, H. X. & Mistretta, C. M. (2006) Bone morphogenetic proteins and noggin: inhibiting and inducing fungiform taste papilla development. Dev Biol, 297, 198 -213.

Appendix

I. Reibring CG, El Shahawy M, Hallberg K, Kannius-Janson M, Nilsson J, Parkkila S, Sly WS, Waheed A, Linde A, Gritli-Linde A. Expression patterns and subcellular localization of carbonic anhydrases are developmentally regulated during tooth formation. *PloS One*. 2014 May 1;9(5):e96007.

II. El Shahawy M, Reibring CG, Neben CL, Hallberg K, Marangoni P, Harfe BD, Klein OD, Linde A, Gritli-Linde A. Cell fate specification in the lingual epithelium is controlled by antagonistic activities of Sonic hedgehog and retinoic acid. *PLoS Genet.* 2017 July 17; 13(7):e1006914.

III. El Shahawy M, Reibring CG, Hallberg K, Neben CL, Marangoni P, Harfe BD, Klein OD, Linde A, Gritli-Linde A. Sonic hedgehog signaling is required for *Cyp26* expression during embryonic development. *Manuscript.*